Dottorato di Ricerca in Scienze Biomediche

CICLO XXIX

Dipartimento di Medicina Molecolare, Sezione di Fisiologia Umana

Coordinator: Chiar.mo Prof. Egidio D'Angelo

Skeletal muscle deterioration in dilated cardiomyopathy: molecular mechanism and effect of prolonged endurance training in a mice model

Dr. Eleonora Bardi

Tutor: Prof. Roberto Bottinelli

Academic Year 2015-2016

"When I was 5 years old, my mother always told me that happiness was the key to life. When I went to school, they asked me what I wanted to be when I grew up. I wrote down 'happy'. They told me I didn't understand the assignment, and I told them they didn't understand life."

John Lennon

Index

Preface

The benefit of exercise training on heart rate response in patients with heart failure has been well documented, as well as the exercise intolerance which is developed by patients and that limits the exercise benefit. Several studies showed that a decrease in the exercise tolerance in patients with chronic heart failure (CHF) is a strong prognostic indicator of cardiovascular events. As the life expectancy of patients with heart disease has improved in recent years, a deeper understanding of the molecular causes of exercise intolerance, is of primary scientific, clinical and social importance.

Exercise intolerance is defined as the reduced ability to perform daily activities that involve dynamic movement of large skeletal muscles because of symptoms of dyspnea or fatigue. Many investigators have sought mechanisms to explain the source of exercise intolerance. Importantly, hemodynamic improvements do not acutely reverse this process. Therefore, several different lines of evidence have converged to identify skeletal muscle pathology as a major contributor to exercise intolerance. While numerous studies have linked enzymatic and histologic abnormalities to exercise intolerance, the underlying mechanisms driving these processes remain poorly understood.

An useful animal model to investigate these aspects at a cellular/molecular level is represented by the $Tg\alpha_q\ 44^*$ mice line, a transgenic mice model of CHF resulting from a cardiac-specific overexpression of constitutively active $G\alpha_q$ protein. This model is characterized by a gradual progression of the disease and for this reason offers the great advantage of studying muscle adaptations from the early to the late stage of the disease. Furthermore, voluntary exercise represents a training modality in which physical activity occurs under non-stressful conditions representing a valid training intervention to assess the presence of exercise intolerance.

The major findings of this thesis can be divided in (i) the characterization of the muscle alterations in skeletal muscle in mice with dilated cardiomyopathy and (ii) the analysis of how these alterations are related to *in vivo* functional performance over time.

Background

General structure of skeletal muscle

Skeletal muscle is the most abundant tissue in the vertebrate body. It is also a very specialized tissue that has both the ability to contract and to conduct electrical impulses. Whole muscle is attached to bone by a tendon, nearly inextensible connective tissue layer called epimysium. The muscle is divided into bundles by thinner layers called perimysium within which we distinguish the fiber bundles or fasciculi. Bundles are an aggregation of myofibers, the latter representing the muscle cells (Fig. 1). Each fiber is a syncytium, i.e. a cell that have many nuclei. The nuclei are oval in shaped and are found at the periphery of the cell, just beneath the thin, elastic membrane (sarcolemma). The sarcoplasm also has many alternating light and dark bands, giving the fiber a striped or striated appearance (hence the name striated muscle). With the aid of an electron microscope it can be seen that each muscle fiber is made up of many smaller units, the myofibrils. This specific arrangement of actin and myosin filaments is known as a sarcomere (Fig. 1).
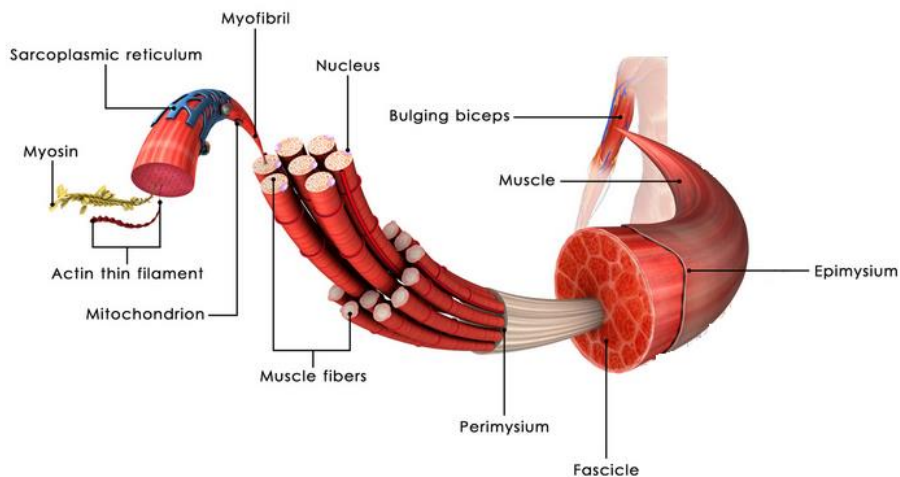
Fig. 1: Muscle anatomy and composition, from macroscopic to microscopic.

Muscle fiber organization

Skeletal muscle fiber is the fundamental unit of muscle, each fiber is a syncytium, (i.e. a cell that have many nuclei) derives embryologically from the multiple division of progenitor cells that give rise to myoblast fusion which leads to the formation of syncytial multinucleated cells. A muscle fiber is from a few mm to several cm long and of variable diameter, 10-100 m; it is surrounded by a membrane, the sarcolemma, which encloses a fluid matrix, the sarcoplasm in which the nuclei, the sarcoplasmic organelles, glycogen granules and myofibrils which constitute the component muscle contractile, are present. The myofibrils, with a diameter between 0.5 and 2 mM, are in turn constituted by myofilaments or protofibrils of two types: thin myofilaments with a diameter of 12 nm and thick myofilaments having a diameter of approximately 4 nm.

Hanson and Huxley H.E (H A N S O N a n d H U X L E Y , 1 9 5 3) , using phase-contrast, polarized light and electron microscopy, showed that the cross-striations resulted from a discontinuous distribution of contractile proteins along the length of the myofibrils. They suggest that the denser regions (the A-bands), were made of thick filaments, mainly made of myosin, interdigitating with thin filaments, mainly made of actin (Fig. 2). The lighter regions, the I-bands, were made of thin filaments. I-bands presented a darker line in the middle, the so called Z-line, from which the thin filaments departed towards the A band (Fig. 2). The distance between two successive Z-lines was called the sarcomere (Fig. 2). In the middle of the A-band Hanson and H.E Huxley (1953) identified a lighter region, the H-zone, where only the thick filaments were present (Fig. 2). In the A-band two different types of filaments were present. The thicker filaments (myosin), with a diameter of ~110 Å, formed a very regular hexagonal array and were spaced ~300 Å apart and the thinner filaments (actin), with a diameter of ~40 Å, that were also arranged in a regular manner, lying fairly symmetrically in between three of the thicker filaments. Thus six actin filaments surrounded every myosin filament. Myosin is the most abundant protein in striated muscle fibers and is the main constituent of thick filaments. It plays the role of the molecular motor of muscle contraction. Sarcomeric myosins belong to II class myosin (Sellers et al., 1996) and are composed by two heavy chains (MHC, molecular weight of each MHC is 200-220 kD), two essential light chains and two regulatory light chains (RLC) (ELC and RLC are together called MLC, with molecular weight 16-26 kD each). The two heavy chains are wound around each other to form a double α-helical structure. At one end both chains are folded into separate globular structures to form the two heads.

In the muscle, the long tail portion forms the backbone of the thick filament and the heads protrude as cross-bridges toward the thin actin filament.

Each head contains two light chains distinct in one essential, or alkaline, light chain and one regulatory, or phosphorylable, light chain.
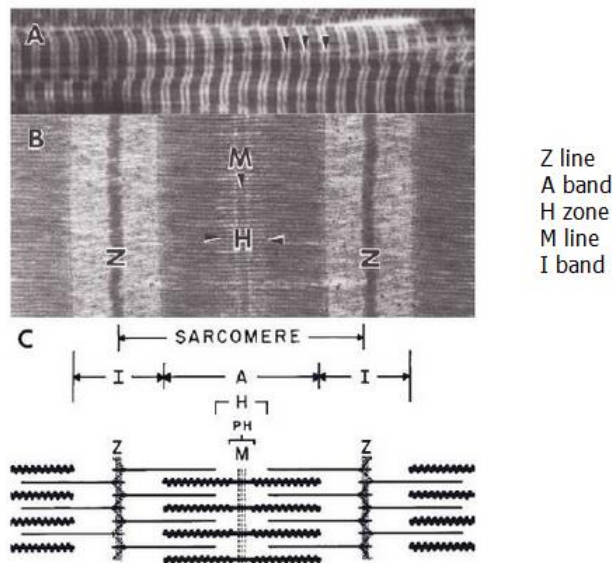
Fig. 2: Structure of sarcomere, the basic unit of striated muscle tissue (A) Photomicrograph of a logitudinal section of skeletal muscle fiber: are visible the bands A, darker, and the bands I, clearer. **(B)** Electron photomicrograph of a sarcomere. A sarcomere is defined as the segment between two neighbouring Z-lines (or Z-discs, or Z bodies). In electron micrographs of cross-striated muscle, the **Z-line** (*the disc in between* the I bands) appears as a series of dark lines. Surrounding the Z-line is the region of the **I-band**. I-band is the zone of thin filaments that is not superimposed by thick filaments. Following the I-band is the **A-band**. An A-band contains the entire length of a single thick filament. Within the A-band is a paler region called the **H-zone**. H-band is the zone of the thick filaments that is not superimposed by the thin filaments. Within the H-zone is a thin **M-line** (the disc in the *middle* of the sarcomere) formed of cross-connecting elements of the cytoskeleton. **(C)** Simplified model of sarcomeres in parallel.

Functional and energetics properties of muscle fiber

The understanding of the mechanisms of skeletal muscle heterogeneity and plasticity progressed very slowly from the pioneering work by Close (CLOSE, 1964) up to the end of the 1980s, when several works and especially those coming from Pette's and Schiaffino's laboratories uncovered the large molecular heterogeneity of the basic contractile unit of striated muscle, the sarcomere (Bär and Pette, 1988; Schiaffino et al., 1989; Pette and Staron, 1990; Schiaffino and Reggiani, 1996) They showed that the heavy chain of myosin (MHC), as well as the light chain (MLC) essential and regulators are encoded by a family of multigenes and therefore existed in different isoforms (Schiaffino and Reggiani, 1996). The secret of the extraordinary capacity of myosin to respond to requests very different functional among them lies precisely in the existence of multiple isoforms of MHC and MLC. Isoforms can be defined as protein which have very similar, but not identical, amino acid sequences, are coded by different genes, and are interchangeable. The attention mostly focused on the MHC isoforms as MHCs are the portion of the molecule that attaches to actin and split ATP, and they are mostly responsible for power generation.

In the human genome as in all mammals, nine genes encoding the sarcomeric MHC class II have been identified. The MHC genes are distributed in two main clusters: the first, located on human chromosome 14, contains genes MHC-β/slow and MHC-α and , the second cluster includes MHC-emb, MHC-neo, MHC-eo genes, and the three genes coding MHCs fast adult and is localized on chromosome 17 (Schiaffino and Reggiani, 1996). Four genes encoding isoforms 1 or β-MHC slow, MHC 2A, MHC 2X and MHC 2B, predominant in adult skeletal muscle in different species of mammals, are expressed in limbs and trunk muscle. Among these MHC 1 or β-slow is also expressed at the level of the myocardium ventricle. The MHC 2B isoform is generally not

expressed in human skeletal muscle. Two other genes encoding the MHC-emb and MHC-neo isoforms, are expressed during development, in adult life only during the regeneration and, in some species, in masticatory muscles. The remaining three isoforms have a limited tissue distribution: MHC-α is expressed in heart and in some species in the mandibular muscle; MHC-eo in extraocular and laryngeal muscle and finally the MHC-m isoform is expressed in the mandibular muscles of carnivores and non human primates (Mascarello et al., 2004).

Since the discovery of MHC isoforms, it was straightforward to assume that they were functionally different and that the functional heterogeneity among skeletal muscles depended on their differential expression. However, it took a considerable amount of work to definitely prove that this was actually the case.

In this respect, the earlier demonstration came with skinned fibers experiments in which contractile properties and MHC isoform content could be determined in the same muscle fiber enabling a direct relationship between function and MHC isoform content (Bottinelli et al., 1991; Bottinelli and Reggiani, 2000). When muscle fibers were grouped on the basis of MHC isoform content, very large differences among groups were observed with type I fibers being the slowest and type IIB fibers being the fastest fiber type. In humans, for example, fibers containing MHC-I (type I) had 10 fold lower unloaded shortening velocity (V_0), maximum power output (V_{max}), rate constant of tension raise ($1/T$), and 3 fold lower ATPase and tension cost than type IIX fibers, type IIA being intermediate. As expected, hybrid fibers were intermediate between pure fiber types. Interestingly, two properties did not differentiate muscle fiber types as much as all the others. Specific force (P_0/CSA) was only 30-40% lower in slow fibers than in fast fibers, whereas no differences were observed among fast fibers. Finally, thermodynamic efficiency was found to be similar in slow and fast human fibers and only slightly higher in slow than in fast rat fibers. The expression of different isoforms of protein and therefore the existence of distinct phenotypes of fibers muscle is the major determinant of muscle performance in vivo.

The finding that fiber types differed significantly in most contractile and energetic properties provided a simple basis for the functional heterogeneity of skeletal muscles. As in all mammals skeletal muscles are mixed muscles expressing the different fibers types in variable proportions (Fig 3A, B, C); it is expected that the higher the percent of fast fibers the higher the shortening velocity of the muscles. The classic work (Thorstensson et al., 1976) showing that velocity of knee extension was proportional to the percentage of fast fiber content of the contracting muscle was the earliest demonstration that this was actually the case. The qualitative mechanism of skeletal muscle heterogeneity and plasticity shown by Close long ago is based on the expression of different myosin isoforms within fiber types and on a differential distribution of fiber types in mammalian muscles. It is now well documented that the soleus muscle of the rat mostly contains type I fibers whereas the EDL muscle mostly contains fast fibers (IIA, IIX and IIB). No surprise that the EDL was found to be much faster than the Soleus muscle (Fig. 3A, B, C).
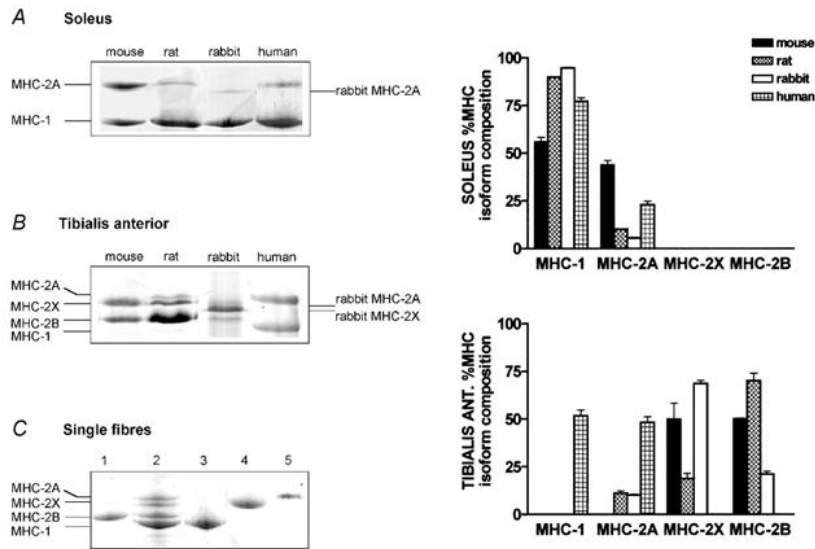
Fig. 3: MHC isoform distribution in soleus (A), tibialis anterior (B) and single muscle fibres (C) of mouse, rat, rabbit and human (A) Different proportions of two MHC isoforms (MHC-2A and MHC-1 or slow) are expressed in mouse, rat, rabbit and human soleus. **(B)** Two MHC isoforms (MHC-2X and MHC-2B) are detectable in mouse tibialis anterior, three isoforms (MHC-2A, MHC-2X, MHC-2B) are expressed in rat and in rabbit tibialis anterior and only two (MHC-2A and MHC-1 or slow) in human tibialis anterior. Note the different migration of fast MHC isoforms in rabbit. **(C)** Examples of MHC composition of single fibers: lane 1, rat pure fast 2B fibre; lane 3, rabbit pure slow fibre; lane 4, mouse pure fast 2X fibre; lane 5, mouse pure fast 2A fiber. Lane 2 shows a mixed rat muscle sample used as a reference. The relative percentage (mean ±s.e.m.) of MHC isoforms of soleus and tibialis anterior is shown in the histograms on the right-hand side of the figure (image, Pellegrino et al., 2003).

Muscle Plasticity

Skeletal muscle is a highly dynamic tissue that undergoes continuous remodeling in response to various metabolic and functional demands. The quantity and quality of muscle can be traced down to the structural and contractile proteins that respond to physiological and pathological conditions including exercise and injury (Blaauw et al., 2013). Individual muscle fibers vary in their mechanical, biochemical and metabolic properties depending upon the fiber type. Various criteria have been used to classify fiber types including histochemical methods (Green et al., 1982), speed of twitch contraction (Burke et al., 1973), fatigability, dominant enzymatic pathway and the myosin heavy chain (MyHC) isoform expression (Larsson and Moss, 1993). Of those, MyHC isoforms are the most frequently used classification criteria and are considered the molecular markers of fiber types. Myosin is the molecular motor and the prime driving protein in force generation. It is also the most abundant protein in the sarcomere comprising ~25% of the total muscle proteins (Balagopal et al., 1997). Due to its abundance and contractile significance, quantitative and qualitative changes in myosin and its isoforms have significant effects on muscle strength. Because fiber type diversity is associated with functional diversity, alterations in muscle fiber types affect contractile, metabolic and biochemical properties of the muscle.

Quantitative and Qualitative Mechanism of Skeletal Muscle Plasticity

It is now clear two major mechanisms of skeletal muscle heterogeneity and plasticity exist: a quantitative mechanism based on a change in muscle mass and a qualitative mechanism independent of muscle mass.

Quantitative mechanism: The quantitative mechanism modifies fibers in size leading muscles to an increase called hypertrophy or a decrease called atrophy.
Skeletal muscle mass can change quite rapidly and these changes can be evoked by a variety of stimuli including mechanical loads, nutrients, neural activity, cytokines, growth factors and hormones (Bodine, 2006; Sandri, 2008). All of these stimuli induce changes in muscle mass by altering the net balance between protein synthesis and protein degradation. Genetic studies in both drosophila and mammals have shown that pathways controlling protein synthesis and protein breakdown are tightly regulated and interrelated. The first level of connection occurs during protein synthesis when the quality control of the cell degrades proteins that are not correctly folded. At a further level, protein degradation systems determine the half- life of protein and, in muscle, are required to replace sarcomeric proteins as a consequence of changes in muscle activity. Importantly, the proteolytic systems can produce alternative energy substrates that are used by the cell to maintain internal homeostasis in conditions of energy stress.

Qualitative mechanism: The qualitative mechanisms is based on the presence of skeletal muscle fiber types with different functional properties: fast and slow fibers. This imply that even whole muscle properties could be modified by changing its relative content in slow and fast fibers. The change of protein content and of protein isoforms towards a new steady-state during an adaptive event can potentially be controlled by modifications in many steps from DNA to assembled translation products. Altered pre-translational, translational and post-translational events are all involved in the molecular regulation of skeletal muscle phenotype. In the plastic process, hybrid fibers represent the ability of adult muscle fibers to shift from a fast to a slow phenotype and vice

versa. Genes coding for myosin heavy chains are activated and inactivated following the sequence I↔IIA↔IIX↔(IIB), according with the stress imposed to the muscle.

Signaling Pathways that control Skeletal Muscle Mass

Skeletal muscle is a highly adaptive tissue, capable of altering muscle fiber size, functional capacity and metabolism in response to physiological stimuli. However, pathological conditions compromise the mechanisms that regulate muscle homeostasis, resulting in loss of muscle mass, functional impairment and compromised metabolism. This condition is characterized by enhanced muscle protein breakdown and amino acids release that sustain liver gluconeogenesis and tissue protein synthesis. Proteolysis is controlled by the two most important cellular degradation systems, the ubiquitin proteasome and autophagy lysosome. These systems are carefully regulated by different signaling pathways that determine protein and organelle turnover. The decrease in cell size, named *atrophy*, involves the net loss of proteins, organelles and cytoplasm. The amount of organelles and proteins in the cell depends from the balance between biogenesis/biosynthesis and removal/destruction. This equilibrium defines the organelle and protein turnover and greatly affects the size and performance of cells including skeletal muscles (Sandri, 2016).

Degradation Pathway

All intracellular proteins and many extracellular proteins are continually "turning over". Although the continual destruction of cell proteins might seem wasteful, this process serves several important homeostatic functions.
Cells contain multiple systems to carry out the degradation process: the Autophagy and the Ubiquitine Proteasome System (UPS).
Therefore, excessive breakdown of cell constituents is prevented: the rates of protein synthesis and degradation in each cell must be balanced precisely because even a small decrease in synthesis or a small acceleration of degradation, if sustained, can result in a marked loss of mass in the organism (Mitch and Goldberg, 1996).

Autophagy-Lysosome System in Skeletal Muscle

The term 'autophagy', derived from the Greek meaning 'eating of self', was first coined by Christian de Duve over 40 years ago, and was largely based on the observed degradation of mitochondria and other intracellular structures within lysosomes of rat liver perfused with the pancreatic hormone, glucagon (Deter and De Duve, 1967).
Autophagy plays a crucial role in the turnover of cell components both in constitutive conditions and in response to various stimuli, such as cellular stress, nutrient deprivation, amino acid starvation and cytokines (Mizushima et al., 2008).

Three different mechanisms have been described in mammals for the delivery of the autophagic cargo to lysosomes: macroautophagy, chaperone-mediated autophagy (CMA) and microautophagy (Fig. 4). Thus far, most data on the role of the autophagic process in muscle are related to macroautophagy. Although it is still unknown whether microautophagy occurs in skeletal muscle, some findings indicate that microautophagy can participate in glycogen uptake into lysosomes when macroautophagy is blocked (Raben et al., 2008; Takikita et al., 2010). CMA has raised interest owing to its potential role in aging, neurodegenerative disorders and lysosomal storage diseases (Kon and Cuervo, 2010).
The involvement of Autophagy in muscle protein breakdown during atrophy was not recognized for a long time. Early evidence showed that lysosomal degradation contributes to protein breakdown in denervated muscle (Furuno et al., 1990; Schiaffino and Hanzlíková, 1972).

Moreover, cathepsin L, a lysosomal protease, was shown to be upregulated during muscle atrophy (Deval et al., 2001). The development of molecular and imaging tools to follow autophagosome formation has greatly improved the characterization of autophagy in normal and atrophying muscles (Klionsky et al., 2008).

Interestingly, fast glycolytic muscles display a higher content of autophagosomes than slow β-oxidative muscles (Mizushima et al., 2004).
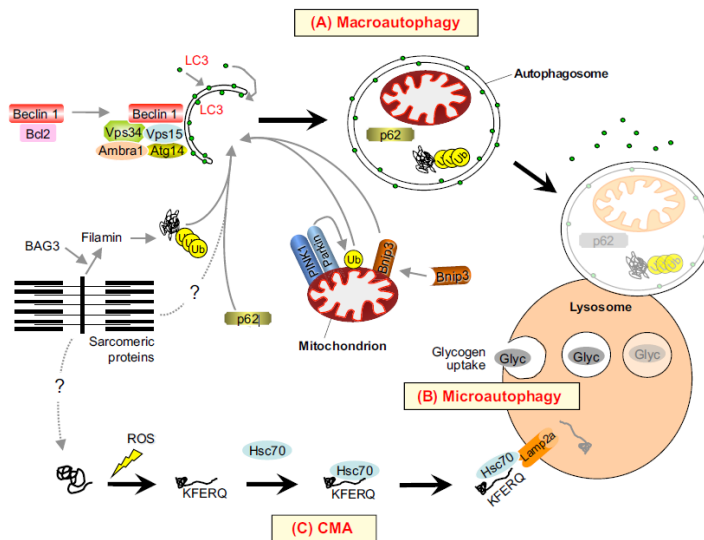
Fig. 4: Macroautophagy, microautophagy and chaperone-mediated autophagy (CMA), and their contribution to protein degradation and organelles removal in skeletal muscle. (A) Macroautophagy is triggered by the activation of a regulatory complex (containing Vps34, Beclin 1, Vps15, Ambra1 and Atg14) that induces LC3 recruitment to the nascent autophagosome (isolation membrane). Selective removal of mitochondria (mitophagy; a specific form of macroautophagy) requires the PINK1-parkin complex and Bnip3 factors. Proteins that are committed for lysosomal degradation (including BAG3 and filamin, shown here) are labeled by polyubiquitin chains and delivered to the autophagosome by the p62 scaffold protein. **(B)** Microautophagy involves the direct engulfment of small portions of cytoplasm into lysosomes. Glycogen (Glyc) is reportedly taken up and broken down by microautophagy in skeletal muscle. **(C)** In CMA, proteins that are damaged by different agents, such as reactive oxygen species (ROS), expose a specific amino acid sequence (the KFERQ motif) that is recognized by the Hsc70 chaperone, which in turn delivers them to the lysosome via interaction with Lamp2a receptors. Dotted lines depict pathways whose molecular mechanisms and roles in adult skeletal muscle have not yet been fully defined (image, Bonaldo and Sandri, 2013).

Macro- and micro-autophagy

This complex process is orchestrated at the molecular level. There are five key stages (Fig. 5): (a) phagophore formation or nucleation; (b) Atg5-Atg12 conjugation, interaction with Atg16L and multimerization at the phagophore; (c) LC3 processing and insertion into the extending phagophore membrane; (d) capture of random or selective targets for degradation; and (e) fusion of the autophagosome with the lysosome, followed by proteolytic degradation by lysosomal proteases of engulfed molecules. Each of this steps involves a number of conserved autophagy-related genes (Atg) that are transcriptionally regulated, reviewed in (Lapierre et al., 2015).

The autophagy process begins from the complex kinase ULK1 which consists of ULK1, Atg13, Atg17 and receives stress signals from mTOR complex 1, when the kinase activity of mTORC1 is inhibited, with the autophagosome formation (Klionsky, 2007; Simonsen and Tooze, 2009; Kundu and Thompson, 2005). This involves Vps34 that forms a complex with Atg6/Beclin 1. Additional regulatory proteins complex with Vps34 and Beclin-1 at the ER and nucleated phagophore to either promote autophagy, such as UVRAG, BIF-1, Atg14L and Ambra (Liang et al., 2006; Fimia et al., 2007), or to inhibit autophagy, such as Rubicon and Bcl-2 (Matsunaga et al., 2009; Pattingre et al., 2005). Current research suggests that phosphorylation of ULK1 Beclin-1 begins the activity of VPS34 complex containing Atg14L, thereby promoting autophagy. There are two ubiquitin-like systems that are key to autophagy (Mizushima, 2007; Kirkin et al., 2009) acting at the Atg5–Atg12 conjugation step and at the Atg8/LC3 processing step. LC3 of the system is important for the transport and the autophagosome maturation; once the autophagosome completes fusion of the expanding ends of the phagophore membrane, the next step towards maturation in this self-degradative process is fusion of the autophagosome with the specialized endosomal compartment that is the lysosome to form the 'autolysosome' (Mizushima, 2007). Within the lysosome, cathepsin proteases B and D are required for turnover of autophagosomes and, by inference, for the maturation of the autolysosome (Koike et al., 2005) to degrade the cargo (Fig. 5).
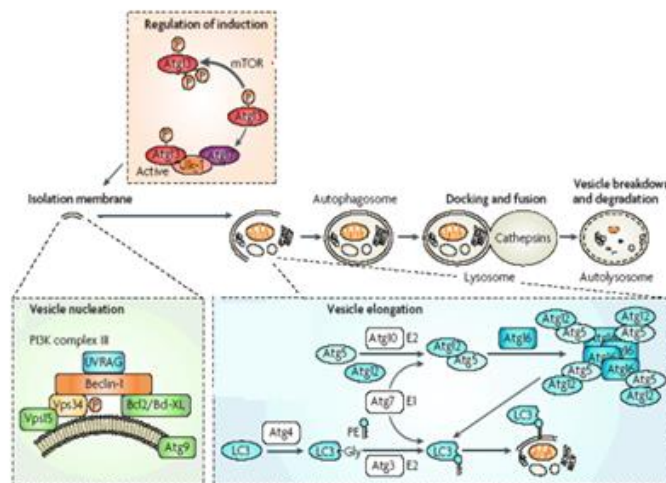
Fig. 5: Molecular circuitry and signaling pathways regulating autophagy. Autophagy is a complex self-degradative process that involves the following key steps: **regulation of induction** activation of Atg1/ULK-1 complexes; **vescicle nucleation** control of phagophore formation by Beclin-1/VPS34 at the ER and other membranes in response to stress signaling pathways; **vescicle elongation** Atg5–Atg12 conjugation, interaction with Atg16L, multimerization at the phagophore and LC3 processing and insertion into the extending phagophore membrane; capture of random or selective targets for degradation, completion of the autophagosome followed by; **docking and fusion** of the autophagosome with the lysosome and **vescicle breakdown and degradation** by lysosomal proteases of engulfed molecules. Autophagy is regulated by important signaling pathways in the cell, including stress-signaling kinases

such as JNK-1, which promotes autophagy by phosphorylating Bcl 2, thereby promoting the interaction of Beclin-1 with VPS34 (Wei et al., 2008). Perhaps the central signaling molecule in determining the levels of autophagy in cells is the mTOR kinase that likely mediates its effects on autophagy through inhibition of Atg1/ULK-1 complexes at the earliest stages in phagophore formation from lipid bilayers (Wei et al., 2008). mTOR is key to integrating metabolic, growth factor and energy signaling into levels of both autophagy, on the one hand, which is inhibited by mTOR when nutrients are plentiful and, on the other hand, to growth-promoting activities, including protein translation, that are stimulated by mTOR signaling (Díaz-Troya et al., 2008). Autophagy is induced by hypoxia and low cytosolic ATP levels that feed through REDD1 and AMP-kinase to inhibit mTOR activity through reduced Rheb GTPase activity. Conversely, autophagy is inhibited by increased growth factor signaling through the insulin receptor and its adaptor, IRS1, as well as other growth factor receptors that activate the Class I group of PI3-kinases and Akt, to promote mTOR activity through inhibition of TSC1/TSC2 and increased Rheb GTPase activity (Díaz-Troya et al., 2008; Sabatini, 2006) (modified image, Maiuri et al., 2007).

Atg5/Atg7-independent autophagy

Although Atg5- and Atg7-dependent autophagy has been shown to be critical for survival during the starvation period in the first few days immediately following birth (Johansen and Lamark, 2011; Kuma et al., 2004, Komatsu et al., 2005), recent evidence has identified an alternative Atg5/Atg7-independent pathway of autophagy (Nishida et al., 2009). This pathway of autophagy was not associated with LC3 processing but appeared to specifically involve autophagosome formation from late endosomes and the *trans*-Golgi (Nishida et al., 2009). Atg7-independent autophagy had been implicated in mitochondrial clearance from reticulocytes (Zhang et al., 2009), and it has consistently been shown that Ulk-1 (a mammalian homologue of Atg1) is required for both reticulocyte clearance of mitochondria (Kundu et al., 2008) and, along with Beclin-1, for Atg5/Atg7-independent autophagy (Nishida et al., 2009). The exact molecular basis of Atg5/Atg7-independent autophagy remains to be elucidated.

Selective autophagy via p62:

Mitophagy

Autophagy is primarily considered to be a non-selective degradation pathway, but the significance of more selective forms of autophagy is becoming increasingly evident. p62/SQSTM1 has been proposed to contribute to selective autophagy of protein aggregates (aggrephagy), depolarized mitochondria (mitophagy) (Fig. 6) and invasive microbes (xenophagy) through ubiquitin-signaling (Rogov et al., 2014; Johansen and Lamark, 2011). We now focus on the role of p62 in the selective autophagy of mitochondria. In mammals, parkin, PINK1, Bnip3 and Bnip3L have been shown to regulate mitophagy, and inactivation of the genes encoding these proteins leads to abnormal mitochondria (Bothe et al., 2000; Hara et al., 2006). PINK1 recruits parkin to mitochondria (Fig. 7), where parkin promotes mitophagy through ubiquitylation of outer mitochondrial membrane proteins that are recognized directly by p62, which brings autophagic vesicles to ubiquitylated mitochondrial proteins (Narendra and Youle, 2011; Youle and Narendra, 2011). Bnip3 and Bnip3L reportedly bind directly to LC3, and can therefore recruit the growing autophagosome to mitochondria (Hanna et al., 2012; Novak et al., 2010).

In atrophying muscle, the mitochondrial network is dramatically remodeled following fasting or denervation, and autophagy via Bnip3 contributes to mitochondrial remodeling (Romanello et al., 2010; Romanello and Sandri, 2010). Expression of the fission machinery is sufficient to cause muscle wasting in mice, whereas inhibition of mitochondrial fission prevents muscle loss during denervation, indicating that disruption of the mitochondrial network is a crucial amplificatory loop of the muscle atrophy program (Romanello et al., 2010; Romanello and Sandri, 2010). Conversely, impairment of basal mitophagy is deleterious to muscle homeostasis, and leads to the accumulation of damaged and dysfunctional mitochondria (Grumati et al., 2010). Besides mitophagy, other forms of selective autophagy probably play important roles in the maintenance of skeletal muscle homeostasis.
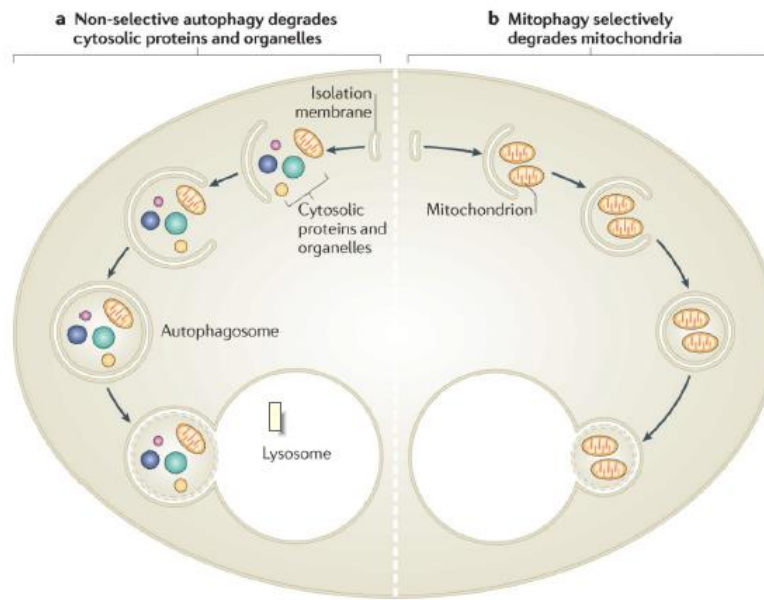
Fig. 6: Non-selective autophagy and mitophagy have different roles (**a**) Non-selective autophagy occurs when cells are deprived of nutrients. It degrades a range of cytosolic contents, including proteins and many types of organelles. After their recruitment into isolation membranes, cytosolic components are sealed into autophagosomes that fuse with lysosomes. The degradation of these components in the lysosome supplies building blocks for re-use and for metabolism to provide ATP. (**b**) By contrast, mitophagy occurs to eliminate mitochondria, either to regulate their number or to specifically remove ones that are damaged. Mitochondria are selectively recruited into isolation membranes, which seal and then fuse with lysosomes to eliminate the trapped mitochondria (image, Youle and Narendra, 2011).
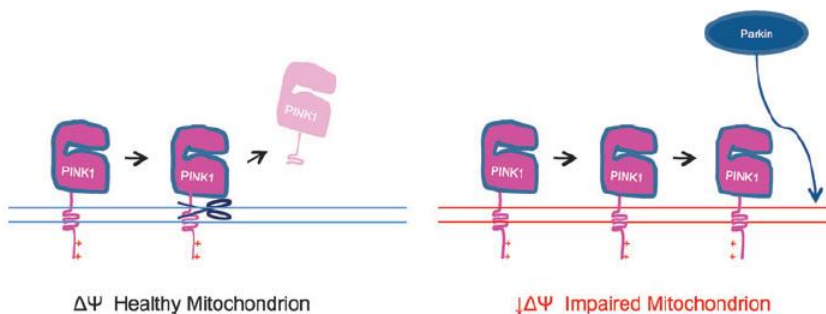
Fix. 7: Cartoon depicting regulation of PINK1 processing by voltage potential across the inner mitochondrial membrane. PTEN induced putative kinase 1 (PINK1) is proteolytically cleaved and degraded in healthy mitochondria but stabilized on mitochondria membrane with low inner membrane voltage (image, Narendra and Youle, 2011).

Ablation of autophagy

Although available data are still limited to a few components of the autophagic machinery, the phenotypes of mice with muscle-specific inactivation of genes encoding autophagy-related proteins clearly demonstrate the essential role of autophagy in muscle homeostasis (Table 1). Ablation of Atg7, the unique E1 enzyme of the autophagic machinery, causes disorganized sarcomeres and activation of the unfolded protein response, which in turn triggers myofiber degeneration; this phenotype is associated with complete inhibition of autophagosome formation, leading to abnormal mitochondria, oxidative stress, accumulation of polyubiquitylated proteins and age-dependent decrease in force (Masiero et al., 2009). These Atg7-null mice are affected by

15

muscle weakness and atrophy, and they display several signs of myopathy. Another study showed that suppression of autophagy exacerbates fasting- and denervation-induced atrophy in Atg7-null mice (Masiero and Sandri, 2010). A similar phenotype was observed in mice with muscle-specific ablation of Atg5, another crucial component of the autophagy machinery (Raben et al., 2008). Another recent study revealed that nutrient-deprivation autophagy factor-1 (Naf-1), a Bcl-2-associated autophagy regulator, is required for the homeostatic maintenance of skeletal muscle in mice. Naf1-null mice display muscle weakness and markedly decreased strength, accompanied by increased autophagy, dysregulation of calcium homeostasis and enlarged mitochondria (Chang et al., 2012).

Recent genetic studies by the group of Eric N. Olson, revealed a key role for histone deacetylases (HDACs) in the control of skeletal muscle homeostasis and autophagic flux (Moresi et al., 2012; Moresi et al., 2010) (see Table 1). Muscle-specific ablation of both HDAC1 and HDAC2 results in partial perinatal lethality, and HDAC1/2 double- knockout mice surviving postnatally develop a progressive myopathy characterized by impaired autophagy. HDAC1 and HDAC2 were found to regulate muscle autophagy by inducing the expression of autophagy genes.

The crucial role of the autophagy-lysosome system in skeletal muscles is confirmed by the fact that alterations of this process contribute to the pathogenesis of several genetic muscle diseases. Autophagy has a dual role in muscle homeostasis: it can be detrimental and contribute to muscle degeneration, but can also be a compensatory mechanism for cell survival.

Gene product	Mouse model	Phenotype	Reference
Autophagy-lysosome			
Atg5	Muscle-specific KO	Muscle weakness, atrophy, myopathic phenotype	Raben et al., 2008
Atg7	Muscle-specific KO, inducible muscle-specific KO	Muscle weakness, atrophy, myopathic phenotype, increased muscle loss during denervation and fasting	Masiero et al., 2009
NAF-1	KO	Increased autophagy, decreased muscle strength	Chang et al., 2012
Lamp2	KO	Accumulation of autophagic vesicles in many tissues, including skeletal muscles	Tanaka et al., 2000
Acetylating enzymes and myogenic regulatory factors			
HDAC1 + HDAC2	Muscle-specific double KO	Perinatal sublethality, progressive myopathy with autophagy blockade	Moresi et al., 2012
HDAC4	Muscle-specific KO	Protection from denervation-induced atrophy	Moresi et al., 2010
HDAC5	KO	Protection from denervation-induced atrophy	Moresi et al., 2010
HDAC4 + HDAC5	Muscle-specific double KO	Marked protection from denervation-induced atrophy	Moresi et al., 2010
Myogenin	Inducible KO	Protection from denervation-induced atrophy	Moresi et al., 2010

KO, knockout.

Table 1: Phenotype of transgenic and KO mice for genes involved in catabolic pathways of skeletal muscle (modified image, Bonaldo and Sandri, 2013)

Ubiquitine Proteasome System

In the ubiquitin-proteasome system, proteins are targeted for degradation by the 26S proteasome through covalent attachment of a chain of ubiquitin molecules. Different classes of enzymes, named E1, E2 and E3, are involved in protein ubiquitination. The E1 is the ubiquitin activating enzyme and is encoded by only one gene. The ubiquitin ligase enzyme, or E3, binds the protein substrate and catalyzes the movement of the ubiquitin from the E2 enzyme to the substrate. This is the rate-limiting step of the ubiquitination process, which affects the subsequent proteasome-dependent degradation. Once the protein is ubiquitinated it is docked to the proteasome for degradation, unless the polyubiquitin chain is removed by the de-ubiquitinating enzymes (Fig. 8). Different E2-E3 pairs function in the degradation of different proteins, and the specificity of the E3s for specific groups of proteins provides exquisite selectivity to this degradation process. The human genome contains around one hundred E2 and more than one thousand E3. This great heterogeneity is involved in the precise regulation of different cellular processes. The content of different E2s and E3s varies between tissues and with different physiological conditions, but it is still unknown which specific E2s and E3s normally work in muscle (Sandri, 2016).
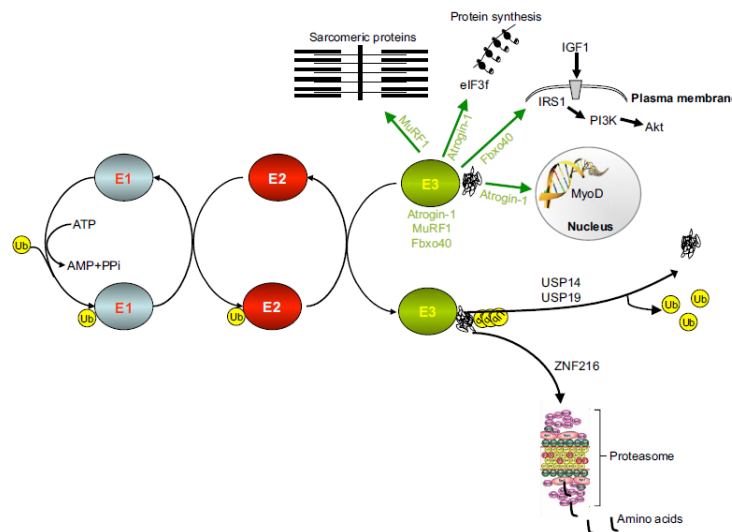
Fig. 8: Ubiquitin-proteasome systems in muscle homeostasis. E1 enzymes activate ubiquitin proteins after the cleavage of ATP. The ubiquitin is then moved from E1 to members of the E2 enzyme class. The final ubiquitylation reaction is catalyzed by members of the E3 enzyme class. E3 binds to E2 and the protein substrate, inducing the transfer of ubiquitin from E2 to the substrate. Once the substrate is polyubiquitylated, it is docked to the proteasome for degradation. Note that polyubiquitin chains can be removed by de-ubiquitylating enzymes (ubiquitin-specific processing proteases (USPs). The components of this system that contribute to muscle wasting are depicted. ZNF216 is involved in the recognition and delivery to the proteasome of ubiquitylated proteins during muscle atrophy. Atrogin-1 regulates the half-life of the MyoD transcription factor and of eIF3f, which is crucial for protein synthesis. Fbxo40 regulates the half-life of IRS1, an essential factor for IGF1/insulin signaling, whereas MuRF1 regulates the half-life of several sarcomeric proteins. E3 ubiquitin ligases are depicted in green, with arrows pointing to their substrates. Note that ubiquitin ligases can have different cellular localizations and can shuttle into the nucleus. IRS1, insulin receptor substrate 1; Ub, ubiquitin (image, Bonaldo and Sandri, 2013).

Atrogin-1/MAFbx and MuRF1 ubiquitin ligases

The first ubiquitin ligases that were identified to play a role in muscle loss were Atrogin-1/MAFbx and MuRF1. These two E3s are considered the master genes of muscle atrophy (Bodine et al., 2001; Lecker et al., 2004). Thus far, MuRF1 ubiquitinates several muscle structural proteins, including troponin I (Kedar et al., 2004), myosin heavy chains (Fielitz et al., 2007; Clarke et al., 2007), actin (Polge et al., 2011), myosin binding protein C and myosin light chains 1 and 2 (Cohen et al., 2009). In comparison, Atrogin-1 substrates seem to be involved in growth-related processes

or survival pathways. Atrogin-1 promotes degradation of MyoD, a key muscle transcription factor, and eIF3-f, an important activator of protein synthesis (Csibi et al., 2010; Tintignac et al., 2005). In recent work, Atrogin-1 was found to interact with sarcomeric proteins, including myosins, desmin and vimentin, as well as, transcription factors components of the translational machinery, enzymes involved in glycolysis and gluconeogenesis and mitochondrial proteins (Lokireddy et al., 2012). Whether these interactions result in ubiquitination of these protein substrates has yet to be proven. In the heart, Atrogin-1 ubiquitinates and reduces the levels of calcineurin A, an important factor triggering cardiac hypertrophy in response to pressure overload (Li et al., 2004). By using an in vivo Pulsed Stable Isotope Labeling of Amino aCids (SILAC) approach in heart, it was recently found that Atrogin1 regulates the half-life of CHMP2B, an ESCRT family member that plays an important role in autophagosome-lysosome fusion (Zaglia et al., 2014). Interestingly, although Atrogin1 is described as a muscle specific ubiquitin ligase, it was found to be modulated in many cancer cells (Wu et al., 2011; Lei et al., 2011; Chou et al., 2010; Frolov et al., 2003) and recently, cMyc was reported as an Atrogin-1 substrate (Mei et al., 2015) therefore, suggesting that this ligase might play a role in tumorigenesis.

It is important to highlight the involvement of these E3 ligases in different catabolic conditions of muscle loss. Mice with MuRF1 knockout are not protected from denervation-induced muscle loss at 7 days and only partially protected (around 30%) at 14 days (Bodine et al., 2001). Moreover, the absence of MuRF1 does not protect from fasting induced atrophy, while muscle mass is spared following glucocorticoid treatment (Baehr et al., 2011). Finally, MuRF1 inhibition prevents age related muscle loss (Hwee et al., 2014; Sandri et al., 2013) but this protection is not functional since aged MuRF1 knockout mice are weaker than age-matched controls (Sandri et al., 2013). Inhibition of Atrogin-1 does not block denervation-and glucocorticoids-induced muscle loss (Baehr et al., 2011; Gomes et al., 2012; Sartori et al., 2013) while muscle mass is only partially spared in fasted Atrogin-1 knockout animals (Cong et al., 2011). Importantly, mice Atrogin-1 knockout are not protected from ageing sarcopenia (Sandri et al., 2013) and die prematurely from a severe restrictive-like hypertrophic cardiomyopathy (Zaglia et al., 2014; Sandri et al., 2013).

Protein Synthesis Signaling Pathway

Skeletal muscle mass increases during postnatal development through a process of hypertrophy, i.e. enlargement of individual muscle fibers, and a similar process may be induced in adult skeletal muscle in response to contractile activity, such as strength exercise, and specific hormones, such as androgens and b-adrenergic agonists. Muscle hypertrophy occurs when the overall rates of protein synthesis exceed the rates of protein degradation. Two major signaling pathways control protein synthesis, the IGF1–Akt–mTOR pathway, acting as a positive regulator, and the myostatin–Smad2/3 pathway, acting as a negative regulator, and additional pathways have recently been identified (Schiaffino et al., 2013) (Fig. 9).

IGF1/Akt/mTOR Signaling Pathway

The insulin-like growth factor 1–phosphoinositide-3-kinase–Akt/protein kinase B–mammalian target of rapamycin (IGF1–PI3K–Akt/PKB–mTOR) pathway acts as a positive regulator of muscle growth. In fact, muscle-specific inactivation of the IGF1 receptor impairs muscle growth due to reduced muscle fiber number and size (Mavalli et al., 2010). Conversely, muscle-specific over-expression of IGF1 causes muscle hypertrophy (Musarò et al., 2001).

Akt stimulates protein synthesis by activating mTOR and its downstream effectors. The kinase mTOR interacts with several proteins to form two complexes: mTOR complex 1 (mTORC1) containing raptor and mTOR complex 2 (mTORC2) containing rictor (Laplante and Sabatini, 2012).

It should be stressed that mTOR responds to multiple upstream signals in addition to Akt, including amino acids, and it controls several cellular processes in addition to protein synthesis, including autophagy. The crucial role of mTOR in mediating muscle growth is supported by genetic and pharmacological evidence. Muscle-specific mTOR knockout causes reduced postnatal growth, due to the reduced size of fast but not slow muscle fibers, and severe myopathy (Risson et al., 2009). A similar phenotype is found in mice lacking raptor in skeletal muscle, whereas those lacking rictor have a normal phenotype, supporting a major role of mTORC1 in mediating the effect of mTOR on protein synthesis (Bentzinger et al., 2008). Rapamycin, a specific mTOR inhibitor, acts especially on mTORC1, although mTORC2 is also affected during chronic treatment (Laplante and Sabatini, 2012). Muscle fiber hypertrophy induced by transfection of adult muscles with a constitutively active Akt construct is also blunted by rapamycin (Bodine et al., 2001b; Pallafacchina et al., 2002).

Two major effectors of mTORC1 that promote protein synthesis are eukaryotic translation initiation factor 4E-binding protein 1 (4E-BP1) and S6 kinase 1. Muscle growth is apparently unaffected by 4E-BP1 knockout (Le Bacquer et al., 2007). In contrast, deletion of S6 kinase 1 causes muscle atrophy and partially prevents the response to constitutively active Akt (Mounier et al., 2011). However, the control of protein synthesis by mTOR is still incompletely characterized (Laplante and Sabatini, 2012). The growth-promoting effect of mTORC1 is repressed by AMP-activated protein kinase (AMPK), and hypertrophy of soleus muscle has been described in AMPK-deficient mice (Mounier et al., 2011). Another aspect of mTOR function that is incompletely understood is the role of mTOR in transcriptional regulation. In both yeast and mammalian cells, TOR/mTOR controls cell growth by coordinately regulating the synthesis of ribosomes and tRNAs and activating transcription by all three nuclear RNA polymerases (I, II and III). However, ribosomal RNA accumulation induced in overloaded muscles after synergist ablation is only partially inhibited by rapamycin (Goodman et al., 2011). On the other hand, blockade of mTOR by rapamycin in cultured myotubes is sufficient to block most IGF1-induced changes in transcription (Latres et al., 2005).

Myostatin-Smad3 Pathway

The second major signaling pathway that regulates muscle growth involves the myostatin, acting as a negative regulator (Lee, 2004). Myostatin inhibits protein synthesis and reduces myotube size when added to differentiated myotubes in culture (Taylor et al., 2001). Furthermore, muscle atrophy is induced in mice by systemically administered myostatin (Lee, 2004). Muscle hypertrophy may also be induced by inhibitory extracellular binding proteins, such as follistatin, whose effect is even greater than the lack of myostatin, because it binds to other TGFb superfamily members, such as activin A, that act as negative regulators of muscle growth like myostatin does (Fig. 9).

Myostatin and activin A interact and activate a heterodimeric receptor complex with serine–threonine kinase activity, comprising a type II receptor, activin receptor 2 (ACVR2 and ACVR2B), and a type I receptor, acting receptor-like kinase 4 and 5 (ALK4 and ALK5). Myostatin/activin A signaling in myofibers is mediated by phosphorylation and nuclear translocation of Smad2 or Smad3 transcription factors, and formation of heterodimers with Smad4. Although the transcriptional targets of the Smad2/Smad4 and Smad3/Smad4 complexes that mediate the inhibitory effect on growth are not known, it is possible that myostatin/activin A signaling interferes with the Akt–mTOR pathway (Sartori et al., 2009; Trendelenburg et al., 2009).

Inhibition of Smad3 activity by follistatin is critical for activation of Akt–mTOR signaling, as constitutively active Smad3 was found to suppress follistatin-induced muscle growth and mTOR activation. It is also possible that a direct interaction between Smad3 and Akt, as demonstrated in other cell systems (Remy et al., 2004; Conery et al., 2004), may be involved in crosstalk between the myostatin/activin A and IGF1 pathways in skeletal muscle.
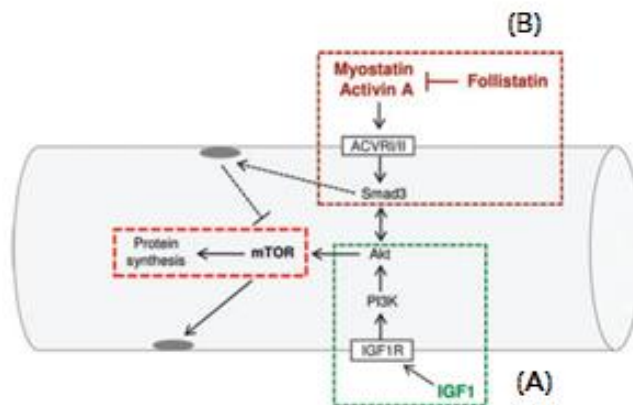
Fig. 9: Signaling modules responsible for skeletal muscle growth. All these modules converge to final common pathway centered on mTOR and its effectors that control protein synthesis. Major signaling pathways. **(A)** IGF1 stimulates mTOR activity and muscle growth via PI3K–Akt. **(B)** Follistatin induces muscle growth by inhibiting myostatin and activin A.
The two pathways cross-talk by direct interaction between Smad3 and Akt. In addition, transcriptional regulation by Smad3/Smad4 heterodimers may repress mTOR and protein synthesis through mechanisms that have not yet been defined. The arrow connecting mTOR with a myonucleus indicates transcriptional roles of mTOR (image, Schiaffino et al., 2013).

Protein synthesis and protein degradation: hypertrophy *vs* atrophy

The changes in protein turnover, leading to muscle hypertrophy or atrophy, do not always proceed according to the simplistic equations suggested by the 'balance' analogy, i.e. muscle hypertrophy results from increased protein synthesis and decreased protein degradation, while muscle atrophy results from decreased protein synthesis and increased protein degradation. Goldberg's analyses on muscle growth showed that, during soleus hypertrophy induced by gastrocnemius tenotomy, decreased protein catabolism as well as increased synthesis of new proteins occurs. Interestingly, during soleus hypertrophy induced by growth hormone, it was observed an increase of protein synthesis without any change in protein degradation rates (Goldberg, 1969). Starvation causes decreased protein synthesis and increased protein degradation in both fast and slow rat muscles (Li and Goldberg, 1976). However, muscle denervation is accompanied by increased protein degradation and increased rather than decreased protein synthesis (Argadine et al., 2009; Quy et al., 2013). One must also consider that fast and slow muscles differ in their protein turnover rates, with slow muscles showing higher rates of both protein synthesis and degradation (Goldberg, 1969).

Cross-talk between MPB and MPS: FoxO family transcription factors

Akt controls both protein synthesis, via mTOR, and protein degradation, via transcription factors of the FoxO family (Fig. 10).
The upregulation of atrogin-1, MuRF1 and several autophagy-related genes is normally blocked by Akt through negative regulation of FoxO transcription factors (Lee et al., 2004; Sandri et al., 2004; Stitt et al., 2004). The FoxO family in skeletal muscle is comprised of three isoforms: FoxO1, FoxO3 and FoxO4. Akt phosphorylates FoxO proteins, promoting their export from the nucleus to the cytoplasm. As predicted, the reduced activity of the Akt pathway observed in different models of muscle atrophy results in decreased levels of phosphorylated FoxO in the cytoplasm and a marked increase of nuclear FoxO (reviewed in Calnan and Brunet, 2008) (Fig. 10). The translocation and activity of FoxO members is required for the upregulation of atrogin-1 and MuRF1, and FoxO3 is sufficient to promote atrogin-1 expression and muscle atrophy when transfected into skeletal muscles in vivo (Sandri et al., 2004). FoxO1 transgenic mice show markedly reduced muscle mass and fiber atrophy, further supporting the notion that FoxO proteins are sufficient to promote muscle loss (Kamei et al., 2004; Southgate et al., 2007). In contrast, FoxO knockdown by RNAi can block the upregulation of atrogin-1 expression during atrophy and muscle loss (Liu et al., 2007; Sandri et al., 2004).

Crosstalk between protein breakdown and protein synthesis is not limited to Akt, but also involves FoxO. Activation of FoxO in *Drosophila* muscle upregulates 4E-BP1 (Demontis and Perrimon, 2010) and represses mTOR via sestrin (Lee et al., 2010). Consistently, in mammals, FoxO3 reduces total protein synthesis in adult muscle (Reed et al., 2012). Thus, when Akt is active, protein breakdown is suppressed, and when FoxO is induced, protein synthesis is further suppressed. This is not trivial, because FoxO activity is regulated by several different post-translational modifications, including phosphorylation, acetylation, and mono- and polyubiquitylation (Huang and Tindall, 2007).

Other findings have revealed a connection between AMPK and FoxO3 (Fig. 10). AMPK phosphorylates several Akt-independent sites on FoxO3, thereby stimulating its transcriptional activity (Greer et al., 2007a; Greer et al., 2007b). Indeed, treatment of muscle cultures with AICAR, an activator of AMPK, increases protein breakdown and atrogin-1 expression via the FoxO family (Nakashima and Yakabe, 2007). In conditions of energy stress FoxO3 is activated via AMPK in myofibers inducing the expression of atrogin-1 and MuRF1 (Romanello et al., 2010). Activation of AMPK also leads to induction of some autophagy-related genes, such as those coding for LC3 and Bnip3.

FoxO activity is also modulated by direct or indirect actions of cofactors and other transcription factors. FoxO has been found to interact with PGC1α, a critical cofactor for mitochondrial biogenesis (Puigserver et al., 2003; Wu et al., 1999) (Fig. 10). Maintaining high levels of PGC1α during catabolic conditions (either in transgenic mice or by transfecting adult myofibers) muscle mass is preserved (Geng et al., 2011; Sandri et al., 2006; Cannavino et al 2014; Cannavino et al 2015; Wenz et al., 2009). Similar beneficial effects were recently obtained by overexpression of PGC1β, a homolog of PGC1α (Brault et al., 2010). The positive action on muscle mass of these cofactors is due to the inhibition of autophagy-lysosome and ubiquitin-proteasome degradation systems. PGC1α and PGC1β reduce protein breakdown by inhibiting the transcriptional activity of FoxO3, but they do not affect protein synthesis. Thus, these cofactors prevent the excessive activation of proteolytic systems by inhibiting the action of the pro-atrophy transcription factors without perturbing the translational machinery.

It was recently reported that the transcription factor JunB blocks atrophy and promotes hypertrophy in adult mouse muscles (Raffaello et al., 2010). Indeed, JunB can block myofiber atrophy of denervated tibialis anterior muscles and cultured myotubes induced by FoxO3 overexpression, dexamethasone treatment or starvation. In these conditions, JunB prevents the activation of atrogin-1 and partially that of MuRF1, thereby reducing the increase in overall protein degradation induced by activated FoxO3. Further analysis revealed that JunB does not inhibit FoxO3-mediated activation of the autophagy-lysosom system, but only the ubiquitin-proteasome degradation, through inhibiting atrogin-1 and MuRF1 induction during catabolic conditions. In fact, JunB directly binds FoxO3, thereby preventing its recruitment to the promoters of key atrogenes. Moreover, JunB overexpression is sufficient to induce dramatic hypertrophy of myotubes and of adult muscle. These hypertrophic changes depend on increased protein synthesis, without affecting the basal rate of protein degradation (Sartori et al., 2009; Trendelenburg et al., 2009). Indeed, JunB overexpression markedly suppresses myostatin expression in transfected myotubes and decreases the phosphorylation of Smad3, the transcription factor downstream of the myostatin-TGFβ signaling pathway (Raffaello et al., 2010).
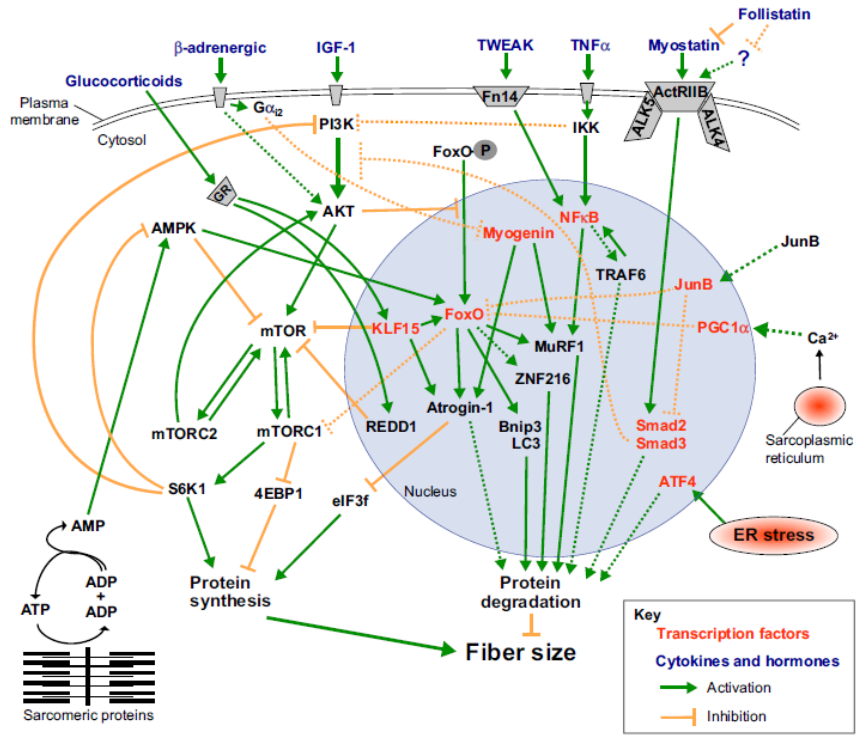
Fig. 10. Major pathways that control muscle fiber size. Protein synthesis and degradation are regulated by several different stimuli, which activate multiple signaling pathways, many of which converge at common intermediates and/or crosstalk with one another. Many of the components shown here could be promising therapeutic targets. See the main text for further details. Dotted lines depict pathways whose molecular mechanisms and role in adult skeletal muscle have yet to be completely defined. GR, glucocorticoid receptor (image, Bonaldo and Sandri, 2013).

Muscle Metabolism

The energy needed for all basic cellular functions, including muscle contraction, is supplied by the hydrolysis of ATP, with ADP and P_i release.

Very little ATP is stored in muscle fibers, only enough to power muscle contraction for a few seconds. The ATP in muscle must be constantly replenished as it is used for various process. ATP is replenished within muscle fibers in three ways: (i) from creatine phosphate (CP), (ii) by glycolysis (anaerobic) and (iii) by cellular respiration (aerobic mitochondrial respiration). The powerhouse of energy production and metabolism are the mitochondria.

Supply of ATP for muscle contraction:
Creatine phosphatase

A rapid turnover of ATP is maintained without the use of oxygen trough Creatin phosphate (CP), an hight energy phosphate compound. Energy is released with the breakdown of CP, for the immediate synthesis of ATP (ADP + CP $\leftrightarrow$ ATP + C + Energy). Different creatin phosphokinase (CPK) isoenzymes catalyze the generation of CP from ATP at the mitochondrial site (CPK-MB and CPK-mi) and generation of ATP from CP at the myofibrillar location (CPK-MM). In human muscles at rest, CP content is slightly higher in fast than slow fibers (Sant'Ana Pereira et al., 1996; Sahlin et al., 1997); moreover the total activity of CPK is equal in fast and slow fibers (Apple and Tesch, 1989) or slightly higher in fast fibers (Yamashita and Yoshioka, 1992) but the greater CP content and the higher activity of CPK-MM suggest that ATP regeneration from CP is likely more effective in fast than in slow fibers.

Supply of ATP for muscle contraction:
Glycolysis

Anaerobic glycolysis is the catabolic pathway from glucose to pyruvate associated with the regeneration of 2-3 mol ATP/mol glucose. In skeletal muscle, glycolysis permits high performance when aerobic metabolism alone is not sufficient. In skeletal muscle at rest, glycolysis provides nearly half of the acetyl-CoA used in Citric acid cycle. In human muscles, a pronounced difference in glycogenolysis rate has been reported between slow and fast fibers during maximal contractions (Vøllestad et al., 1992; Greenhaff et al., 1993). The differential expression of glycolytic genes in fast and slow muscles has been confirmed by PCR and microarray studies in both mouse and human (Plomgaard et al., 2006; Chemello et al., 2011).
The pyruvate produced can be either (i) converted to lactate by lactate deidrogenase enzymes and exported or (ii) decarboxylated to acetyl-CoA and enter in the tricarboxylic acid cycle (TCA). As mention above the end product of glycolysis, pyruvate, can enter the tricarboxylic acid via the pyruvate dehydrogenase (PDH) complex, which in skeletal muscle controls the glucose oxidation pathway by catalyzing the irreversible decarboxylation of pyruvate to acetyl coenzyme A. PDH is negatively regulated by phosphorylation mediated by pyruvate dehydrogenase kinases (PDK1 to -4). Thanks to its inhibitory control on PDH, PDK acts as switch of fuel oxidation from carbohydrate to fat. PDK activity is less active in glycolytic than in oxidative muscles (Peters et al., 2001) PDH activity is enhanced by a pyruvate dehydrogenase phosphatase (PDP), which is also more abundant and more active in slow oxidative fibers (Leblanc et al., 2007). In summary

ATP regeneration through the glycolytic pathway is more effective in fast than in slow fibers as the glycolytic activity is about two times higher in fast fibers, moreover in both fiber types this is not sufficient to cope with maximal ATP consumption, thus setting a limit to the use of this source for contractile activity and leads pyruvate having two different fates: lactate or acetyl CoA. The presence of different LDH isoforms and PDH regulation via kinase (PDK) and phosphatase (PDP) control the switch between the two alternative pathways. The balance between the two alternatives is shifted towards acetyl CoA in slow fibers and towards conversion to lactate in fast fibers.

Supply of ATP for muscle contraction: aerobic cellular respiration

Aerobic energy metabolism takes place in mitochondria, and it results in the greatest release of energy; thus as the name implies it requires oxygen.

ATP resynthesis via mitochondrial oxidative phosphorylation utilizes acetyl-CoA derived either from pyruvate generated by the activity of PDH or from fatty acids (FA) via-oxidation and can provide 18 ATP per acetate.

In mitochondria of muscle cells, hydrogen atoms are extracted from the reducing equivalents that are formed during the citric acid cycle, in a process called oxidative phosphorylation. Consequently, special electron transport proteins extract the hydrogen atoms and transfer them finally to molecular oxygen. The energy released during the transfer of electrons to oxygen is conserved as ATP.

Oxidative Metabolism in muscle fiber

ATP regeneration based on TCA cycle is more effective in slow than in fast fibers due mainly to differences in (i) substrate availability (ii) mitochondrial structure and (iii) oxidative enzyme content and activity.

(i) *Substrate availability* Acetyl-CoA is provided by two sources: from (a) Fatty Acids (FA) via activation to acyl-CoA, transfer into the mitochondria and via carnitine-acyl- transferase and degradation to acetyl- CoA via β-oxidation, and (b) from pyruvate, derived from glycolysis via PDH. The contribution of FA from β-oxidation to the TCA cycle is higher in slow than fast fibers. In fact, type 1 fibers have greater availability and higher utilization of free fatty acids than type 2 fibers. The mitochondrial carnitine shuttle trough Carnitine palmitoyltransferase I (CPT I), and carnitine palmitoyltransferase II (CPT II) has an obligatory role in β-oxidation by permitting acyl-CoA translocation from the cytosol; in slow fibers CPT I is more active (Kim et al., 2002). Finally, the activity of 3-hydroxy-acyl-CoA dehydrogenase (HAD), a key enzyme of β-oxidation, is higher in slow than in fast fibers.

(ii) *Mitochondrial structure* Mitochondrial content varies significantly in relation to fiber type. In human fibers, the mitochondrial volume varies from 6% in type 1 fibers to 4.5% in type 2A fibers and 2.3% in type 2X fibers (Hoppeler et al., 1985). In the rat, the fraction volume occupied by mitochondria ranges from 2.2% in fast glycolytic fibers of gastrocnemius to 10% in slow oxidative fibers of soleus (Ogata and Yamasaki, 1997).

Beside their density, mitochondria of slow and fast fibers also differ in their ultrastructure; thus slow fiber mitochondria exhibit more densely packed crista (Jackman and Willis, 1996).

(iii) *Oxidative enzyme content and activity* Using isolated mitochondrial preparations it has been shown that citric acid cycle enzyme activities are approximately twice higher and electron

transport chain (ETC) exhibits twice the capacity for coenzyme oxidation in mitochondria from slow muscles compared with those from fast muscles of the rabbit (Jackman and Willis, 1996). Mitochondrial generation of hydrogen peroxide is two- to three-fold higher in white fast glycolytic muscles than in slow oxidative soleus of the rat (Anderson and Neufer, 2006).

Therefore, ATP regeneration based on TCA cycle is more effective in slow than in fast fibers due to the greater mitochondrial density and greater TCA cycle fuelling based on β-oxidation, which is about three times higher in slow than in fast fibers. Diversity is also present in the regulation of mitochondrial activity between slow and fast fibers, with different effects of the stimulation due to ADP, more effective in fast fibers, and the stimulation due to creatine, more effective in slow fibers. Importantly, once mitochondrial respiration and ATP regeneration are activated, in slow fibers a complete energy balance can be achieved, i.e., consumption is covered by regeneration, also in view of the relatively low ATP consumption. Such condition of balance is never achieved in fast fibers.

Redox homeostasis in skeletal muscle

Oxygen free radicals or, more generally, reactive oxygen species (ROS), as well as reactive nitrogen species (RNS), are products of normal cellular metabolism. ROS and RNS are well recognized for playing a dual role as both deleterious and beneficial species, since they can be either harmful or beneficial to living systems (Valko et al., 2007). Beneficial effects of ROS occur at low/moderate concentrations and involve physiological roles in cellular responses, as for example in defense against infectious agents and in the function of a number of cellular signalling systems. One further beneficial example of ROS at low/moderate concentrations is the induction of a mitogenic response. The harmful effect of free radicals causing potential biological damage is termed oxidative stress and nitrosative stress (Kovacic and Jacintho, 2001; Valko et al., 2001; Ridnour et al., 2005; Valko et al., 2006). The latter occur in biological systems when there is an overproduction of ROS/RNS and/or a deficiency of enzymatic and non-enzymatic antioxidants. Oxidative stress results from the metabolic reactions that use oxygen and represents a disturbance in the equilibrium status of pro-oxidant/antioxidant reactions in living organisms. The excess ROS can damage cellular lipids, proteins, or DNA inhibiting their normal function. Because of this, oxidative stress has been implicated in a number of human diseases as well as in the ageing process. The delicate balance between beneficial and harmful effects of free radicals is a very important aspect of living organisms and is achieved by mechanisms called "redox regulation".

Reactive oxygen species (ROS)

Free radicals can be defined as molecules or molecular fragments containing one or more unpaired electrons in atomic or molecular orbitals (Gutteridge and Mitchell, 1999; Halliwell, 2007). Free radicals can be generated as products of homolytic, heterolytic, or redox reactions, producing either charged or uncharged radical species. Note that reactive oxygen species (ROS) is a general term that refers not only to oxygen-centered radicals, but also includes non radical reactive derivatives of oxygen (e.g., hydrogen peroxide) (Halliwell, 2007). Similarly, the term reactive nitrogen species (RNS) refers to both nitrogen radicals along with other reactive molecules in which the reactive center is nitrogen. Radicals derived from oxygen represent the most important class of radical species generated in living systems.

Superoxide anion radical ($O_2^{\bullet-}$)
Molecular oxygen (dioxygen) has a unique electronic configuration and is itself a radical. The addition of one electron to dioxygen forms the superoxide anion radical ($O_2^{\bullet-}$) (Miller et al., 1990). This anion is negatively charged and is relatively membrane impermeable. Nonetheless, compared with other free radicals, superoxide has a relatively long half-life that enables diffusion within the cell. It is considered the "primary" ROS, and can further interact with other molecules to generate "secondary" ROS, either directly or prevalently through enzyme- or metal-catalyzed processes (Valko et al., 2005). It can react rapidly with some radicals such as NO and with some iron-sulfur clusters in proteins (Valko et al., 2007). The production of superoxide mostly occurs within mitochondria (Cadenas and Sies, 1998). Direct production of superoxide also occurs in some specific enzymatic reactions such as those catalyzed by xanthine oxidase, NAD(P)H oxidase enzymes and phospholipase (PL) A2-dependent.
The dismutation of superoxide anion to oxygen and hydrogen peroxide, catalyzed by the enzyme superoxide dismutase (SOD), represents the largest source of the dangerous hydrogen peroxide in the cell (Liochev and Fridovich, 2002). Importantly, the toxic action of superoxide depends largely on the interaction with hydrogen peroxide, ($O_2^{\bullet-} + H_2O_2 \rightarrow O_2 + {}^{\bullet}OH + OH^-$; Haber–

Weiss reaction) which causes the formation of the radical hydroxyl (OH •), an extremely reactive species.

Hydrogen peroxide (H_2O_2)

Hydrogen peroxide is stable, permeable to membranes, and has a relatively long half-life within the cell. In addition to dismutation of superoxide anion, hydrogen peroxide can be formed even for direct production in some enzymatic reactions at the level of microsomes, peroxisomes and mitochondria. It is cytotoxic although it is considered a weak oxidizing agent. The toxicity resides in the fact that it is in capable of giving rise to the hydroxyl radical through reactions catalyzed by metal ions ($H_2O_2 + Fe^{2+} \rightarrow •OH + OH^- + Fe^{3+}$ Fenton reaction) (Bergendi et al., 1999; Valko et al., 2005; Valko et al., 2007). For these chemical reasons the redox state of the cell is largely linked to an iron (and copper) redox couple and is maintained within strict physiological limits.

Mechanisms of maintenance of "redox homeostasis"

Free radicals and reactive species operate at low, but measurable concentrations in the cells. Their "steady state" concentrations are determined by the balance between their rates of production and their rates of removal by various antioxidant systems. To maintain redox homeostasis, muscle fibers contain a network of antioxidant defense mechanisms to reduce the risk of oxidative damage during periods of increased ROS production. The term antioxidant has been defined in many ways, but in the context of our discussion, antioxidants will be broadly defined as any substance that delays or prevents the oxidation of a substrate.

Enzymatyc Antioxidant

The main antioxidant enzymes include superoxide dismutase, glutathione peroxidase, and catalase (Tab. 2). Additional antioxidant enzymes such as peroxiredoxin, glutaredoxin, and thioredoxin reductase also contribute to cellular protection against oxidation.

Superoxide dismutase (SOD)

Superoxide dismutase (SOD) was discovered in 1969 by McCord and Fridovich (McCord and Fridovich, 1969) and forms the first line of defense against superoxide radicals as SOD dismutates superoxide to form hydrogen peroxide (H_2O_2) and oxygen (O_2) (Fig. 11). In mammals, three isoforms of SOD (SOD1, SOD2, SOD3) exist, and all require a redox active transition metal in the active site to accomplish the catalytic breakdown of the superoxide anion (Culotta et al., 2006). SOD1 is primarily located in the cytosol and the mitochondrial intermembrane space. SOD2 is located in the mitochondrial matrix. Finally, SOD3 is located in the extracellular space. In skeletal muscle, 15–35% of the total SOD activity is in the mitochondria, and the remaining 65–85% is in the cytosol (Powers et al., 1994). In rat skeletal muscle, SOD activity is highest in oxidative muscles that contain a high percentage of type I and type IIa fibers compared with muscles with low mitochondrial volumes (i.e., type IIx or IIb fibers) (Criswell et al., 1993).

Glutathione peroxidase (GPX)

Analysis of the selenoproteome has identified five glutathione peroxidases in mammals (Brigelius-Flohe, 2006; Drevet, 2006). All of these GPX enzymes catalyze the reduction of H_2O_2 or organic hydroperoxide (ROOH) to water (H_2O) and alcohol, respectively, using reduced glutathione (GSH) or in some cases thioredoxin or glutaredoxin as the electron donor (Bjornstedt et al., 1994; Bjornstedt et al., 1997; Holmgren et al., 2005) (Fig. 11). When GSH is the electron donor, it donates a pair of hydrogen ions and GSH is oxidized to glutathione disulfide (GSSG) (Fig. 11). Cells must possess a pathway capable of regenerating GSH. The reduction of GSSG back to GSH is accomplished by glutathione reductase, a flavin containing enzyme whereby NADPH provides the reducing power. Many tissues produce NADPH by glucose-6-phosphate dehydrogenase via the pentose pathway, but skeletal muscles produce NADPH primarily via isocitrate dehydrogenase (Lawler et al., 1993; Lawler and Demaree, 2001). Although the reaction catalyzed by all GPXs appears to be the same, individual GPXs differ in substrate specificity (i.e., varying range of hydroperoxides) and cellular localization (i.e., cytosol vs. mitochondria) (Brigelius-Flohe, 1999). The varying substrate specificity and cellular location across GPX isoforms appears to optimize GPX's function as a cellular antioxidant enzyme. Indeed, the fact that many GPX isoenzymes will reduce a wide range of hydroperoxides ranging from H2O2 to complex organic hydroperoxides makes GPX an important intracellular antioxidant to protect against ROS-mediated damage to membrane lipids, proteins, and nuclei acids.

Identical to SOD, the relative amount of GPX present in skeletal muscle fibers differs across fiber types: highly oxidative fibers (i.e., type I) exhibit the highest GPX activity, whereas rodent muscle fibers with low oxidative capacity (i.e., type IIB) exhibit the lowest levels of GPX (Lawler et al., 1993).

Catalase (Cat)
Catalase (Cat) serves several biochemical functions, but the principal purpose of CAT is to catalyze the break-down of H_2O_2 into H_2O and O_2 (Fig. 11). Although Cat and GPX share common substrates, Cat has a much lower affinity for H_2O_2 at low concentrations compared with GPX.

Cat protein levels are highest in highly oxidative muscle fibers and lowest in fibers with low oxidative capacity (Laughlin et al., 1990; Leeuwenburgh et al., 1994; Pereira et al., 1994; Powers et al., 1994).

The thioredoxin (TRX)
The thioredoxin (TRX) antioxidant system is composed of thioredoxin (TRX) and thioredoxin reductase (TRXR) (Fig. 11) (Arnér and Holmgren, 2000; Holmgren et al., 2005; Yoshioka et al., 2006; Berndt et al., 2007). The mammalian TRX is a highly conserved 12-kDa protein and cells contain two TRX systems, the cytosolic (TRX1) and the mitochondrial (TRX2) (Berndt et al., 2007). Functionally, TRX is the major ubiquitous disulfide reductase responsible for maintaining proteins in their reduced state (Arner & Holmgren, 2000). Oxidized TRX is then reduced by electrons from NADPH via thioredoxin reductase (Holmgren, 1985) (Fig. 11). Along with the prevention of protein oxidation, numerous other physiological functions of TRX have been described including reduction of transcription factors, protection against oxidative stress, and control of apoptosis (Arnér and Holmgren, 2000). Moreover, thioredoxin reductase also contributes as an antioxidant enzyme by reducing hydroperoxides and functioning as a NADPH-dependent dehydroascorbate reductase to recycle vitamin C (Arnér and Holmgren, 2000).

Peroxiredoxin (PRX)
Peroxiredoxin (PRX) was discovered in 1988 and is a novel peroxidase capable of reducing both hydroperoxides and peroxynitrate with the use of electrons provided by a physiological thiol like TRX (Kim et al., 1985; Rhee et al., 2005a) (Fig. 11). Mammalian cells express six isoforms of PRX (PRXI–VI) that are distributed differentially within the cell: PRXI, II, and VI are found in the cytosol; PRXIII is located in the mitochondrion; PRXIV is located in the extracellular space; and PRXV is located in both mitochondria and peroxisomes (Rhee et al., 2005a). Unfortunately, a kinetic analysis of PRX reaction rates at physiological concentrations of substrates has not been reported for any of the PRX isoforms. Nonetheless, the molar efficiencies of PRXs are generally smaller than GPX or CAT by several orders of magnitude (Flohé et al., 2003). Therefore, although PRXs may defend against cellular oxidative stress, the importance of their antioxidant role in mammalian cells remains unclear (Flohé et al., 2003). Moreover, growing evidences suggest that in addition to antioxidant properties, these peroxidases may also play a role in the regulation of H_2O_2 as a second messenger in receptor-mediated signaling (Kang et al., 2005; Rhee et al., 2005b; Rhee et al., 2005c).

Heat shock proteins
The production of heat shock proteins in living organisms, can be induced by any stress, but more frequently by thermal stress and for this reason are called heat shock proteins. The Hsps have been identified in virtually all species belonging to the eubacteria, archaea and higher organisms

and animals. Also a considerable similarity between the Hsps in different species has been verified, which is indicative of an early differentiation of the evolutionary course that makes them conserved in all living organisms (Lindquist and Craig, 1988). This also suggests the existence of such a protective function in all organisms. Many of the stress proteins are present at low levels and their main function is to reduce to a minimum the harmful effects of any stress (Schlesinger, 1990; Gutteridge & Mitchell, 1999).

The stress proteins are molecular chaperones, and have, therefore, the task of ensuring the correct folding and the restoration of the native structure. They have been classified into six families, essentially on the basis of molecular weight: hsp100 (100-110 kDa), hsp90 (83-90 kDa), hsp70 (66-78 kDa), hsp60, hsp40 and hsp small (15-30 kDa). They are in different compartments cell where they are appointed to carry out specific functions.

The Hsp70 family is the most conserved and the most studied and include the inducible form Hsp70, the shape constitutively expressed Hsc70, the mitochondrial form Hsp75, and the shape localized in the endoplasmic reticulum, Grp78. The inducible isoform of the protein Hsp-70 is expressed especially in slow muscles rather than fast ones. As a result of various stress such as ischemia or physical exercise Hsp-70 activation occurs both in slow and fast muscles (Lindquist & Craig, 1988; Schlesinger, 1990; Gutteridge & Mitchell, 1999).

Non-enzymatic Antioxidants

Nonenzymatic antioxidants include low-molecular-weight compounds, such as vitamins (vitamins C and E), β-carotene, uric acid, and Glutathione GSH, a tripeptide (L-γ-glutamyl-L-cysteinyl-Lglycine) that comprise a thiol (sulfhydryl) group (Tab. 3).

Vitamin C
Vitamin C (Ascorbic Acid) Water-soluble vitamin C (ascorbic acid) provides intracellular and extracellular aqueous-phase antioxidant capacity primarily by scavenging oxygen free radicals. It converts vitamin E free radicals back to vitamin E. Its plasma levels have been shown to decrease with age (Bunker, 1992; Mezzetti et al., 1996).

Vitamin E (α-TCP)
Vitamin E (α-Tocopherol, α-TCP) Lipid-soluble vitamin E is concentrated in the hydrophobic interior site of cell membrane and is the principal defense against oxidant-induced membrane injury. Vitamin E donates electron to peroxyl radical which is produced during lipid peroxidation (Fig. 11). α-Tocopherol is the most active form of vitamin E and the major membrane-bound antioxidant in cell.
Vitamin E triggers apoptosis of cancer cells and inhibits free radical formations.

Glutathione (GSH)
Glutathione GSH is highly abundant in all cell compartments and is the major soluble antioxidant. GSH/GSSG ratio is a major determinant of oxidative stress. GSH shows its antioxidant effects in several ways (Masella et al., 2005). It detoxifies H_2O_2 and lipid peroxides via action of GSH-Px (Fig. 11). GSH donates its electron to H_2O_2 to reduce it into H_2O and O_2 (Fig. 11). GSSG is again reduced into GSH by GSH reductase that uses NAD(P)H as the electron donor (Fig. 11). Gluthatione peroxidase (GPX) are also important for the protection of cell membrane from lipid peroxidation (Fig. 11). Reduced glutathione donates protons to membrane lipids and protects them from oxidant attacks (Curello et al., 1985). GSH is a cofactor for several detoxifying enzymes, such as GPX and transferase. It has a role in converting vitamin C and E back to their active forms. GSH protects cells against apoptosis by interacting with proapoptotic and antiapoptotic signaling pathways (Masella et al., 2005). It also regulates and activates several transcription factors, such as AP-1, NF-kB, and Sp-1.

Carotenoids (β-Carotene)
Carotenoids are pigments found in plants. Primarily, β-carotene has been found to react with peroxyl ($ROO^{\bullet}$), hydroxyl ($^{\bullet}OH$), and superoxide ($O^{\bullet}_2{}^-$) radicals (El-Agamey et al., 2004). Carotenoids show their antioxidant effects in low oxygen partial pressure but may have pro-oxidant effects at higher oxygen concentrations (Rice-Evans et al., 1997). Both carotenoids and retinoic acids (RAs) are capable of regulating transcription factors. β-Carotene inhibits the oxidant-induced NF-κB activation and interleukin (IL)-6 and tumor necrosis factor-a production. Carotenoids also affect apoptosis of cells. Antiproliferative effects of RA have been shown in several studies. This effect of RA is mediated mainly by retinoic acid receptors and vary among cell types. In mammary carcinoma cells, retinoic acid receptor was shown to trigger growth inhibition by inducing cell cycle arrest, apoptosis, or both (Donato and Noy, 2005; Niizuma et al., 2006).

ROS and exercise

Regular exercise is increasingly used as a therapeutic strategy to prevent age-related muscular atrophy as well as a number of diseases, including heart failure and diabetes. It is noteworthy that the benefits of exercise may not be equal between different conditions, due to the blunted adaptive responses of skeletal. The metabolic and structural changes induced by exercise ultimately affect the contractile properties of the muscle fibers and as contracting muscles generate ROS/ RNS; these signaling molecules play crucial roles in the adaptive response to exercise. ROS/RNS generate unique signaling cascades that are essential in skeletal muscle contraction and adaptation, but also play a role in a wide array of cell processes including cell proliferation, immune response and antioxidant defenses.

There are a number of potential endogenous sources of ROS/RNS in skeletal muscle (Fig. 11). A part of ROS appear to come from uncoupling of mitochondrial electron transport chain at the level of complexes I and III (in part II too). The 2% of the electrons (C-I, C-II and C-III, see white stars in Fig. 11) reactive with the oxygen generating superoxide anion ($O_2^{\bullet-}$). Recent studies indicate that cytoplasmic generation, rather than electron leakage from the electron transport chain, are primarily responsible for the increase in ROS/RNS generation within healthy skeletal muscle following contractions (Pearson et al., 2014; Sakellariou et al., 2013; Sakellariou, Jackson and Vasilaki 2014; Ward et al., 2014). As ROS/RNS are too reactive to produce a signaling effect by diffusion throughout the cell, it is now considered that they produce an effect localized to their site of generation (Poole, 2015). Other responsible ROS generators, are some enzymes including: (i) aconitase (ACO), (ii) α-ketoglutarate dehydrogenase (KGDH), (iii) pyruvate dehydrogenase (PDH) and (iv) the Monoamine Oxidase (MAO); overall exarcebate at least hydrogen peroxide production (H_2O_2) (see white stars in Fig. 11).

Importantly, more recently it has been understood that ROS are major signals involved in muscle homeostasis, i.e. in maintaining normal skeletal muscle structure and function (Dröge, 2002; Smith & Reid, 2006; Brigelius-Flohé, 2009; Musarò, Fulle and Fanò 2010). ROS production due to heavy exercise training (Sastre et al., 1992; Palazzetti et al., 2003; Aguiló et al., 2005) has been shown to determine muscle damage, documented by increased lipid peroxidation, protein carbonylation, increase in serum creatine kinase and altered glutathione redox status. On the contrary, ROS production during moderate exercise caused positive adaptations among which are increases in insulin sensitivity, mitochondria biogenesis and antioxidant defence systems (Powers and Jackson, 2008; Jackson, 2010; Ristow et al., 2009). Consequently, antioxidant administration may counter muscle damage following heavy exercise (Sastre et al., 1992; Palazzetti et al., 2004), but also positive adaptations following moderate exercise (Ristow et al., 2009). The mechanisms underlying the opposite effects of ROS on muscle homeostasis in different conditions are still unclear. It could be that small, compartmentalized, or transient (minutes) increases in ROS mostly modulate intracellular signals by reversible oxidation of specific protein residues (Ghezzi, 2005; Janssen-Heininger et al., 2008) and consequently affect gene expression (Jackson et al. 2002; Powers et al., 2005; Powers et al., 2010). The latter phenomenon could occur in response to moderate exercise. In heavy exercise, disuse and pathological conditions, sustained (hours, days), large increases in ROS could (i) have a direct, non-specific, large scale oxidative effect on proteins, which would become more susceptible to proteolysis; (ii) damage plasma membrane and sarcoplasmic reticulum altering calcium homeostasis and activating proteases (e.g. calpains), enhancing proteolysis, (iii) damage lysosome and cause a leakage of catabolic enzymes in the cytosol. Oxidized proteins could be more susceptible to proteolysis because they are more easily targeted by the ubiquitin–proteasome system, which is up-regulated by ROS (Davies, 1987;

Shang et al., 1997), because their recognition by calpain and caspase is enhanced (Smuder et al., 2010), or because they could be directly degraded by proteasome without being ubiquitinated (Grune et al., 2003), or for all the above causes.
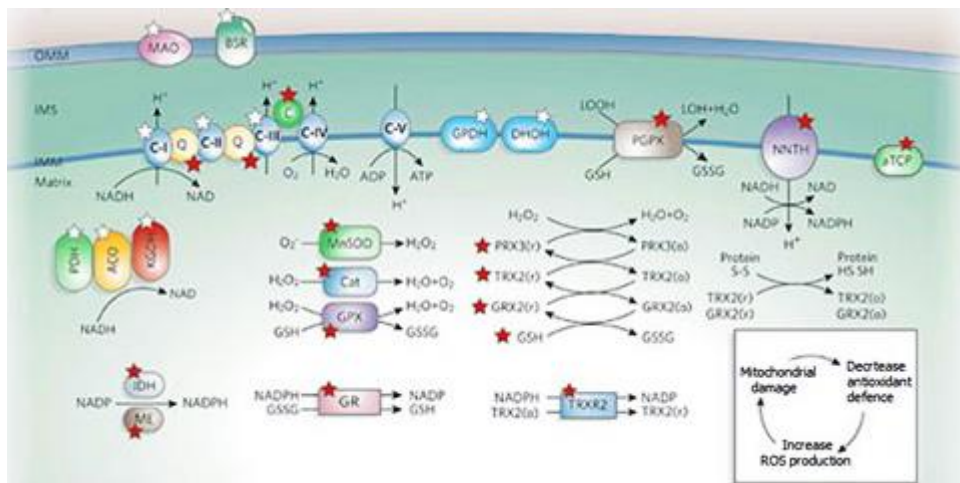

Fig. 11: Cartoon depicting the processes and components involved in ROS generation (white stars) and antioxidant defence (red stars). Mitochondria are the primary cellular consumers of oxygen and contain numerous redox enzymes capable of transferring single electrons to oxygen, generating the ROS superoxide ($O_2^{.-}$). Mitochondrial enzymes so far known to generate ROS include the tricarboxylic acid (TCA) cycle enzymes aconitase (ACO) and α-ketoglutarate dehydrogenase (KGDH); the electron-transport chain (ETC) complexes I, II and III; pyruvate dehydrogenase (PDH) and glycerol-3-phosphate dehydrogenase (GPDH); dihydroorotate dehydrogenase (DHOH); the monoamine oxidases (MAO); and cytochrome b_5 reductase (B5R). The transfer of electrons to oxygen, generating superoxide, is more likely when these redox carriers are abundantly charged with electrons and the potential energy for transfer is high, as reflected by a high mitochondrial membrane potential. ROS generation is decreased when available electrons are few and potential energy for the transfer is low. Mitochondria also contain an extensive antioxidant defence system to detoxify the ROS generated by the reactions described above. Both the membrane-enclosed and soluble compartments are protected. **Nonenzymatic components** of the system include α-tocopherol (aTCP), coenzyme Q10 (Q), cytochrome *c* (C) and glutathione (GSH). **Enzymatic components** include manganese superoxide dismutase (MnSOD), catalase (Cat), glutathione peroxidase (GPX), phospholipid hydroperoxide glutathione peroxidase (PGPX), glutathione reductase (GR); peroxiredoxins (PRX3/5), glutaredoxin (GRX2), thioredoxin (TRX2) and thioredoxin reductase (TRXR2). The regeneration of GSH (through GR) and reduced TRX2 (through TRXR2) depends on NADPH, which is derived from substrates (through isocitrate dehydrogenase, IDH, or malic enzyme, ME) or the membrane potential (through nicotinamide nucleotide transhydrogenase, NNTH). So, like ROS generation, antioxidant defences are also tied to the redox and energetic state of mitochondria. GSSG, glutathione disulphide; LOH, lipid hydroxide; LOOH, lipid hydroperoxide; o, oxidized state; r, reduced state. In structurally and functionally intact mitochondria, a large antioxidant defence capacity balances ROS generation, and there is little net ROS production. Mitochondrial damage with decrease of antioxidant defence capacity is a prerequisite for net ROS production. Once this occurs, a vicious cycle (inset) can ensue whereby ROS can further damage mitochondria, causing more free-radical generation and loss or consumption of antioxidant capacity. For example, the Fe–S cluster in aconitase is easily inactivated by superoxide, the iron is released, and this induces hydroxyl radical production (image, Lin and Beal, 2006).

TABLE 2. Enzymatic Scavenger of Antioxidant Defense

Name of Scavenger	Acronym	Catalyzed Reaction
Superoxide dismutase	SOD	$M^{(n+1)+}\text{-SOD} + O_2^- \rightarrow M^{n+}\text{-SOD} + O_2$ $M^{n+}\text{-SOD} + O_2^- + 2H^+ \rightarrow M^{(n+1)+}\text{-SOD} + H_2O_2$
Catalase	CAT	$2\ H_2O_2 \rightarrow O_2 + 2\ H_2O$ $H_2O_2 + Fe(III)\text{-E} \rightarrow H_2O + O = Fe(IV)\text{-E}(.+)$ $H_2O_2 + O = Fe(IV)\text{-E}(.+) \rightarrow H_2O + Fe(III)\text{-E} + O_2$
Glutathione peroxidase	GTPx	$2GSH + H_2O_2 \rightarrow GSSG + 2H_2O$ $2GSH + ROOH \rightarrow GSSG + ROH + H_2O$
Thioredoxin	TRX	Adenosine monophosphate + sulfite + thioredoxin disulfide = 5'-adenylyl sulfate + thioredoxin Adenosine 3',5'-bisphosphate + sulfite + thioredoxin disulfide = 3'-phosphoadenylyl sulfate + thioredoxin
Peroxiredoxin	PRX	$2\ R'\text{-SH} + ROOH = R'\text{-S-S-}R' + H_2O + ROH$
Glutathione transferase	GST	$RX + GSH = HX + R\text{-S-GSH}$

TABLE 3. Nonenzymatic Scavenger of Antioxidant Defenses

Chemical Name of Scavenger	Name of Scavenger
All trans retinol 2	Vitamin A
Ascorbic acid	Vitamin C
α-Tocopherol	Vitamin E
β-Carotene	
Glutathione	

Table 2 and 3: List of Enzymatic Scavenger and Non enzymatic Scavenger of Antioxidant Defences, shown in table 2 and 3, respectively (modified image, Birben et al., 2012).

Mitochondrial Quality Control and Muscle Mass Maintenance

Mitochondria are continuously challenged by reactive oxygen species (ROS), an inexorable by product of oxidative phosphorylation. In order to prevent an excessive production of ROS but also the release of dangerous factors such as cytochrome c, AIF (Apoptosis-inducing factor) or endonuclease G, mammalian cells contain several systems that maintain mitochondrial integrity and function.

This mitochondrial quality control includes pathways related to protein folding and degradation as well as systems involved in organelle shape, movement and turnover (Fig. 12). The activation of each specific quality control system depends on the degree of mitochondrial damage. Dysfunctional mitochondria trigger catabolic signaling pathway swhich feed-forward to the nucleus to promote the activation of muscle atrophy. Exercise, on the other hand, improves mitochondrial function by activating mitochondrial biogenesis and mitophagy, possibly playing an important part in the beneficial effects in several diseases. Optimized mitochondrial function is strictly maintained by the coordinate activation of different mitochondrial quality control pathways. (Romanello and Sandri, 2016).

Mitochondrial network:
not only a matter of shape

Mitochondria are dynamic organelles that continuously change remodeling their size, shape and function through fusion and fission events.

Fusion leads to elongated mitochondria with increased interconnectivity into a tubular network. On the contrary, fission fragments the network into unconnected shorter organelles. In physiological conditions, most mammalian cells show a continuous filamentous mitochondrial network with the exception of cardiomyocytes that display fragmented mitochondria that do not form a network (Song and Dorn, 2015). However, the mitochondrial pool rapidly changes its morphology according to the cellular needs. Increased mitochondrial fusion facilitates the redistribution of metabolites, proteins and mtDNA within the network. Moreover, fusion between healthy and damaged organelles allows to dilute the damaged material into the healthy network, avoids the accumulation of dysfunctional mitochondria and maintains their overall fitness (i.e function) (Twig et al., 2008). On the other hand, mitochondrial fragmentation is a mechanism that segregates dysfunctional or damaged components of the mitochondrial network, allowing their removal via mitophagy (Otera and Mihara, 2011). However, excessive fission generates isolated mitochondria which are less efficient in ATP production and are dysfunctional because they consume ATP to maintain their membrane potential (Benard et al., 2007).

Fusion machinery

Mfn1 and Mfn2 are integrated protein into the OMM (outer mitochondrial membrane) and have two cytosolic heptad repeat domains (HR1 and HR2) which interact to form a dimeric antiparallel coiled-coil structure. Then Mfn1/2 can interact homotypically (Mfn1-Mfn1, Mfn2-Mfn2) or heterotypically (Mfn1-Mfn2) to promote the tethering of two adjacent mitochondria and further the OMMs fusion (Koshiba et al., 2004). The two mitofusins conserve high degree of homology but they seem to have different roles: Mfn1 has higher GTPase and organelle fusion activity, while Mfn2 has greater affinity for GTP (Ishihara et al., 2004). Additionally, Mfn2 and not Mfn1 is expressed on the mitochondria-associated endoplasmic reticulum membranes (MAM) and less express on the endoplasmic/sarcoplasmic reticulum (ER/SR) (de Brito and Scorrano, 2009). Indeed, Mfn2 bridges mitochondria to ER/SR facilitating important processes linked to ER-mitochondria interactions like calcium homeostasis and signaling (de Brito and Scorrano, 2009; Ngoh et al., 2012; Sebastian et al., 2012; Munoz et al., 2013; Ainbinder et al., 2015). Recent studies have highlighted Mfn2 as a modulator of the UPR (unfolded protein response) during ER stress. In fact, Mfn2 deficiency leads to fragmented ER network and ER stress (Ngoh et al., 2012; Sebastian et al., 2012; Munoz et al., 2013; Bhandari et al., 2015). Furthermore, Mfn2 is modified at the post-translational level; when is phosphorylated by PINK1, it becomes a receptor for the ubiquitin ligase Parkin (Chen and Dorn, 2013). In addition, the E3 ligases Mul1 also promote Mfn2 ubiquitination and proteasomal degradation (Leboucher et al., 2012; Lokireddy et al., 2012). Altogether, Mfn2 promotes mitochondrial fusion, enhances ER-mitochondria and activates mitophagy via PINK1/Parkin pathway.

The profusion protein Opa1 is regulated by proteolytic processing. There are different splicing variants of Opa1 (8 in humans and 4 in mice) which are tissue specific. Opa1-dependent mitochondrial fusion needs Mfn1 (Cipolat et al., 2004).

Fission machinery

In mammalian cells, mitochondrial fission depends on the cytosolic GTPase dynamin-related protein 1 (DRP1), that mediates the fragmentation of mitochondria and peroxisomes (Schrader, 2006). Drp1 translocates to mitochondria in response to cellular and mitochondrial signals.

DRP1 is recruited to the OMM where it assembles into multimeric ring complexes that form active GTP-dependent mitochondrial fission sites (Smirnova et al., 2001). DRP1 lacks hydrophobic membrane-binding domains and for this reason its recruitment on OMM is dependent on mitochondrial membrane proteins that act as receptors. Accordingly, Drp1 interacts with the integral OMM proteins: Fis1, Mff, mitochondrial elongation factor 2/mitochondrial dynamics protein 49 (MIEF2/MiD49) and MIEF1/MiD51. Fis1 is the major DRP1 receptor in yeasts (Karren et al., 2005). Fis1 is a membrane protein homogenously distributed in the OMM via a trans membrane domain located in the C-terminal region, and only a small portion of the molecule protrudes into the intermembrane space (IMS). Overexpression of Fis1 induces mitochondrial fragmentation, but because it does not possess enzymatic activity, its role is probably restricted to anchoring effector proteins to mitochondria. Accordingly, mitochondrial fragmentation caused by Fis1 overexpression can be blocked by expression of a dominant-negative mutant of DRP1 (James et al., 2003). However, recent evidence suggest that Mff has an higher affinity for DRP1 in mammalian (Otera et al., 2010).
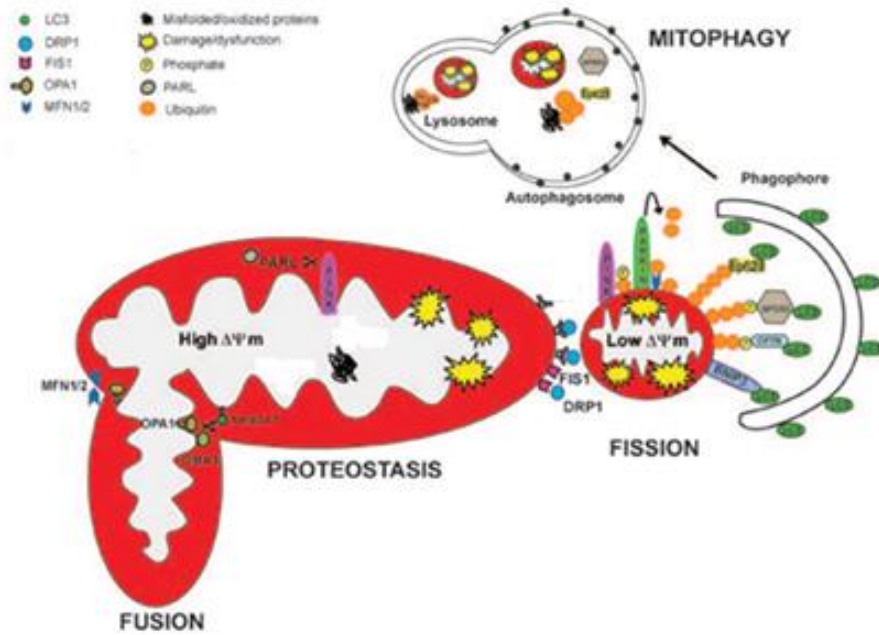
Fig. 12: Mitochondrial quality control pathways are depicted. The fusion starts with tethering of mitochondria, continues with fusion of OMM (outer mitochondrial membrane) that involves the GTPase mitoprotein Mfn1/2, and concludes with fusion of IIM (inner mitochondrial membrane) and cristae remodelling, that involves mitoprotein OPA1. The fission requires GTPase DRP1 that is recruited to the OMM where interacts with OMM-integral protein receptor Fis1 and Mff. The fission divedes the mitochondria in two fragments with different $\Delta\Psi$m. Depolarized will be removed by mitophagy. PINK1 accumulates on the surface of depolarized mitochondria where phosphorilates ubiquitinaded OMM proteins and Parkin that will ubiquitinate Mfn1/2. The ubiquitinated proteins will be recognized and redirect to mitophagy (modified image, Romanello and Sandri, 2016).

Mitochondrial clearance and mitochondrial function: energy and oxidative stress

Impaired skeletal muscle oxidative metabolism is associated with the development of a number of chronic diseases ,with a reduction in the expression of a number of metabolic and mitochondrial genes (Mootha et al., 2003; Patti et al., 2003). In addition, defective in mitochondrial metabolism is thought to contribute to the development of muscle-wasting disorders, such as that seen in aging (Mishra & Misra, 2003), COPD (chronic obstructive pulmonary disease; Balasubramanian & Varkey, 2006) and some muscular dystrophies (Bernardi & Bonaldo, 2008). Taken together, these findings highlight the importance of oxidative metabolism and skeletal muscle phenotype in human health and performance.

It is widely recognized that the age-related decline in autophagy in conjunction with accumulation of damaged proteins contribute to the deficiency of autophagy-lysosomal pathway (Rajawat et al., 2009). The activity of AMPK, mitophagy, and mitochondrial biogenesis are coordinately regulated to maintain a healthy pool of mitochondria in cellular homeostasis (Calvani et al., 2013). A crosstalk exists between autophagy and mitochondrial quality control, which is crucial for homeostasis of long-lived cells. The removal of damaged mitochondria by mitophagy is an essential process for maintaining normal muscle function at basal level and in response to various stress stimuli. Enlarged mitochondria with highly interconnected networks and aberrant morphology are frequently observed in aging muscle. Fission segregates of the mitochondrial network are damaged or senescent, and allow for the autophagic removal, while enlarged mitochondria as a poor substrate can evade degradation by hindering the autophagic disposal of dysfunctional organelles (Yoon et al., 2006). The impaired clearance of damaged mitochondria is thought to be involved in skeletal muscle loss with oxidative damage and bio-energetic failure (Lee et al., 2012). ROS can promote the accumulation of oxidized proteins that have the tendency to aggregate in lysosomes, resulting in a further ROS production and autophagic function decrease. Impaired autophagy stimulates further accumulation of damaged mitochondria, and enhances the generation of ROS (Terman et al., 2010). The accumulation of dysfunctional mitochondria and the impairment of autophagy lead to increased oxidative stress and decreased ATP production (Fan J. et al., 2015).

PGC-1α

PGC-1 α has been extensively described as the master regulator of mitochondrial biogenesis. PGC-1α coordinately increases mitochondrial biogenesis (through fusion and fission events) and respiration rates, as well as the uptake and utilization of substrates for energy production. In order to exert such a wide array of functions PGC-1α directly coactivates multiple transcription factors, including nuclear receptors–such as the PPARs (Vega et al., 2000; Wang et al., 2003), the thyroid hormone receptor (TR) (Puigserver et al., 1998), glucocorticoid receptors (GRs) (Vega et al., 2000), estrogen receptors (ERs) (Puigserver et al., 1998; Feige and Auwerx, 2007; Wu et al., 1999; St-Pierre et al., 2003; Lehman et al., 2000; Vega et al., 2000) estrogen-related receptors (ERRs) (Huss et al., 2002; Schreiber et al., 2003) and non-nuclear receptor transcription factors, such as myocyte enhancer factor-2 (MEF-2) (Michael et al., 2001) and the family of forkhead O-box (FoxO) transcription factors (Puigserver et al., 2003).

PGC-1α is mainly expressed in tissues with high energy oxidative capacity, like heart, skeletal muscle, liver, brown adipose tissue and brain, and is robustly induced in conditions that require energy, such as cold, fasting and exercise (Puigserver et al., 1998; Mootha et al., 2004). Muscle-specific PGC-1α transgenic animals display increased mitochondrial number and function, as well

as a higher relative amount of type I oxidative fibers (Lin et al., 2002). Conversely, mice with a muscle-specific deletion of PGC-1α show abnormal glucose homeostasis linked to a moderate reduction in the number of oxidative type I fibers, decreased endurance capacity and mitochondrial gene expression (Handschin et al., 2007). Altogether, these data provide compelling evidence that PGC-1α is a key regulator of mitochondrial biogenesis in muscle.

Interestingly, there is a strong overlap in the genes transcriptionally regulated by AMPK and PGC-1α, suggesting that PGC-1α might be an important mediator AMPK-induced gene expression. In support of this hypothesis, AMPK activation leads to increased PGC-1α expression, and AMPK requires PGC-1α activity to modulate the expression of several key players in mitochondrial and glucose metabolism. A closer link has been provided by recent findings showing that AMPK can directly interact and phosphorylate PGC-1α. Direct phosphorylation of PGC-1α by AMPK seems to increase transcriptional activity of PGC-1α, even though the reasons why, where, and how that happens are still elusive. Phosphorylation of PGC-1α by AMPK may, hence, be part of the link between the sensing of the energetic status and the induction of transcriptional programs that control energy expenditure.

Recent studies have shown that PGC-1α also exerts a regulatory mechanism for the expression of endogenous antioxidant proteins. Reduced mRNA levels of SOD1 (CuZn-SOD), SOD2 (Mn-SOD), and/or GPx1, (Leick et al., 2008) as well as SOD2 protein content, (Geng et al., 2010, Leick et al., 2010) were observed in skeletal muscle from PGC-1α knockout mice, while PGC-1α overexpression induces an upregulation of SOD2 protein content in skeletal muscle (Wenz et al., 2009).

Recent observations indicate that PGC-1α may also play a role in anti-inflammatory effects. Studies in PGC-1α KO animals indicated that PGC-1α modulates local or systemic inflammation and might regulate the expression of inflammatory cytokines and inflammatory markers such as TNF-α and IL-6 (Arnold et al., 2011, Handschin, 2009). PGC-1α KO mice show higher basal mRNA expression of TNF-α, IL-6 in skeletal muscle, as well as higher serum IL-6 levels. In addition, PGC-1α – overexpression in mice show lower TNF-α and IL-6 mRNA levels in skeletal muscle.

Dilated Cardiomyopathy (DCM)

Dilated cardiomyopathy (DCM) is a complex clinical syndrome, progressive and irreversible, that often results in death due to congestive heart failure (CHF, chronic heart failure), or heart attack (SCD, sudden cardiac death).

Dilated cardiomyopathy is the cause of CHF in a substantial proportion of patients and, despite advances in treatment, has a mean survival time of 5 years (Dec and Fuster, 1994; Richardson et al., 1996). The only effective treatment for end-stage dilated cardiomyopathy is heart transplantation but, since there is a limited number of donor organs, other forms of therapy are being (Levin et al., 1995; Batista et al., 1996).

Exercise Intolerance and the "Muscle Hypothesis"

A clinical hallmark of the CHF is the exercise intolerance (EI). The ability to exercise is a good index to assess the quality of life and mortality, in fact, it has been amply demonstrated that exercise is beneficial for the prevention and treatment of various pathological conditions (Pedersen & Saltin, 2006) and that has a positive effect on the rehabilitation and treatment of cardiac patients (Wisløff et al., 2002; Kemi et al., 2007; Stølen et al., 2009; Piepoli et al., 2011).

Exercise intolerance is related to the structural and functional aberrations in the transport of oxygen (O_2). The CHF reduces the availability of O_2 in the muscle, increasing, at the same time, the requests (Poole et al., 2012). The severity of CHF swings from moderate to severe, and is commonly assessed in terms of kinetic rate of O_2 consumption (VO_2max) (Elahi et al., 2010). In CHF patients, cardiac output (Q_{tot}) at rest, and in particular during physical exercise, is reduced as a result of decreased ejection fraction and stroke volume. The heart rate response is insufficient to compensate the reduction in stroke volume thus, the start condition, is a global vasoconstriction that occurs, not only in the muscle, but in all peripheral organs, and that affects the distribution and redistribution of Q_{tot} to and within skeletal muscle (Poole et al., 2012). Where arise vascular diseases, endothelial cells can lose their ability to release vasodilatory substances and, in certain pathological conditions, release factors that induce vasoconstriction; this vasoconstriction is enhanced by higher working level of catecholamines, angiotensin II, arginine, vasopressine and endothelin-1 (Thomas et al., 2001; Teerlink, 2005).

The hemodynamic changes are not enough to explain the generation of symptoms in CHF, e.g. reduced exercise tolerance; in fact, improved hemodynamics by cardiotonic agents, resulting in improved cardiac performance, it does not lead to increased exercise tolerance.

Attention has therefore been focused on peripheral factors such as alterations in skeletal muscle perfusion and intrinsic skeletal muscle abnormalities. Indeed, numerous studies in patients (Mancini et al., 1989; Sullivan et al., 1990; Drexler et al., 1992; Massie et al., 1996; Sullivan et al., 1997) and animal models of heart failure (Arnolda et al., 1991; Sabbah et al., 1993; Bernocchi et al., 1996; Simonini et al., 1996b; Simonini et al., 1996a; Delp et al., 1997) have described muscle histological abnormalities, including fiber atrophy, fiber-type transformation toward more fast phenotype and reduced oxidative enzyme activity. However, whether these abnormalities result in functional alterations of the contractile machinery or sites of energy production, has never been directly assessed.

For this reason, attention is focused on skeletal muscle, at the level of which is thought to reside primarily responsible mechanism of exercise intolerance in patients with HF ("*muscle hypothesis*" see Coats et al., 1994) (Poole et al., 2012).

Some studies have shown the existence of intrinsic abnormalities in skeletal muscle in patients with heart failure that would lead to the establishment of an early anaerobic metabolism, which would limit exercise capacity. Considering the importance of the peripheral muscle abnormalities, their knowledge would help the development of more appropriate training protocols and more effective drug therapies, targeted to improve the prognosis of CHF patients.

Exercise as therapy in chronic HF

In 2001, a European task force proposed a classification of HF based on two criteria: symptoms of HF at rest or during exercise (typically breathlessness and fatigue), and objective evidence of cardiac dysfunction at rest (Remme et al., 2001). Symptoms and functional exercise capacity are used to classify the severity of HF, according to the NYHA classification system (i.e. New York Heart Association) (Fig. 13), and to judge the patient's response to treatment. A decreased functional capacity is negatively related to individual's ability to perform daily activities of life and, therefore, their independence and quality of life. In patients with chronic HF, exercise training can reverse , in part, the situation allaying symptoms, improving exercise capacity and quality of life, and reducing disability, hospitalization and , thus, mortality (Piepoli et al., 2004; Hunt et al., 2001; van Tol et al., 2006). For all details see Review Crimi et al. (2009).

Neurohumoral effects of exercise

Patients with HF exhibit neurohumoral changes: the sympathetic and renin-angiotensin‑aldosterone systems are enhanced (by release of catecholamines, renin, vasopressin, atrial natri uretics) in an attempt to increase myocardial contractility, heart rate and vasoconstriction, and expand extra cellular fluid volume (Anand et al., 2003; Azevedo et al., 2000; Benedict et al., 1994). Continuous neurohumoral activation leads to deterioration of myocardial function with inflammatory response, organ damage, and skeletal muscle deterioration, therefore a worsened exercise tolerance.

Different protocols of exercise training reveal a reduction of sympathetic hyperactivity (Coats et al., 1992; Belardinelli et al., 1995; Shemesh et al., 1995; Gordon et al., 1997; Hambrecht et al., 2000; Passino et al., 2006) and muscle sympathetic nerve activity (Passino et al., 2006; de Mello Franco et al., 2006). Exercise training can also reduce the levels of circulating neurohormones including Ang II, aldosterone, vaso pressin and natriuretic peptides (Passino et al., 2006; Braith et al., 1999; Wisløff et al., 2007) resulting in improved cardiac function, reduced vasoconstriction with better peripheral and skeletal blood delivery, and, ultimately, improved exercise tolerance.

Endothelial effects of exercise

The worsening in vasodilatation in the microcirculation of patients with HF could be due to a decrement of NO endothelial production (i.e. nitrix oxide) (Katz et al., 1999; Ramsey et al., 1995) and to an increment of endothelin concentration (Lerman et al., 1992). The impaired of NO production can be derived by reduced endothelial nitric oxide synthase (eNOS) expression or activity, by asymmetric dimethyl arginine, NO scavenging by reactive oxygen species, and reduced availability of l-arginine and tetrathydropbiopterin (Rush et al., 2005; Linke et al., 2003). Oxidative stress has a major role in NO inactivation (Linke et al., 2003).

Regular exercise promotes NO release and, therefore, improves endothelium-dependent vasodilatation to slow vascular damage (Napoli et al., 2004; Napoli et al., 2006). Evidence suggests that improved endothelial function could be related mechanisms by which exercise

training can exert its beneficial effects in HF (Watanabe et al., 2008; Arany et al., 2008; Bjørnstad et al., 2008; Sarto et al., 2007).

Anti-inflammatory effects of exercise

In the last decade, it was highlighted a central role of inflammation in the pathophysiology of HF (Adamopoulos et al., 2001; Blum and Miller, 2001). Levels of proinflammatory cytokines, such as tumor necrosis factor (TNF) and interleukin (Il)-6, (Torre-Amione et al., 1996; Tsutamoto et al., 1998) are elevated in patients with HF. Cytokine activation can negatively affect myocardial contractility by inducing activation of inducible nitric oxide synthase (iNOS), increasing oxidative stress, inhibiting sarcoplasmic reticulum Ca^{2+} release and promoting myocyte apoptosis and cardiac remodeling (Ferdinandy et al., 2000; McTiernan et al., 1997; Bozkurt et al., 1998). Increased cytokine production can also lead to endothelial dysfunction by increased production of reactive oxygen species.

Regular exercise training has an anti-inflammatory effect: in experimental models of HF, exercise training reduces plasma levels of inflammatory cytokines (TNF, soluble TNF, Il-6, Il-6 receptor, Il-1β) (Adamopoulos et al., 2002), increases plasma levels of the anti-inflammatory cytokines (Nunes et al., 2008), also in skeletal muscle (Damy et al., 2004), and can stimulate the innate immune system, by influencing macrophage and lymphocyte function (Batista et al., 2007; Batista et al., 2008).

Cardiovascular effects of exercise

Physical training can also have beneficial effects on cardiac performance in patients with chronic HF (Hambrecht et al., 2000; Kenchaiah et al., 2009; Arena et al., 2008a; Arena et al., 2008b; Di Valentino et al., 2010; Myers et al., 2008, Nilsson et al., 2008; Chase et al., 2008; Bensimhon et al., 2008; Beckers et al., 2008) with significant improvements in left ventricular ejection fraction, end-diastolic and systolic volumes (Haykowsky et al., 2007), and maximal heart rate, systolic blood pressure and cardiac output (van Tol et al., 2006). Experimental data demonstrate that exercise training can improve heart function by restoring cardiomyocyte contractility and calcium sensitivity. Exercise training re-establishes calcium cycling by normalizing the activity of Ca^{2+}-regulating proteins, such as sarcoplasmatic reticulum Ca^{2+} ATPase, phospholamban, the ryanodine receptor and the Na^{2+} and Ca^{2+} exchanger, which increases myofilament Ca^{2+} sensitivity and, thus, myocyte contractility (Lu et al., 2002; Rolim et al., 2007; de Waard et al., 2007; Medeiros et al., 2008).

Effects of exercise on skeletal muscle

It has been described that the HF lead to skeletal muscle myopathy contributing to exercise capacity limitation. Apoptosis is not normally present in skeletal muscle, but has been reported to be present in approximately 50% of patients with HF (Vescovo et al., 1998). It was also observed alteration in the capillary density, a shift from aerobic capacity to glycolytic capacity and a reduction in mitochondrial density and structure with decreased cytochrome oxidase activity and oxidative enzymes (Sinoway and Li, 2005). These abnormalities cause an increase in muscle fatigability, an alteration in oxidative metabolism, an increase in oxidative stress, and ineffective high energy phosphate use (as shown by increased inorganic phosphate and phosphocreatine levels) with early accumulation of lactate during exercise. Reduced perfusion, neuro humoral changes, endothelial dysfunction and inflammatory activation can all participate in skeletal muscle abnormalities (Sinoway and Li, 2005).

The exercise training is able to reverse changes potentially responsible for reducing of skeletal muscle performance (Ventura-Clapier et al., 2007). In fact, in experimental models of HF, exercise training shows a beneficial effect increasing muscle oxidative capacity (De Sousa et al.,

2002), normalizing skeletal muscle metabolism (Brunotte et al., 1995), and reducing oxidative stress (Lawler et al., 2006). It was also observed an augment in the mitochondrial content (Belardinelli et al., 1995; Hambrecht et al., 1995; Gordon et al., 1997; Hambrecht et al., 1997; Gustafsson et al., 2001; Damy et al., 2004). Clinical studies have shown contrasting effects of exercise training on muscle fiber type distribution and capillary densities, which probably reflects differences in training level and duration (Belardinelli et al., 1995; Hambrecht et al., 1997; Keteyian et al., 2003; Larsen et al., 2002).

NYHA Class	Symptoms
I	Cardiac disease, but no symptoms and no limitation in ordinary physical activity, e.g. no shortness of breath when walking, climbing stairs etc.
II	Mild symptoms (mild shortness of breath and/or angina) and slight limitation during ordinary activity.
III	Marked limitation in activity due to symptoms, even during less-than-ordinary activity, e.g. walking short distances (20–100 m). Comfortable only at rest.
IV	Severe limitations. Experiences symptoms even while *at rest*. Mostly bedbound patients.

Fig. 13: The New York Heart Association (NYHA) Functional Classification provides a simple way of classifying the extent of heart failure. It places patients in one of four categories based on how much they are limited during physical activity; the limitations/symptoms are in regard to normal breathing and varying degrees in shortness of breath and/or angina pain (image by The Criteria Committee of the New York Heart Association. *Nomenclature and Criteria for Diagnosis of Diseases of the Heart and Great Vessels*. 9th ed. Boston, Mass: Little, Brown & Co; 1994:253-256).

Gα$_q$ signalling

In the last few years the interactome of Gα$_q$ has expanded considerably, contributing to improve our understanding of the cellular and physiological events controlled by this G alpha subunit (Sánchez-Fernández et al., 2014). Despite the size and diversity of the GPCR (G-protein coupled receptors) superfamily, there are a relatively small number of G proteins able to initiate many different intracellular signaling cascades. In the human genome 35 genes encode G proteins, 16 of which correspond to α-subunits, five to β and 14 to γ (Milligan and Kostenis, 2006). On the basis of sequence similarity, the Gα subunits have been divided into five different families i.e. G$_s$, G$_i$, G$_q$, G$_{12}$ (Simon et al., 1991) and the newly discovered G$_v$ (Oka et al., 2009).

Classically, Gα$_q$ action has been tied to the binding and activation of the β-isoforms of phospholipase C (PLCβ) as major downstream effectors (Rhee, 2001). However, to date Gα$_q$ is known to interact with more than 20 proteins and the real complexity of Gα$_q$ pathways is only starting to be unravelled (Dowal et al., 2006).

Several lines of evidence underscore the importance of G$_q$ protein-mediated signaling pathway in transmitting hypertrophic signals to downstream cellular events. Enhanced G$_q$-mediated signaling leads to the development and ultimate decompensation of cardiac hypertrophy (Mende et al., 2001; Edes et al., 2008).

Transgenic DCM *Tgα$_q$***44h* model

The G$_q$ protein belongs to the G protein family, GTP-dependent, and its activation is linked to the development of HF (Drelicharz et al., 2009). In fact, previous studies demonstrated as transgenic models expressing various components of G$_q$-mediated signalling pathway, e.g. myocardial expression of a constitutively active alpha 1B-adrenergic receptor or overexpression of protein kynase C beta2 isoform, causes cardiomyopathy (Milano et al., 1994, Wakasaki et al., 1997).

To study the progression of dilated cardiomyopathy, it was created a line of transgenic mice with heart tissue-specific expression of G$_q$ protein, including the G$_q$ protein α subunit itself, which mimics a constitutive activation of G-protein coupled receptors (GPCRs), i.e. α1 adrenergic, angiotensin AT1 , endothelin ET-A (D'Angelo et al., 1997, Mende et al., 1998, Akhter et al., 1998). In this transgenic model, the development of the phenotype does not require the continued presence of the transgenic protein (Mende et al., 1998). In fact, transient expression of a hemoagglutinin (HA)-tagged, a constitutively active G protein α$_q$ (HAα$_q$*), is enough to lead to cardiac hypertrophy and dilation (Mende et al., 1999).
Two independent transgenic lines, αq*52 and αq*44, are available, obtained in the same genetic background by microinjection of HAα$_q$* cDNA under the control of the α-MHC promoter (Mende et al., 2001).
In the two transgenic models, the cardiac phenotype is the same, however, in the *α$_q$***44* model, the onset of the cardiac phenotype is delayed by approximately nine months (Fig. 14, by Mende et al., 2001) and, therefore, represents a useful model for the study of mechanisms involved in the progression of exercise intolerance.
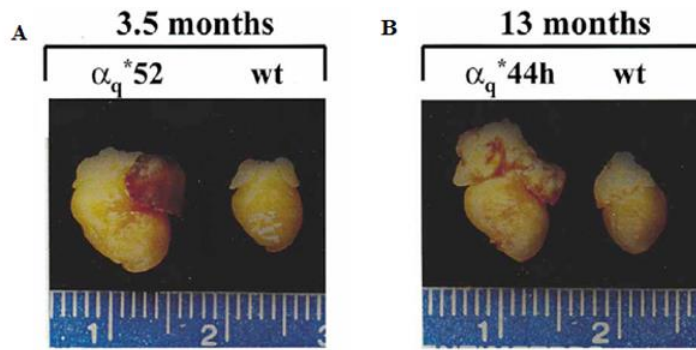
Fig. 14: Cardiac phenotype in DCM trangenic model, (**A**) in $\alpha_q{}^*52$ and (**B**) in $\alpha_q{}^*44h$. In the panel **A** was showed the DCM cardiac phenotype in $\alpha_q{}^*52$ at the end-stage (3.5 months) respect to wild type; in the panel **B** was showed the DCM cardiac phenotype in $\alpha_q{}^*44h$ at the end-stage (13 months) respect to wild type. In the trangenic model $\alpha_q{}^*44h$ the onset of the phenotype is delayed by approximately 9 months respect to $\alpha_q{}^*52$ (image by Mende et al., 2001).

Aim

Aim

The general aim of this study was to understand skeletal muscle adaptations to CHF and to clarify the molecular mechanisms causing exercise intolerance. For this purpose we used the Tgαq*44h mice model which offers the opportunity to study the progression of skeletal muscle deterioration associated to dilated cardiomyopathy.

To achieve our goals the following experimental strategies has been used:

- the use of a mouse model in which the disease develops gradually and mimic the progression of the human disease;

- the study of the time course of muscle adaptations analyzing different stages of the disease, starting from the time preceding the onset of structural and functional alterations of skeletal muscle (4-6 months) to the early onset (10-12 months) until to the final stage of the disease (12-14 months);

- the study of the effect of exercise at each stage of the disease in order to clarify the molecular mechanisms underlying the effects of such intervention on CHF;

- the assessment of structural, functional and molecular analysis at each stage of the disease;

- the comparison of CHF and exercise training adaptations between soleus and gastrocnemius, in order to understand if CHF and exercise differently influence slow and fast muscles.

Materials & Methods

Sperimental Population

The transgenic DCM $Tg\alpha_q*44$ mice, generated as described in (Mende et al., 2001), and age-matched control FVB mice, offered by the collaboration with Prof. J. Zoladz (Department of Muscle Physiology, Faculty of Rehabilitation, University School of Physical Education, Krakow, Poland), were used in experimental procedures (Tab. 4, 5).

Adult female FVB (n=71) and Tg (n=71) mice divided into 3 age groups (group 1, age: 4 month old; group 2, age: 10 month old; group 3, age: 12 month old at the start of this study) were used for all analysis. The mice were subdivided into sedentary (n=30) and training (n=41) FVB groups and into sedentary (n=30) and training (n=41) Tg groups (Tab. 4, 5).

The training groups were placed in the cages equipped with a running wheel allowing to record its voluntary wheel running activity (VWRA) during a period of 8 weeks. Mice were housed 1 per cage (a floor area of 355 x 235 x 190 mm) and maintained at 22-24°C, under a 12 h light cycle with ad libitum access to water and rodent chow.

All experimental protocols were conducted according to the Guidelines for Animal Care and Treatment of the European Union and approved by the Local Bioethics Committee in Kraków (approvals No. 914/2012 and 27/2014).

FVB UnTr 6mo-old n=8	FVB UnTr 12mo-old n=9	FVB UnTr 14mo-old n=13
Tg UnTr 6mo-old n=12	Tg UnTr 12mo-old n=8	Tg UnTr 14mo-old n=10

Table 4: Sperimental population used. **FVB UnTr**, control mice untrained; **Tg UnTr**, DCM trangenic mice untrained.

FVB Tr 4-6mo-old n=15	FVB Tr 10-12mo-old n=13	FVB Tr 12-14mo-old n=13
Tg Tr 4-6mo-old n=13	Tg Tr 10-12mo-old n=14	Tg Tr 12-14mo-old n=14

Table 5: Sperimental population subjected to free wheel running. **FVB Tr**, control mice trained; **Tg Tr**, DCM trangenic mice trained.

In vivo functional evaluation

Voluntary wheel-running activity (VWRA)

Mice were individually housed in cages equipped with a running wheel. Animals were acclimatizied to cages for 2 days with wheel locked. Wheels were unlocked on the third day, and the VWRA of each studied mouse was recorded continually using the Running Wheel System (Columbus Instruments Inc., Ohio, USA). The system was programed to record all mice running episodes within the running wheel that lasted more than 10 seconds. Moreover the mice has been filmed by a digital camera placed in the animal house allowing as to view on-line the mice behavior without disturbing its normal live. Based on the number of revolutions of the wheel and its radius the distance and the running velocity of the mice has been calculated. The data stored in a computer were downloaded manually on a weekly basis. The distance of run and the velocity of running has been expressed as a men ± SD value per 24 h, covered by each mouse, and further averaged for the entire period of training i.e. for 56 days. Based on the recorded individual data of VWRA we have ranged the studied mice according to the total distance covered within the 8 weeks of study. We have noticed, that despite of having a free access to the running wheels some mice were not interest to run. Based on the total distance covered within 56 days of study, by individual mouse, we have selected the subgroups of the best runners in each group of the FVB and the Tg mice, for further comparisons.

The animals from all experimental groups were sacrified 24 hours from last running activity to avoid any acute effect of the last bout of exercise, with cervical dislocation and its muscles (soleus and gastrocnemius) from both legs has been removed. Muscles were immediately frozen in liquid nitrogen (-196°C) and stored at -80°C for further analisys performed.

Proteomic Analysis

Samples preparation

Muscle Lysis and Protein Extraction

Still frozen muscles using liquid nitrogen are ground into a powder using a ceramic pestle. The powder thus obtained was homogenized with a lysis buffer containing 20mM TRIS-HCl, 1% triton x100, 10% Glycerol, 150mM NaCl, 5 mM EDTA, 100mM NaF and 2mM NaPPi supplemented with 1X inhibitors protease phosphatase (Protease Inhibitor Cocktail, Sigma-Aldrich, St. Louis MO) and 1mM PMSF. The lysis of tissue was performed on ice for 20 minutes. The homogenate obtained was centrifuged at 13500 rpm for 20 min at 4°C and the supernatant was transferred to a clean eppendorf tube and stored at -80°C until ready to use.

Quantification of Protein extract

The protein concentration of the lysates was determined using the RC DC™ (reducing agent and detergent compatible) protein assay (Bio-Rad).

RC-DC TM. is a colorimetric assay for protein determination in the presence of reducing agents and detergents. The RC DC protein assay is based on the Lowry protocol (LOWRY et al., 1951), one of the most used methods to evaluate protein amount; proteins in the samples are treated with copper and other solution to have a final blue colored product which absorbance it is read at 750 nm and it is directly proportional to protein concentration according to the law of Lambert-Beer. The absorbance value of each sample is read in a spectrophotometer and the concentration protein is calculated by interpolating the values on a calibration curve whose points are scalar concentrations of a solution of known concentration (1.45 mg/ml) of Bovine serum albumin (BSA).

Myosin Heavy Chain composition (MHC)

The previously prepared and quantified samples are mixed in a buffer called BUFFER Laemmli, (62.5mM Tris-HCl pH 6.8, 2.3% SDS, 10% glycerol, 5% beta-mercaptoethanol and 0.01% bromophenol blue) (Laemmli, 1970).
The sodium dodecylsulfate (SDS, anionic detergent) present in the buffer, has a dual function: on the one hand, being a detergent, favors the denaturation of proteins in combination with other reducing agents (beta mercaptoethanol), on the other, intercalates every two amino acids , conferring a negative electric charge to the denatured protein; proteins can be well resolved according to their mass in an electrophoretic run.

SDS PAGE

The content of myosin heavy chains (MHC) was determined using an electrophoretic approach previously described in detail. Four bands can be separated and quantified by densitometric analysis, to evaluate the relative proportion of the four MHC isoforms, MHC-1, MHC-2A, MHC and MHC-2X-2B, in each sample (Pellegrino et al., 2003). The separation and identification of myosin heavy chains (MHC), was determined by electrophoresis on sodium dodecyl sulfate polyacrylamide gel (SDS-PAGE), as described by Talmadge (Talmadge et al., 1996). For the electrophoretic run, was used a batch system consists of two polyacrylamide gel (PAA,

acrylamide-bisacrilamide 50: 1) containing 10% SDS in a solution of Tris-HCl pH 6.8 (stacking gel) or Tris-HCl pH 8.8 (Running Gel). The addition of two catalysts 10% APS (ammonium persulfate) and TEMED promotes the polymerization between acrylamide and bisacrylamide leading to the formation of pores, more or less large, depending on the amount of the two polymers. The stacking gel, which contains PAA to 4%, favors the packing of the samples at the interface with the running gel; in the latter it is instead added different percentages of the two polymers so as to obtain the separation of proteins of interest in an appropriate way. In our case, we used a percentage of the 8% and the quantities reported in the following table (Tab. 6). It is prepared by a top and bottom running buffer (Tab. 6) and the operating conditions are 200V (constant voltage) for 2 hours, followed by 250V for another 24 hours. At the end of the run, the proteins can be analyzed by staining with Coomassie Blue or Silver Stain for a quantitative or qualitative quantification, respectively.

SOLUZIONS	RUNNING GEL	STACKING GEL
Acrylamide/Bis 50:1	8%	4%
Glycerol	30%	30%
SDS 10%	0,4%	0,4%
TRIS 1.5M	0.2M	
TRIS 0.5M		0.07M
EDTA		0.004M
Glycine	0.1M	
APS	0.10%	0.10%
TEMED	0.05%	0.05%
SOLUZIONS	UPPER BUFFER	LOWER BUFFER
SDS	0.1%	0.05%
TRIS	0.1M	0.5M
Glycine	0.15M	0.15M

Table 6: Protocol of 8% polyacrylamide gel.

Staining with Coomassie Brillant Blue

This staining method is able to detect less than 0.1 µg of protein in a single band. After the electrophoresis, the gel is immersed in a fixing solution for 1h under stirring (solution composition shown in Table 7); then transferred in the Coomassie Blue staining, which stains both the protein bands that the background. After a washing in water, they are used the solutions A and B (Tab. 7) to destain the background and maintain bands.

53

Densitometric Analysis

The identification of the isoforms and the determination of the amount of one isoform over another, was performed using a scanner (Epson Expression 1680 Pro) and a software (2202 Ultroscan Laser densitometry LKB). During the analysis, the protein bands were visualized as peaks and their areas measured and compared. In this way it was possible to determine the percentage ratio of the different isoforms. The analysis of each sample is repeated three times and the average of the three measurements taken into account. The distribution value in MHC, obtained from each sample, is then averaged with the other values of the samples belonging to the same group in order to assess the average distribution in MHC isoform.

SOLUTIONS	FIXING	Coomassie Blue	Destain A	Destain B
METHANOL	50%	50%		
Acetic Acid	12%	10%	10%	5%
Coomassie Blue R-250		0.6%		
ETHANOL			30%	5%

Table 7: Solutions for Coomassie Blue Staining.

Western Blot

The Western blot technique was invented in 1979 by Towbin (Towbin et al., 1979), simple and rapid, it allows to identify a particular protein in a mixture of proteins, using the recognition by specific antibodies. The mixture of proteins (protein-lysate) is separated according to molecular weight by electrophoresis on polyacrylamide gel and, subsequently, the gel is transferred to a nitrocellulose or polyvinylidene fluoride membrane (PVDF); It proceeds to the recognition of the target protein through the use of a specific antibody and the protein-antibody binding can be displayed using different techniques, including autoradiography, chemiluminescent or colored products.

As mentioned above for the myosin isoforms, the total protein are prepared in the same way.
To allow complete denaturation, samples were heated at 95°C for 5 min or 50°C for 20 min and proteins can be well resolved according to their mass in an electrophoretic run.

SDS PAGE

For the experiment were used preformed gels (BIORAD) in wich the proportion of polymers varies uniformly from 12% (the top of the gel) to 20% (at the bottom of the same). An equal amount of protein sample (Tab. 8) was loaded on the gel and subjected to electrophoresis; the electrophoretic run was carried out at constant current (100V) for about 1.5 h in a running buffer at pH 8.8 (25mM Tris, Glycine 192mm, 1% SDS). To monitor the separation of the proteins, a protein marker was loaded, consisting of a mixture of a molecular weight proteins known

(Preistained Protein Ladder Marker, BIORAD). At the end of the electrophoretic run the apparatus was disassembled and the gels recovered for the next step.

Electro-blotting

The proteins resolved by electrophoresis, are transferred (blotting) into a nitrocellulose or polyvinylidene fluoride membrane (PVDF) applying an electric field in which the proteins, yet negatively charged, will migrate from the negative pole to the positive pole. The transfer was carried out at a constant voltage at 100V for 2h at 4°C or at 35mA Overnight (O/N) in a transfer buffer containing 25mM Tris, Glycine 192mm, and 20% methanol. The successful transfer of the proteins was verified by staining with Ponceau Red (SIGMA ALDRICH) in TCA (0.2% Ponceau Red in 3% trichloroacetic acid, TCA) of the nitrocellulose/PVDF for 5 minutes under stirring at room temperature; this coloration can be easily removed with brief washes in water. The Red Ponceau, by binding to proteins on the nitrocellulose/PVDF membrane, provides information not only on the transfer of proteins, but it gives us an idea about the uniformity of the amount of protein loaded; the image, then, is scanned and used for subsequent analysis.

Blocking of aspecific sites and incubation with primary antibodies

To minimize the background, the aspecific binding sites on the nitrocellulose/PVDF membrane are saturated with a blocking solution consisting of fat-free milk (MILK) to 5% or from bovine serum albumin (BSA) in 2-8% TBS-Tween-20 (0.05%), for 1h at room temperature with constant agitation. At the end of incubation, three washes are carried out, each of 10 min, with TBS-Tween-20 and the membrane incubated O/N at 4°C with the specific primary antibody, appropriately diluted in a solution by MILK 5% or BSA 2-8% in TBS-Tween-20 (Tab. 8).

Incubation with secondary antibodies and acquisition

Subsequently, it is repeated three washes in TBS-Tween-20, and the membrane incubated for 1h at room temperature with constant stirring with a secondary antibody of goat anti-mouse (DAKO) or anti-rabbit conjugated with the enzyme HRP (Horseradish Peroxidase) (Cell Signalling) appropriately diluted in a 5% solution by MILK with TBS-Tween 20 (Tab. 8). After removing the excess of antibody with two washes of 10 minutes each in TBS-Tween-20, and a last in TBS, it was carried out the detection of proteins using ECL Advance detection system (Amersham) which highlights HPRT the substrate by a chemiluminescent reaction. The membrane was gained through an analysis sowtware ImageQuant LAS 4000 (GE Healthcare Life Sciences) and the exposure time adjusted in an automatic manner or editable depending on the intensity of the emitted signal.

	protein lysate (µg)	saturazion	Ab I	company	Ab II	company
PGC-1α	40	MILK 5%	1:1000 MILK 5%	Abcam	anti-Rb 1:10000 MILK 5%	Cell Signalling
p-AMPK α	40	BSA 5%	1:1000 BSA 5%	Cell Signalling	anti-Rb 1:10000 MILK 5%	Cell Signalling
AMPK α	40	BSA 5%	1:1000 BSA 5%	Cell Signalling	anti-Rb 1:10000 MILK 5%	Cell Signalling
SOD1	20	MILK 5%	1:1000 MILK 5%	Abcam	anti-Rb 1:10000 MILK 5%	Cell Signalling
Catalase	20	MILK 5%	1:1000 MILK 5%	Abcam	anti-Rb 1:10000 MILK 5%	Cell Signalling
Drp1	40	BSA 5%	1:1000 BSA 2%	Cell Signalling	anti-Rb 1:10000 MILK 5%	Cell Signalling
Mfn1	20	MILK 5%	1:1000 MILK 5%	Abcam	anti-ms 1:5000 MILK 5%	DAKO
Mfn2	20	MILK 5%	1:1000 MILK 5%	Abcam	anti-Rb 1:10000 MILK 5%	Cell Signalling
LC3B	40	MILK 5%	1:1000 MILK 5%	SIGMA ALDRICH	anti-Rb 1:10000 MILK 5%	Cell Signalling

Table 8: List of antibodies used.

Data analysis

The various bands, present on the scanned images, are quantified with program Adobe Photoshop and is defined a BAP value (Brightness Area Product) given by the product of the brightness for the area of the band itself. The target protein levels were then normalized with respect to the amount of Housekeeping/ponceau protein. The data are expressed as the ratio between the BAP of target protein and of housekeeping.

Oxy Blot

Secondary modifications of proteins, such as oxidation by oxygen free radicals and other reactive oxygen species (ROS), have been evaluated. The carbonyl groups are introduced at the level of the side chains of the protein through a site-specific mechanism.

The level of carbonylation was evaluated using the OxyBlotTM kit (AbNova) that provides reagents for the immunodetection and is sensitive to these carbonyl groups. The carbonyl groups are derivatized with 2,4-dinitrophenylhydrazone (DNP hydrazone) by reaction with 2,4-dinitrophenylhydrazine (DNPH). The protein-DNP-derivatized samples are separated by electrophoresis on polyacrylamide gel (gel Anykd Biorad) followed by Western blotting. This step is followed by saturation of aspecific binding sites with 3% BSA solution. Then the membranes are incubated with the primary antibody, specific for the DNP portion of the proteins, and thereafter with horseradish peroxidase-conjugated antibody directed against the primary antibody (secondary antibody: goat anti-rabbit IgG). The membranes are then treated with a chemiluminescent reagent (ECL Advance, as described earlier). and positive bands that emit light are captured with sowtware of ImageQuant LAS 4000 analysis (GE Healthcare Life Sciences).

The level of oxidation between FVB transgenic controls and Tg, is quantified by comparing the signal intensity for immuno-positive compared to the total protein content of protein loaded into the gel by means of analysis of ponceau signal.

Gene Expression Analysis

Samples preparation

Extraction of mRNA from muscle tissue

The still frozen muscle tissue, are pulverized with a pestle and mortar sterile, previously treated with RNase Zap (SIGMA ALDRICH), to remove the possible presence of RNase. Approximately 20 mg of powder for each sample is used for RNA extraction with SV Total RNA Isolation System (Promega, Italy). The extraction of 'RNA requires four basic steps: (i) effective destruction of cells or tissues, (ii) the denaturation of nucleoprotein complexes, (iii) inactivation of endogenous ribonuclease (RNase) and (iv) removal of contaminants such as DNA and proteins. The most important step is the immediate inactivation of endogenous RNase. The SV Total RNA Isolation System combines the destructive and protective properties of guanidine thiocyanate (GTC) and, of the β-mercaptoethanol to inactivate the ribonucleases present in cell extracts. The GTC, in association with SDS, acts to inactivate the nucleoprotein complexes, allowing the RNA to be released into solution devoid of protein. Dilutions of cell extracts, in the presence of high concentrations of GTC causes selective precipitation of cellular proteins, while RNA remains in solution. After centrifugation, to remove precipitated proteins and cellular debris, RNA is selectively precipitated with ethanol and bound to the silica glass surface present in the column. The binding reaction takes place rapidly due to the disruption of the water molecules by the chaotropic salts, favoring, thus, the absorption of nucleic acids to the silica. The RNase-free DNase I is applied directly onto the silica membrane to digest the possible contamination of genomic DNA. The total RNA is further purified from possible contaminating salts, proteins and cellular impurities by a series of washes. Finally, the total RNA is eluted from the membrane by the addition of Nuclease-Free Water. This procedure produces a pure population of total RNA after only one cycle of purification, without organic extractions or precipitations.

RNA quantification

The nucleic acids absorb ultraviolet light in a specific wavelength pattern. Through the use of the Nano Drop, an mRNA sample, equal to 2μl, is exposed to ultraviolet light at 260 nm and, through a photo detector, is measured the light that passes through the sample. More light is absorbed by the sample, higher is the concentration of nucleic acid content. We also evaluated the contamination by proteins by evaluating the ratio of the absorbance at 260 and 280 nm (A260/280), which for pure RNA is ~1.98-2.

Reverse transcription and cDNA synthesis

For retrotrascribe the messenger RNA (mRNA), it is necessary to use an enzyme, reverse transcriptase, able to synthesize a second helix, complementary, forming a double helix of DNA, said cDNA, which will be amplified by Real-Time PCR. In this study, a quantity of 300 ng of RNA for each sample was retrotrascribed by the action of the enzyme Superscript III (Invitrogen) according to the following protocol:

(i) in the volume corresponding to 300 ng of RNA of each sample, was added 1μl of random primers (non-specific)
(ii) 1μl Deoxyribonucleosides (10 mM of dATP, dGTP, dCTP and dTTP at neutral pH)
(iii) RNase-free water to reach the final volume of 13.5 μl

(iv) the mixture thus obtained, is heated to 65°C for 5 minutes to induce denaturation of the double helix and to allow pairing of the primers to their complementary sequences

(v) incubation on ice for at least 1 minute

(vi) added 4 μl of 5X First-Strand Buffer, 1 μl of 0.1 M DTT, 1 μl of RNaseOUT ™ Recombinant RNase Inhibitor (40 units/ml) and 0.5 μl of SuperScript ™ III RT (200 units/mL).

(vii) the mixture thus composed, was incubated at 25°C for 5 minutes, at 50°C for 60 minutes (anealing and extension). After the temperature is increased to 70°C for 15 minutes to stop the reaction.

Primer design

For the design of primers, we were used the NCBI databases (http://www.ncbi.nlm.nih.gov/entrez) and BLAST (http://www.ncbi.nlm.nih.gov/BLAST) and the specificity of each primer constructed, validated by the use of free software online, Wizard and Primer3 primer (http://frodo.wi.mit.edu/primer3) (Melting temperature; amounts in GC; primer length; length amplified). The sequences of the primers were purchased from SIGMA ALDRICH, resuspended in sterile water to a final concentration of 100 μM and stored at -20°C (Tab. 9).

	Primer forward	Primer reverse
MuRF1	ACCTGGTGGAAAACATC	CTTCGTGTTCCTTGCA CATC
Atrogin-1	GCAAACACTGCCACATTCTC TC	CTTGAGGGGAAAGTG AGACG
Cathepsinl	GCGCGTGACTGGTTGAG	AAAGGCAGCAAGGAT GAGTG
PGC-1alpha	ACCCCAGAGTCACCAAATGA	CGAAGCCTTGAAAGGGT TATC
Ppia HK gene	Quanti Tect Primer Assay (Qiagen, Valencia, CA, USA)	

Table 9: List of sequence of primers used.

Efficiency primer validation

The amplicons exponentially doubling at every cycle. However, the amplification depends on the effectiveness of each primer to bind specifically to the sequence without creating structures in hairpin or stem-loop or dimers of primers. The traditional method to determine the amplification efficiency requires a calibration curve, in which a sample is serially diluted with a known concentration.

For each pair of primers, the calibration curve with serial dilution (10-1) has been performed; the Ct values thus obtained, were analyzed with respect to the initial amount of template in a semi-logarithmic scale; the values thus obtained, were positioned with respect to a straight line, and calculated the slope, using the equations:

Exponential amplification:
10$^{(-1/slope)}$

or, Efficiency Reaction:
[10$^{(-1/slope)}$]-1

it has made it possible to calculate the efficiency of each reaction.

The optimal values of the slope are equal to -3.322 for a 2 efficiency, i.e the 100%.
In this project only the primers with an R^2 of value between 0.97 and 0.99, was taken into consideration.
To assess the presence of dimers of primers, only one melting peak, corresponding to specific amplicon, must appear; on the contrary, all the primers showed more melting peaks, were not taken into account for the Real Time-PCR experiments.

Real Time-PCR

The Real Time PCR is a method that is based on the amplification and quantification of DNA. The technique, unlike a traditional PCR "end point", exploits the use of fluorescent molecules or probes, which allow to follow in real time and quantify the amplification reaction.
In our case, it used the probe SYBR Green I, a fluorescent molecule does not specify that binds to the minor groove of the DNA double helix level.
Samples of the muscles c-DNA were prepared using the SYBR® Green PCR Master Mix (Applied Biosystems, Warrington, UK) consisting of a HotStart Taq DNA Polymerase, a SYBR Green I probe, MgCl2 at a concentration of 5 mM, dNTP , and the fluorescent dye ROX passive reference. The latter serves as an internal reference to normalize the signal emitted by the SYBR Green I probe, thereby enabling to correct possible variations between the wells due to experimental errors and/or due to fluctuations of the fluorescence. For each gene to be studied, the reaction was carried out in duplicate.
The mixture, having a final volume of 30 μl, contained 15μl of SYBR Green PCR Master Mix, 0.6 μl of oligo primers specific to each gene, 3 μl of cDNA mold of each sample and 12 μl of sterile H$_2$O to bring to volume.
The reaction was performed using the AB PRISM 7500 instrument (Applied Biosystems, Warrington, UK).
The protocol used for the reaction of gene amplification consists of 4 steps:

(i) a pre-incubation cycle of 10 minutes at 95°C to activate the HotStart Taq polymerase and denature the DNA
(ii) 45 cycles of amplification, each of them divided in a phase in which the sample is brought to 95°C for 15 seconds for denaturation, a step of 60 seconds at 60°C in which there is the annealing of primer and a step of 30 seconds at 72°C in which there is the elongation of the DNA strand. In this last phase the probe intercalates DNA and acquire the basic fluorescence to quantify.

Analysis of Melting curve

Through the analysis of a graph, in which the abscissa is the number of cycles and the ordinate the logarithm of the fluorescence, is obtained for each sample a sigmoid in which one can observe a region to increase exponentially (Fig. 15). The data is automatically analyzed by the software once you have chosen the central point of the exponential part of the curve for the sample with the highest concentration (the one that reaches the loop-line after a smaller number of cycles).

In the relative quantification, the concentration of the gene of interest (target) is expressed as a function of the concentration of a reference gene (housekeeping gene), which is assumed to be constant between the different tissues of an organism, in all stages of development (expressed constitutively) and should not suffer modifications due to the experimental treatment. In our case, to normalize the samples was chosen the housekeeping gene *Ppia* (cyclophilin A).

The ΔCT was calculated by subtracting the CT of control FVB mice to CT of Tg mice transgenic for both for both target genes for the housekeeping gene; the values obtained by the target genes were normalized on the values obtained by the housekeeping gene.
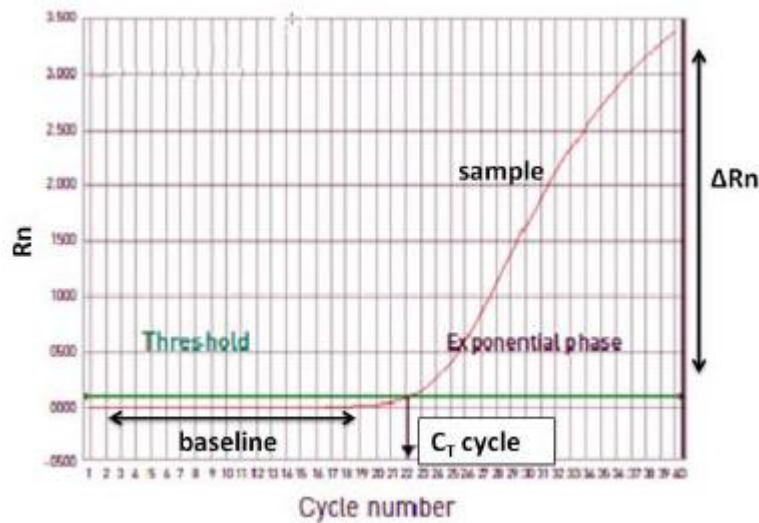
Fig. 15: **Model of an amplification plot in a single sample**; at the level of the base line (*baseline*) does not occur any significant change in the fluorescence signal (*Rn*); during the exponential phase, the fluorescence signal increases proportionally with respect to the amount of amplification products.
The *Threshold* is the line of the fluorescence signal level determined automatically by the software and is set above the baseline and sufficiently low as to fall within the exponential growth region of the amplification curve.
The C_T is the cycle number of the amplification cycle when the fluorescence signal crosses the threshold.

Statistical analysis

All data are expressed as mean values ± standard error of the mean (s.e.m). Statistical analysis was performed using two-way ANOVA analysis of variance with Bonferroni *post hoc* test and Student's *t*-test, and the level of significance was set to p≤0.05.

Results

Skeletal muscle deterioration by dilated cardiomyopathy (DCM)

The results obtained from the animal model of dilated cardiomyopathy ($Tg\alpha_q*44$ transgenic mice model) are described and discussed in this section.

The analysis were performed on gastrocnemius and soleus muscle taken as an example of "fast" and "slow" muscle, at different stages of the disease, 6, 12 and 14 months of age. All experiments were performed on *Tg* DCM and FVB age-matched control mice, with and without a protocol of 2 months of free wheel running.

Effect of 2 months of voluntary wheel running activity (VWRA)

In order to test the presence of exercise intolerance (EI) and to verify the effect of endurance training on muscle adaptive responses, the *in vivo* functional performance was analyzed on Tg DCM mice and compared to the effect of exercise *per se* on FVB control mice.

The functional performance of individual mice was calculated as mean of total distance (Km) and total time (h), recording 24h no stop during the 2 months of voluntary activity. A significant reduction of total distance of running and of total time of running was observed at 14 months in Tg+EX mice respect to age-matched FVB+EX control mice (Fig. 16).
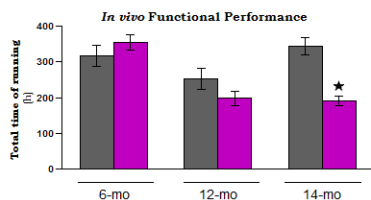
A   **B**
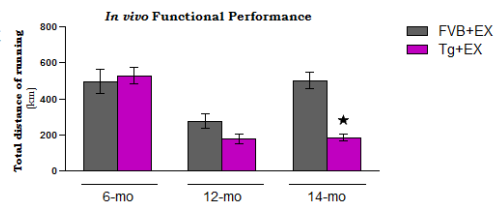
Fig. 16: *In vivo* functional test. (A) Total distance of running and **(B)** total time of running (mean±SEM) covered during 2 months of VWRA, in control exercised mice (FVB+EX) and in transgenic DCM exercised mice (Tg+EX), at 6, 12 and 14 months of age. n=11/13 for each group. Data are shown as mean±s.e.m. Two-way ANOVA analysis-Bonferroni *post hoc* test, level of significance set to p≤0.05.
A: Total distance of running; ★ Tg+Ex sign diffent from age-matched FVB+EX (p<0.001)
B: Total time of running; ★ Tg+Ex sign diffent from age-matched FVB+EX (p<0.001)

In order to better determine the effect of VWRA on functional performance, the functional performance at the beginning and at the end of the VWRA was also compared.

This effect was calculated through the comparison of average value of distance and time covered daily by mice in the first 3 days (start time: 2°, 3° and 4° day, excluding the first day for the accommodation phenomenon) and in the last 3 days of VWRA (end time: 58°, 59° and 60° day), assuming that at the start time mice are still not considered trained and the distance covered by mice reflects the basal functional capacity of both FVB and Tg mice. As indicated in Figure 17, the in vivo performance has improved significantly both in FVB and Tg mice at all stages of the disease. In fact, a significant increase of daily distance was observed in FVB mice at 6 and 12 months of age (Fig. 17A) and in Tg mice at 6, 12 and 14 months of age (Fig. 17B).

Figure 17 panel C shows the in vivo functional basal activity of FVB and Tg mice. No significant differences were observed in functional performance of FVB and Tg mice before the 2 months of VWRA. Interestingly, after 2 months of VWRA a reduction of the daily distance was observed in Tg mice only at 14 months of age, i.e. at the late stage of the disease (Fig. 17D).

As regard the average time of the daily activity at the start and end time, no significant differences were observed in FVB mice, whereas a significant increase was found in Tg mice at 6 months of age (Fig.17E and F).

From the comparison of the time of daily activity, a significant reduction was observed at 14 months of age in FVB and Tg mice both at the beginning (Fig.17G) and at the end (Fig.17H) of VWRA.

**A**   **B**

C   **D**

64
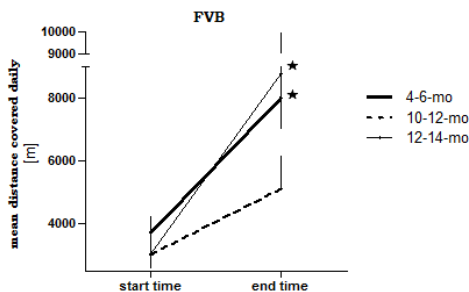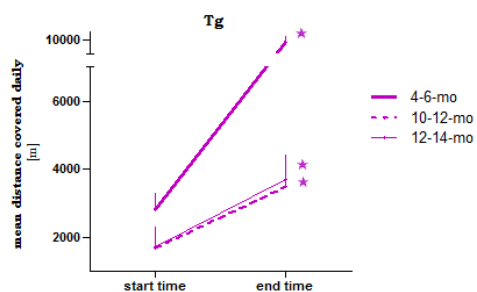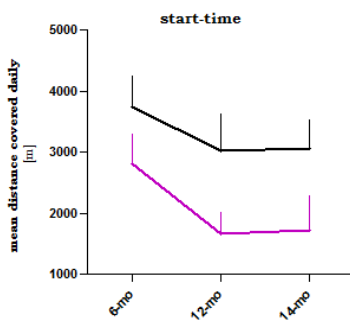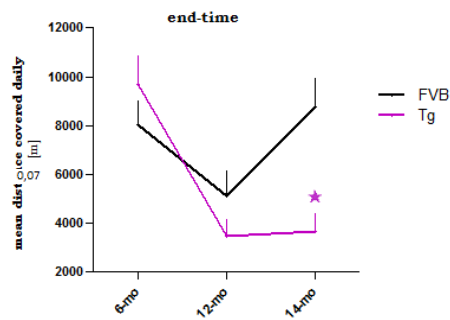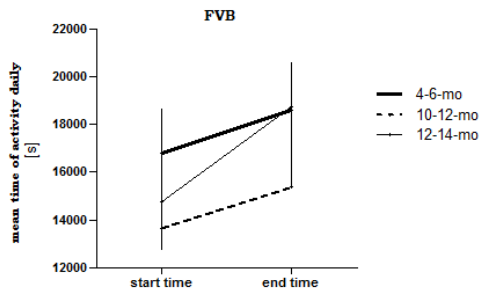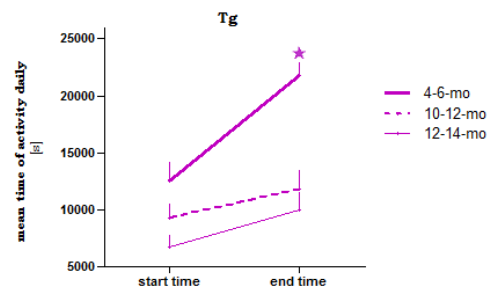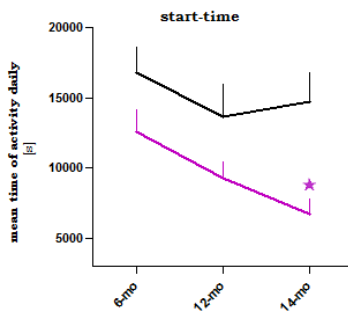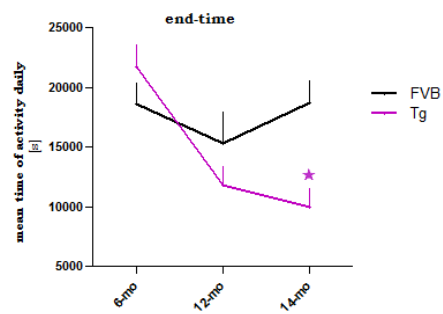
Fig. 17: *In vivo* **functional test.** Mean of distance covered daily during end time respect to start time in FVB+EX mice **(A)** and in Tg+EX mice **(B)**; mean of distance covered daily during start time **(C)** and during end time **(D)** between FVB+EX and Tg+EX; mean of time of activity daily during end time respect to start time in FVB+EX mice **(E)** and in Tg+EX mice **(F)**; mean of time of activity daily during start time **(G)** and during end time **(H)** between FVB+EX and Tg+EX.

n=11/13 for each group. Data are shown as mean±s.e.m. Student's *t*-test analysis, level of significance set to p≤0.05.

A: mean distance of running daily; ★ end time sign diffent from start time

B: mean distance of running daily; ★ end time sign diffent from start time

D: mean distance of running daily; ★ end time Tg+EX sign diffent from end time age-matched FVB+EX

F: mean time of activity daily; ★ end time sign diffent from start time

G: mean time of activity daily; ★ start time Tg+EX sign diffent from start time age-matched FVB+EX

H: mean time of activity daily; ★ end time Tg+EX sign diffent from end time age-matched FVB+EX

Effect of DCM and endurance exercise on Myosin Heavy Chain (MyHC) isoform composition

Gastrocnemius and soleus muscles of Tg and FVB mice, at 6-12-14 months of age, were collected in order to analyze the effect of dilated cardiomyopathy and exercise on muscle phenotype (MyHC isoforms composition).

Gastrocnemius muscle

Effect of cardiomyopathy: In Tg cardiopathic mice, a significant slow-to-fast shift in MyHC isoforms expression was observed at 6 months, respect to the age-matched FVB mice, with a reduction of type 1 and 2A, and an increase of type 2B isoforms percentage (Fig. 18A). At 12 months, Tg mice did not show significant change in MyHC composition respect to age-matched FVB mice, in fact, only a trend in type 2A reduction and type 2B increase was observed (Fig. 18C). Instead, Tg 14 months old mice, showed a significant slow-to-fast shift of MyHC isoforms composition, respect to age-matched FVB mice, with a reduction of type 1 and 2A isoforms, and an increase of type 2X and 2B (Fig. 18E).

Effect of exercise: In FVB+EX mice no significant change in MyHC pattern expression was observed after exercise, respect to the age-matched FVB mice, at any time analyzed (Fig. 18A, C and E).

In Tg+EX mice, a significant fast-to-slow shift in MyHC isoforms expression was observed at 6 months, respect to age-matched Tg mice, with an increase of type 1 and 2A, and a reduction of type 2B (Fig. 18A). At 12 months, Tg+EX mice, did not show significant change in MyHC pattern expression respect to age-matched Tg mice (Fig. 18C) whereas, at 14 mo, a significant fast-to-slow shift in MyHC pattern expression was observed respect to age-matched Tg mice, with an increase of type 2A and a reduction of type 2X (Fig. 18E).

Soleus muscle

Effect of cardiomyopathy: In Tg cardiopathic mice, a significant slow-to-fast shift in MyHC isoforms expression was observed at 6 months, respect to age-matched FVB mice, with a reduction of type I and an increase of type IIX (Fig. 18B). At 12 and 14 months, Tg mice did not show significant change in MyHC composition respect to age-matched FVB mice (Fig. 18D and F).

Effect of exercise: In FVB+EX mice no significant change in MyHC pattern expression was observed after exercise, respect to age-matched FVB mice, at any time analyzed (Fig. 18B, D and F).

In Tg+EX mice, a significant fast-to-slow shift in MyHC isoforms expression was observed at 6 months, respect to age-matched Tg mice, with an increase of type IIA and a reduction of type IIX (Fig. 18B) At 12 and 14 months, Tg+EX mice, did not show significant change in MyHC pattern expression respect to age-matched Tg mice (Fig. 18D and F).
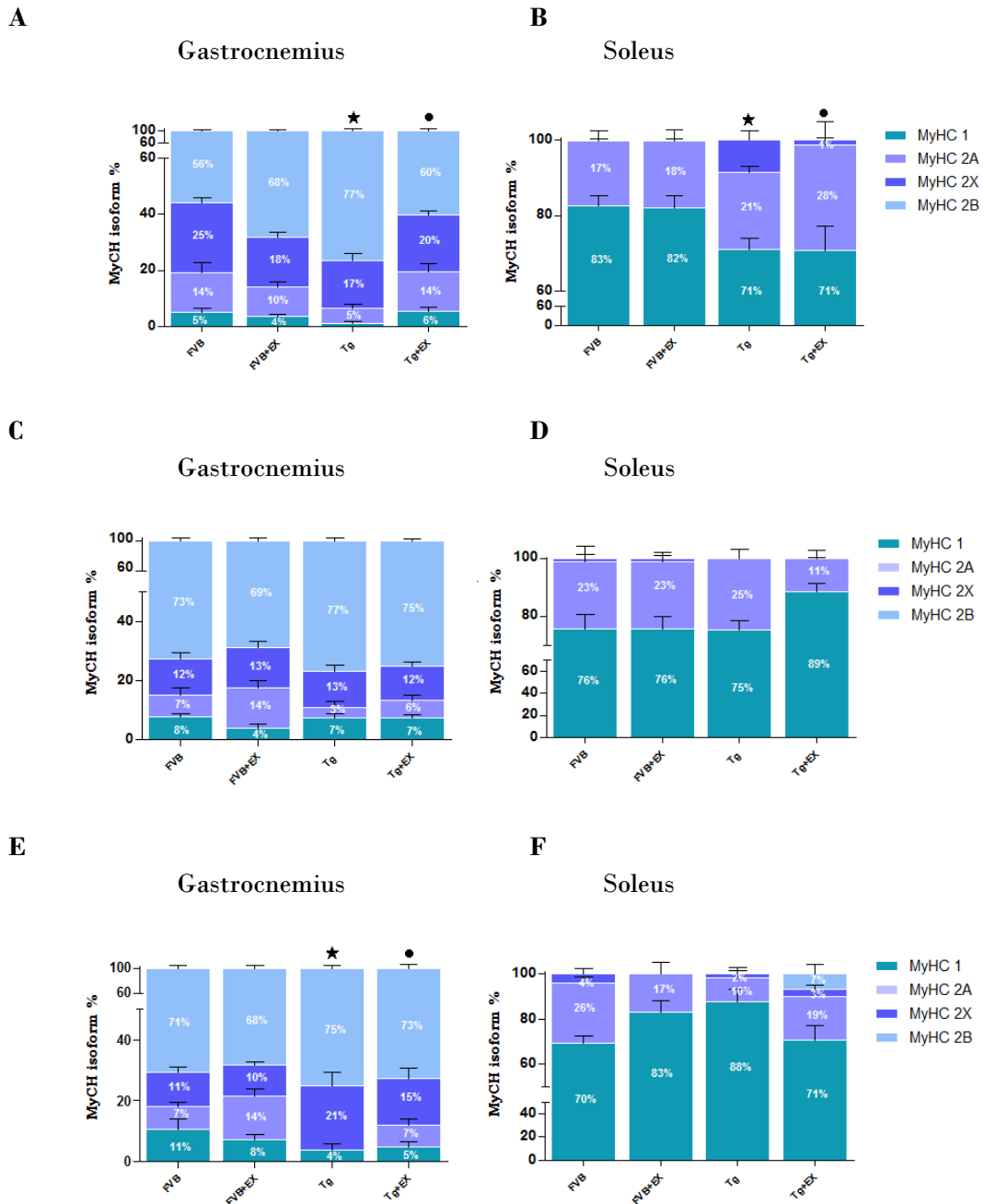
Fig. 18: Relative distribution of MHC isoform at 6 months of age, in Gastrocnemius (**A**) and in Soleus muscle (**B**); at 12 months of age, in Gastrocnemius (**C**) and in Soleus muscle (**D**); at 14 months of age, in Gastrocnemius (**E**) and in Soleus muscle (**F**), in FVB, FVB+EX, Tg and Tg+EX respectively.

n=11/13 for each group. Data are shown as mean±s.e.m. Student's *t*-test analysis, level of significance set to p≤0.05.

A: MyHC isoform %; ★ Tg sign diffent from FVB; ● Tg+EX sign different from Tg

B: MyHC isoform %; ★ Tg sign diffent from FVB; ● Tg+EX sign different from Tg

E MyHC isoform %; ★ Tg sign diffent from FVB; ● Tg+EX sign different from Tg

Effect of DCM and endurance training on skeletal muscle metabolism

Several factors is tought to be in part responsible for exercise intolerance during heart failure, including alteration in metabolic adaptations. The following metabolic key molecules were analyzed: (i) PGC-1alpha protein and mRNA expression, the transcription factor involved in mitochondrial biogenesis, (ii) AMPK protein expression, the cellular energy sensor, (iii) DRP1 protein expression, involved in mitochondrial fission machinery, (iv) Mfn1 and Mfn2 protein expression, involved in mitochondrial fusion machinery, and (v) oxidative and (vi) glycolitic enzymes, in gastrocnemius and soleus muscle.

Oxidative metabolism:

PGC-1α

Gastrocnemius muscle

Effect of cardiomyopathy: In Tg cardiopathic mice, a significant PGC-1α protein and gene expression reduction was observed respect to age-matched FVB mice, at all stages of the disease, with the exception of PGC-1α protein expression at 14 months and PGC-1α gene expression at 6 months, that resulted unchanged in Tg mice (Fig. 19A and 20A).

Effect of exercise: In FVB+EX mice, a significant PGC-1α protein expression reduction was observed at 12 months, respect to age-matched FVB mice (Fig. 19A).

In Tg+EX mice, a significant PGC-1α protein expression up-regulation was observed at 14 months, respect to age-matched Tg mice (Fig. 19A).

Soleus muscle
No differences in PGC-1α protein and gene expression were observed for each group, at any time analyzed (Fig. 19B and 20B), with the exception of significant PGC-1α gene expression reduction in Tg cardiopathic mice, at 14 months (Fig. 20B).

A

Gastrocnemius

B

Soleus

A

Gastrocnemius

B

Soleus

Energy metabolism:

AMPK

Gastrocnemius muscle

Effect of cardiomyopathy: In Tg cardiopathic mice, a significant reduction in the ratio between the phosphorylated and total AMPK (pAMPK/AMPK) was observed respect to age-matched FVB mice, at all stages of disease (Fig. 21A).

Effect of exercise: In FVB+EX mice, a significant reduction in the ratio between the phosphorylated and total AMPK (pAMPK/AMPK) was observed respect to age-matched FVB mice, at all stages of disease (Fig. 21A).

Differently from FVB+EX, in Tg+EX mice, a significant up-regulation in the ratio between the phosphorylated and total AMPK (pAMPK/AMPK) was observed at 6 and 14 months, respect to age-matched Tg and FVB+EX mice (Fig. 21A).

Soleus muscle
No difference in the ratio between the phosphorylated and total AMPK (pAMPK/AMPK) was observed in Tg and in FVB+EX mice, at any time analyzed (Fig. 21B).

Effect of exercise: In Tg+EX mice, a significant up-regulation in the ratio between the phosphorylated and total AMPK (pAMPK/AMPK) was observed at 6 months, respect to age–matched Tg mice (Fig. 21B) and, at 14 months, respect to age-matched FVB+EX mice (Fig. 21A).

A

Gastrocnemius
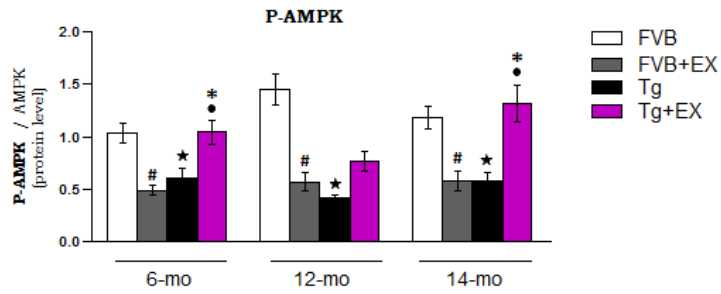
B
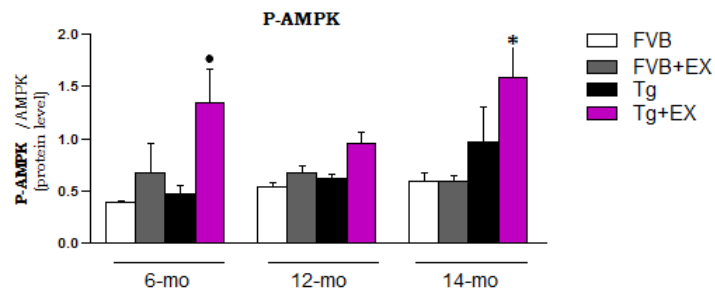
Soleus

Fig. 21: Western blot analysis of P-AMPK/AMPK relative ratio. Relative protein level in Gastrocnemius muscle **(A)** and relative protein level in soleus muscle **(B)** at 6, 12 and 14 months of age, in FVB, FVB+EX, Tg and Tg+EX respectively.

n=4 for each group in Gas; n=3 for each group in soleus. Data are shown as mean±s.e.m. Two-way ANOVA analysis-Bonferroni *post hoc* test; level of significance set to p≤0.05.

A: P-AMPK/AMPK relative ratio; ★ Tg sign diffent from FVB; ● Tg+EX sign different from Tg; * Tg+EX sign different from FVB+EX; # FVB+EX sign different from FVB

B: P-AMPK/AMPK relative ratio; ● Tg+EX sign different from Tg; * Tg+EX sign different from FVB+EX

Mitochondrial dynamic:
DRP1-fission related protein

Gastrocnemius muscle

Effect of cardiomyopathy: In Tg cardiopathic mice, a significant DRP1 protein expression reduction was observed at 6 and 12 months, respect to age-matched FVB mice (Fig. 22A).

Effect of exercise: No difference in DRP1 protein expression was observed in FVB+EX mice, at any time analyzed (Fig. 22A).

In Tg+EX mice, a significant DRP1 protein expression up-regulation was observed at 14 months respect to age-matched Tg mice (Fig. 22A).

Soleus muscle

No difference in DRP1 protein expression was observed for each group, at any time analyzed (Fig. 22B).

A
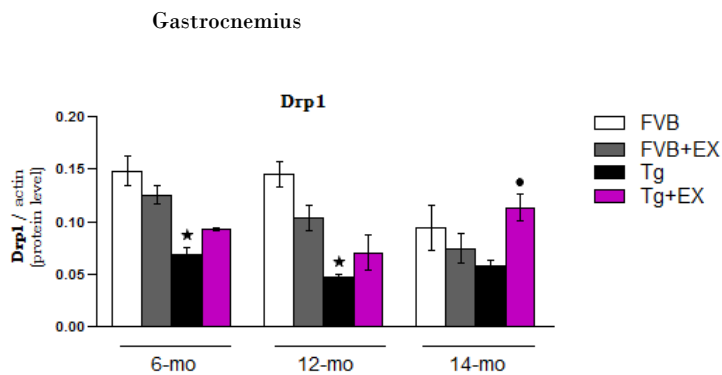
B
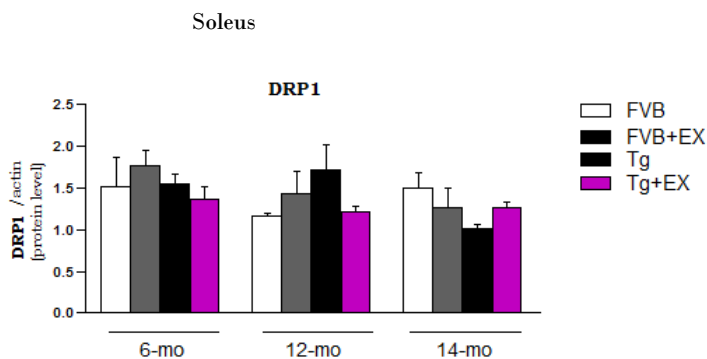
Fig. 22: Western blot analysis of DRP1 normalized on actin ponceau protein. Relative protein level in Gastrocnemius muscle **(A)** and effect of ageing **(B)**, and relative protein level in soleus muscle **(C)** and effect of ageing **(D)** at 6, 12 and 14 months of age, in FVB, FVB+EX, Tg and Tg+EX respectively.
n=4 for each group in Gas; n=3 for each group in soleus. Data are shown as mean±s.e.m. Two-way ANOVA analysis-Bonferroni *post hoc* test; level of significance set to $p \leq 0.05$.
A: DRP1 relative protein level; ★ Tg sign diffent from FVB; ● Tg+EX sign different from Tg

Mitochondrial dynamic:
Mfn1/2-fusion related protein

Gastrocnemius muscle

Since alterations in master control of oxidative metabolism i.e. PGC-1α were found only in gastrocnemius, the mitochondrial fusion, oxidative and glycolitic enzymes, have been investigated only in gastrocnemius muscle.

Effect of cardiomyopathy: In Tg cardiopathic mice, Mfn1 protein expression reduction was observed at 12 and 14 months, respect to age-matched FVB mice, which reached the statistical significance at 12 months (Fig. 23A). No difference in Mfn2 protein expression was oserved (Fig. 23B).

Effect of exercise: In FVB+EX mice, a significant Mfn1 protein expression reduction was observed respect to age-matched FVB mice, at alla stages of disease (Fig. 23A) and only at 12 months Mfn2 (Fig. 23B).

In Tg+EX mice, a significant Mfn1 protein expression reduction (Fig. 23A) and Mfn2 protein expression up-regulation (Fig. 23B) was observed at 6 mo, respect to age-matched Tg mice. Furthermore, a significant Mfn1 and Mfn2 protein expression up-regulation (Fig. 23A and B) was observed at 14 and at 12 months respectively, respect to age-matched FVB+EX mice.

A
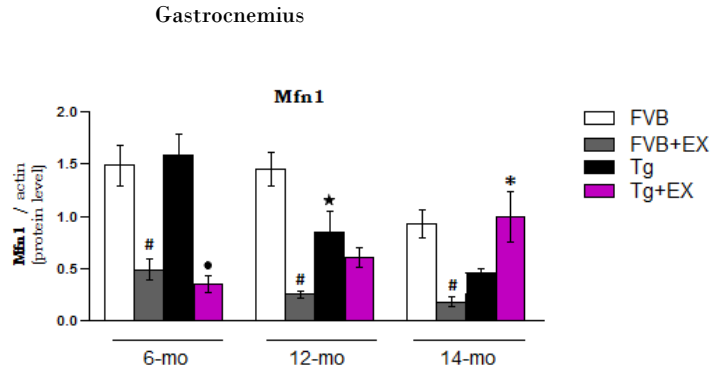
Gastrocnemius

B
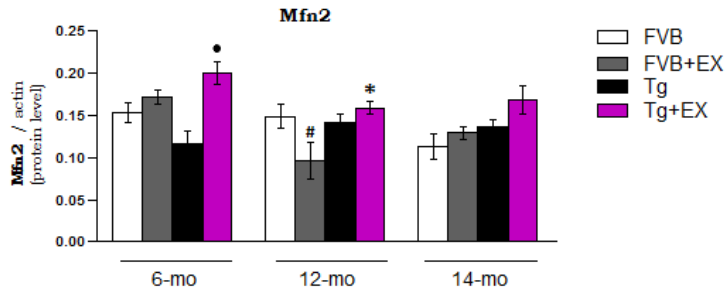
**Fig. 23: Western blot analysis of Mfn1 and Mfn2 normalized on actin ponceau protein.** Relative protein level in Gastrocnemius muscle of Mfn1 (**A**) and relative protein level in Gastrocnemius of Mfn2 (**B**) at 6, 12 and 14 months of age, in FVB, FVB+EX, Tg and Tg+EX respectively.

n=4 for each group in Gas. Data are shown as mean±s.e.m. Two-way ANOVA analysis-Bonferroni *post hoc* test; level of significance set to p≤0.05.

A: Mfn1 relative protein level; ★ Tg sign diffent from FVB; ● Tg+EX sign different from Tg; * Tg+EX sign different from FVB+EX; **#** FVB+EX sign different from FVB

B: Mfn2 relative protein level; ● Tg+EX sign different from Tg; * Tg+EX sign different from FVB+EX; **#** FVB+EX sign different from FVB

Oxidative and glycolitic enzymes

Gastrocnemius muscle

<u>Effect of cardiomyopathy:</u> In Tg cardiopathic mice, a significant complex IV protein expression reduction was observed at 12 months, respect to age-matched FVB mice (Fig. 24D). However, a trend in complex I, II and III protein expression reduction was also observed at 12 months (Fig. 24A, B and C).

<u>Effect of exercise:</u> No difference in OXPHOS complexes protein expression was observed in FVB+EX and Tg+EX mice, at any time analyzed (Fig. 24A, B, C, D and E).

A

Gastrocnemius
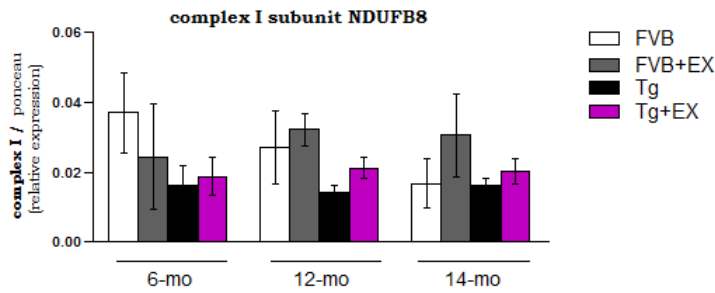
B
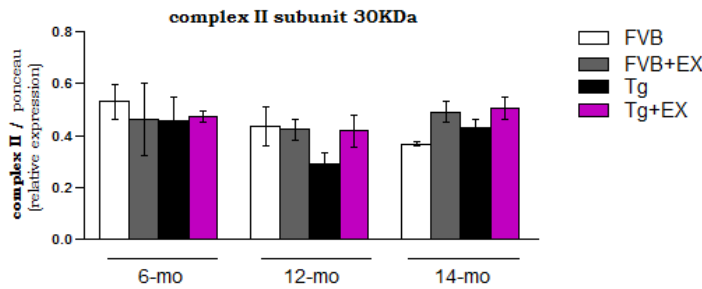
C
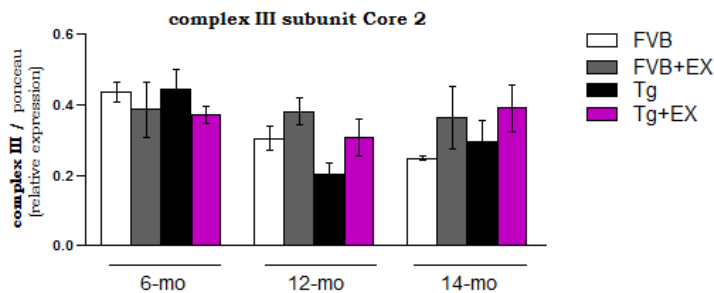
D
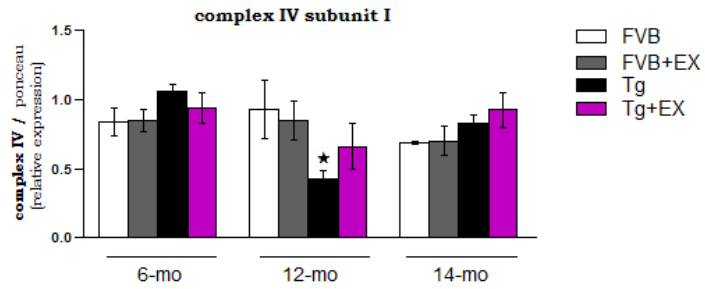
E
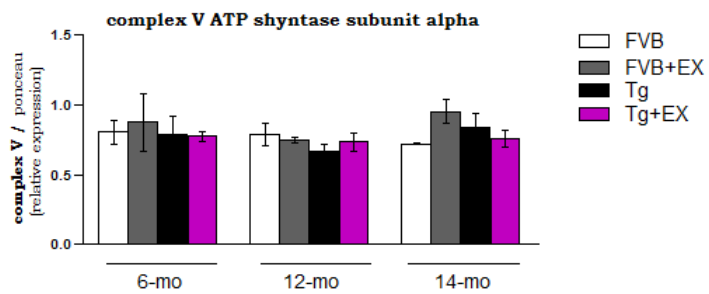
Fig. 24: Western blot analysis of OXPHOS complexes normalized on ponceau. Relative protein level in Gastrocnemius muscle of complex I (**A**); of complex II (**B**); of complex III (**C**); of complex IV (**D**) and of complex V (**E**) at 6, 12 and 14 months of age, in FVB, FVB+EX, Tg and Tg+EX respectively.
n=4 for each group in Gas. Data are shown as mean±s.e.m. Two-way ANOVA analysis-Bonferroni *post hoc* test; level of significance set to p≤0.05.
D: OXOPHOS complex protein expression; ★ Tg sign different from FVB

Gastrocnemius muscle

<u>Effect of cardiomyopathy:</u> In Tg cardiopathic mice, a significant TPI protein expression up-regulation was observed at 12 months, respect to age-matched FVB mice (Fig. 25).

<u>Effect of exercise:</u> In FVB+EX, TPI protein expression significantly increased at 12 months, respect to age-matched FVB mice (Fig. 25).

No difference in TPI protein expression was observed in Tg+EX, at any time analyzed (Fig. 25).
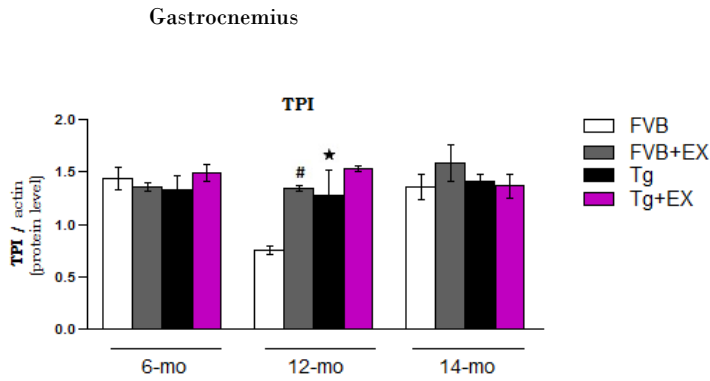
Gastrocnemius

Fig. 25: Western blot analysis of TPI normalized on actin ponceau protein. Relative protein level in Gastrocnemius muscle at 6, 12 and 14 months of age, in FVB, FVB+EX, Tg and Tg+EX respectively.
n=4 for each group in Gas. Data are shown as mean±s.e.m. Two-way ANOVA analysis-Bonferroni *post hoc* test; level of significance set to $p \leq 0.05$.
A: TPI relative protein level; ★ Tg sign diffent from FVB; # FVB+EX sign different from FVB

Effect of DCM and endurance training on skeletal muscle Redox-homeostasis

One of the potential mechanism involved in development of exercise intolerance, is oxidative stress. To clarify its involvement in DCM muscle response, we analyzed redox-status in fast gastrocnemius and slow soleus muscle, before and after 2 months of endurance training, both in wild type and cardiopathic mice (i) by studying antioxidant defense system adaptations (SOD1 and Catalase) and (ii) by measuring protein oxidation index.

Anti-oxidant defence system

Gastrocnemius muscle

Effect of cardiomyopathy: In Tg cardiopathic mice, a SOD1 protein expression reduction was observed at 12 and 14 months, statistically significant at 14 months, respect to age-matched FVB mice (Fig. 27A). A Catalase protein expression reduction was observed only at 12 months (Fig. 28A).

Effect of exercise: No differeces in SOD1 and Catalase protein expression were observed in FVB+EX mice, at any time analyzed (Fig. 27A and 28A), with the exception of SOD1 protein expression reduction at 14 months (Fig. 27A).

In Tg+EX mice, a significant SOD1 protein expression reduction was observed at 6 months, respect to age-matched FVB+EX mice (Fig. 27A). Furthermore, a significant SOD1 protein expression up-regulation was observed at 14 months, respect to age-matched Tg and FVB+EX mice (Fig. 27A). No difference in Catalase protein expression was observed (Fig. 28A).

It was also evaluated the presence of the final product of a redox alteration through the analysis of protein carbonylation levels.

Effect of cardiomyopathy: In Tg cardiopathic mice, a significant protein oxidation index increase was observed at 12 and 14 months, respect to the age-matched FVB mice (Fig. 29A).

Effect of exercise: No differece in protein oxidation index was observed in FVB+EX mice, at any time analyzed (Fig. 29A).

In Tg+EX mice, protein oxidation was prevented only at 12 months (Fig. 29A).

Soleus muscle
No differences in SOD1 and Catalase protein expression and in oxidation index were observed for each group, at any time analyzed (Fig. 27B, 28B and 29B).

A

Gastrocnemius

B
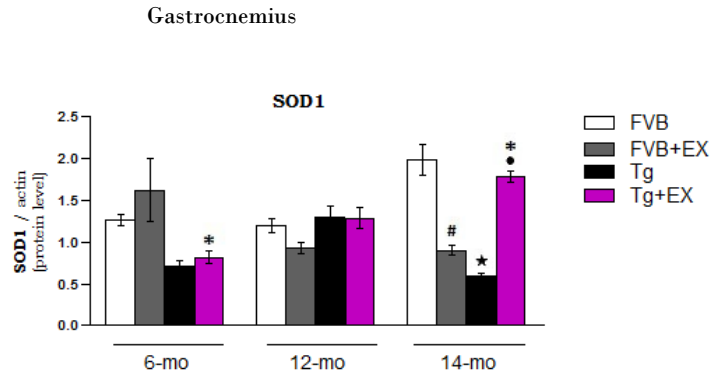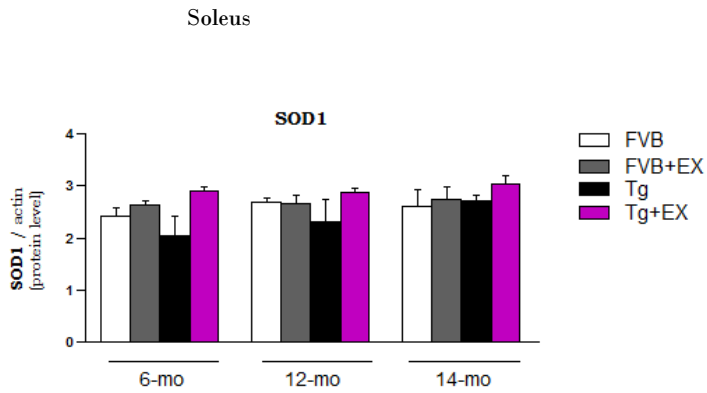
Soleus

Fig. 27: **Western blot analysis of SOD1 normalized on actin ponceau protein.** Relative protein level in Gastrocnemius muscle **(A)** and relative protein level in soleus muscle **(B)** at 6, 12 and 14 months of age, in FVB, FVB+EX, Tg and Tg+EX respectively. n=4 for each group in Gas; n=3 for each group in soleus. Data are shown as mean±s.e.m. Two-way ANOVA analysis-Bonferroni *post hoc* test; level of significance set to p≤0.05.

A: SOD1 relative protein level; ★ Tg sign diffent from FVB; ● Tg+EX sign different from Tg; * Tg+EX sign different from FVB+EX; # FVB+EX sign different from FVB

A

Gastrocnemius

B
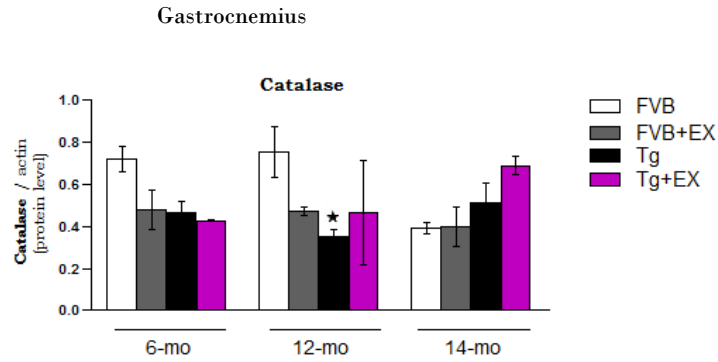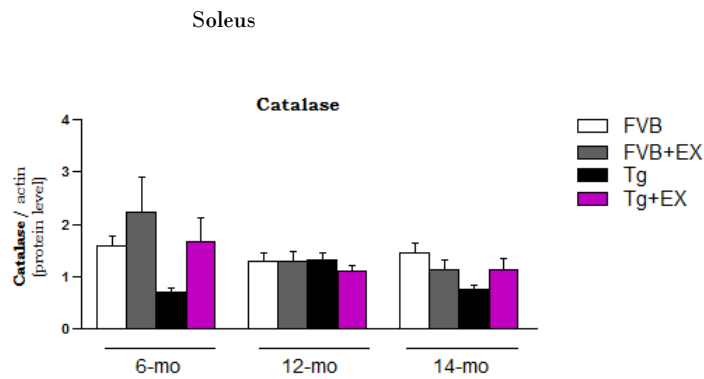
Soleus

Fig. 28: **Western blot analysis of Catalase normalized on actin ponceau protein.** Relative protein level in Gastrocnemius muscle **(A)** and relative protein level in soleus muscle **(B)** at 6, 12 and 14 months of age, in FVB, FVB+EX, Tg and Tg+EX respectively. n=4 for each group in Gas; n=3 for each group in soleus. Data are shown as mean±s.e.m. Two-way ANOVA analysis-Bonferroni *post hoc* test; level of significance set to p≤0.05.
A: Catalase relative protein level; ★ Tg sign diffent from FVB

A

Gastrocnemius
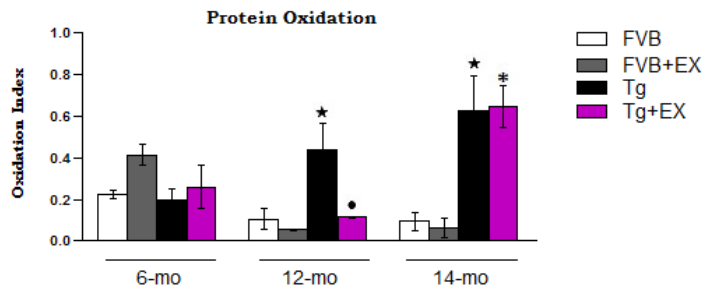
B
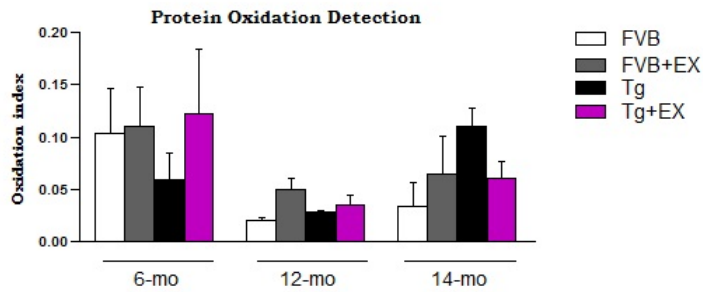
Soleus

Fig. 29: Western blot analysis of Protein Oxidation normalized on ponceau. Protein oxidation accumulation in Gastrocnemius muscle (**A**) and protein oxidation accumulation in soleus muscle (**B**) at 6, 12 and 14 months of age, in FVB, FVB+EX, Tg and Tg+EX respectively.

n=4 for each group in Gas; n=3 for each group in soleus. Data are shown as mean±s.e.m. Two-way ANOVA analysis-Bonferroni *post hoc* test; level of significance set to p≤0.05.

A: Protein oxidation index; ★ Tg sign diffent from FVB; ● Tg+EX sign different from Tg; * Tg+EX sign different from FVB+EX

Effect of DCM and endurance training on skeletal muscle degradation pathway

The contribution of the ubiquitin proteasome and the autophagy system to DCM and the time course of their activation, before an after 2 months of endurance exercise, was assessed in this thesis. The exercise-dependent ubiquitine proteasome and autophagy activation is still unclear, but evidence suggests that these systems are required to garantee cellular quality during endurance exercise (Lo Verso et la., 2014; Grumati et al., 2011).

Real time PCR and Western Blots analyses were used to assess the mRNA expression and the protein level of key factors of the above pathways, in both gastrocnemius and soleus muscles.

Ubiquitine proteasome pathway:
Atrogin-1 and MuRF1

To assess the ubiquitin proteasome pathway contribution in DCM, gene expression of Atrogin1 and MuRF1 ubiquitin ligases were studied, in both gastrocnemius and soleus muscle.

Gastrocnemius muscle

Effect of cardiomyopathy: In Tg cardiopathic mice, a significant Atrogin1 and MuRF1 gene expression reduction was observed at 12 months, respect to age-matched FVB mice (Fig. 30A and 31A).

Effect of exercise: No differeces in Atrogin1 and MuRF1 gene expression were observed in FVB+EX mice, at any time analyzed (Fig. 30A and 31A).

In Tg+EX mice, a significant Atrogin1 and MuRF1 gene expression up-regulation was observed at 6 and 12 months, respect to age-matched Tg and FVB+EX mice (Fig. 30A and 31A), with the exception of Atrogin1 gene expression at 12 months, statistically significant only respect to age-matched Tg mice (Fig. 30A).

Soleus muscle

Effect of cardiomyopathy: In Tg cardiopathic mice, a significant Atrogin1 and MuRF1 gene expression reduction was observed at 12 months, respect to age-matched FVB mice (Fig. 30B and 31B), with the exception of MuRF1 that was not statistically significant (Fig. 31B).

Effect of exercise: No differeces in Atrogin1 and MuRF1 gene expression were observed in FVB+EX mice, at any time analyzed (Fig. 30B and 31B).

In Tg+EX mice, high level of Atrogin1 mRNA was observed at 6 and 12 months, respect to age-matched Tg mice and at 6 months was also statistically significant respect to FVB+EX mice (Fig. 30B). However, a trend in MuRF1 gene expression up-regulation was also observed at 6 and 12 months (Fig. 31B).

A

Gastrocnemius
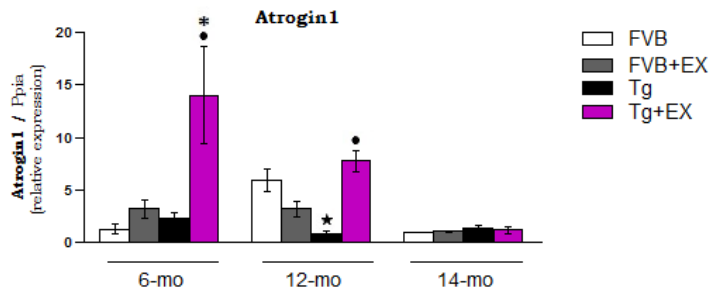
B
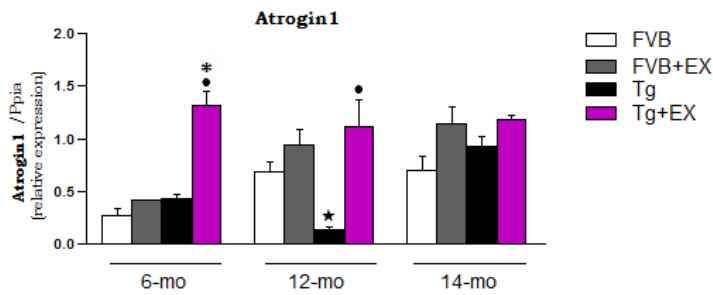
Soleus

Fig. 30: Gene expression analysis of Atrogin-1 normalized on Ppia gene. Relative mRNA expression in Gastrocnemius muscle **(A)** and relative mRNa expression in soleus muscle **(B)** at 6, 12 and 14 months of age, in FVB, FVB+EX, Tg and Tg+EX respectively. n=4 for each group in Gas; n=3 for each group in soleus. Data are shown as mean±s.e.m. Two-way ANOVA analysis-Bonferroni *post hoc* test; level of significance set to p≤0.05.

A: Atrogin-1 gene expression; ★ Tg sign diffent from FVB; ● Tg+EX sign different from Tg; ✱ Tg+EX sign different from FVB+EX

B: Atrogin-1 gene expression; ★ Tg sign diffent from FVB; ● Tg+EX sign different from Tg; ✱ Tg+EX sign different from FVB+EX

A

Gastrocnemius
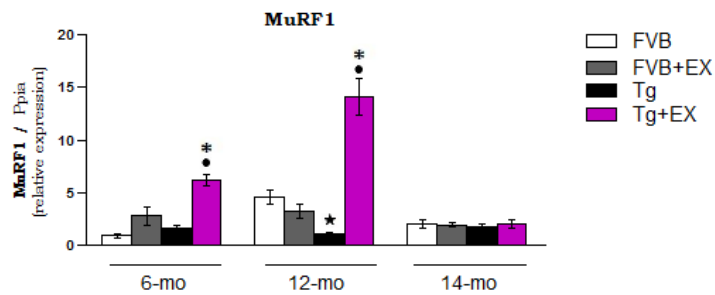
B
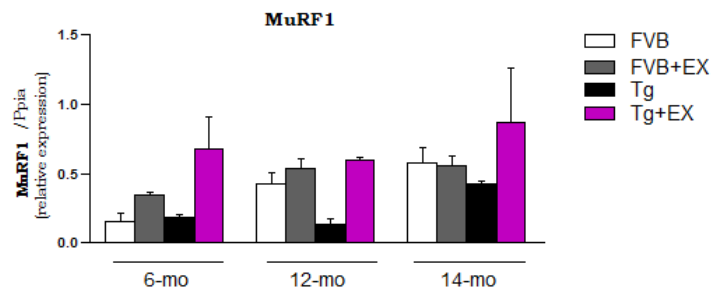
Soleus

Fig. 31: Gene expression analysis of MuRF1 normalized on Ppia gene. Relative mRNA expression in Gastrocnemius muscle **(A)** and relative mRNa expression in soleus muscle **(B)** at 6, 12 and 14 months of age, in FVB, FVB+EX, Tg and Tg+EX respectively. n=4 for each group in Gas; n=3 for each group in soleus. Data are shown as mean±s.e.m. Two-way ANOVA analysis-Bonferroni *post hoc* test; level of significance set to p≤0.05.
A: MuRF1 gene expression; ★ Tg sign diffent from FVB; ● Tg+EX sign different from Tg; * Tg+EX sign different from FVB+EX

Autophagy pathway:
LC3 and Cathepsin L

To assess autophagy pathway involvement in DCM, LC3 protein level and CathepsinL gene expression, two key markers of autophagy machinery, were studied in both gastrocnemius and soleus muscle.

Gastrocnemius muscle

<u>Effect of cardiomyopathy:</u> In Tg cardiopathic mice, a significant reduction in the ratio between the active and precursor LC3 (LC3II/LC3I) was observed at 14 months, respect to age-matched FVB mice (Fig. 32A). No difference in ChatepsinL gene expression was observed (Fig. 33A).

<u>Effect of exercise:</u> In FVB+EX mice, a significant reduction in ratio between the active and precursor LC3 (LC3II/LC3I) was observed at 14 months, respect to age-matched FVB mice (Fig. 32A). No difference in ChatepsinL gene expression was observed (Fig. 33A).

In Tg+EX mice, a significant increase in LC3II/LC3I ratio (at 6 months) and ChatepsinL gene expression (at 12 months) was observed, respect to age-matched Tg and FVB+EX mice (Fig. 32A and 33A).
Furthermore, the exercise failed to prevent autophagy inhibition found at 14 months in Tg cardiopathic mice. In fact, a significant reduction in LC3II/LC3I ratio was observed at 14 months, respect to age-matched FVB mice (Fig. 32A).

Soleus muscle

No differences in LC3II/LC3I ratio and in CathepsinL gene expression were observed for each group, at any time analyzed (Fig. 32B and 33B).

A

Gastrocnemius

B
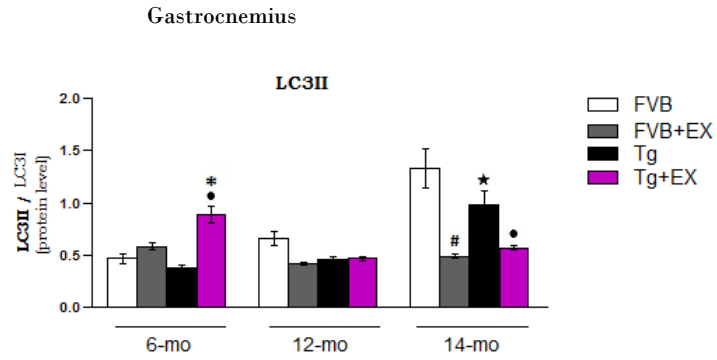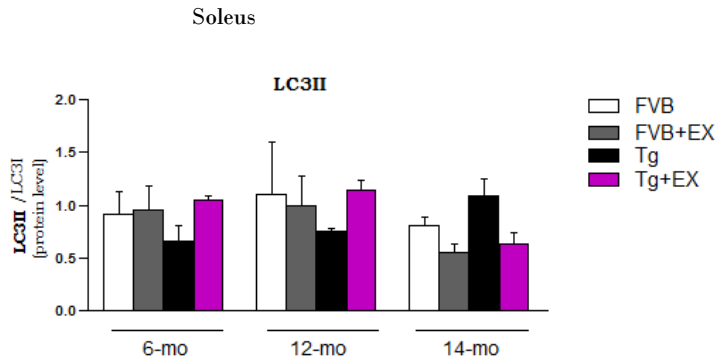
Soleus

Fig. 32: Western blot analysis of LC3II/LC3I relative ratio. Relative protein level in Gastrocnemius muscle (**A**) and relative protein level in soleus muscle (**B**) at 6, 12 and 14 months of age, in FVB, FVB+EX, Tg and Tg+EX respectively.

n=4 for each group in Gas; n=3 for each group in soleus. Data are shown as mean±s.e.m. Two-way ANOVA analysis-Bonferroni *post hoc* test; level of significance set to p≤0.05.

A: LC3II/LC3I relative ratio; ★ Tg sign diffent from FVB; ● Tg+EX sign different from Tg; ✳ Tg+EX sign different from FVB+EX; # FVB+EX sign different from FVB

A
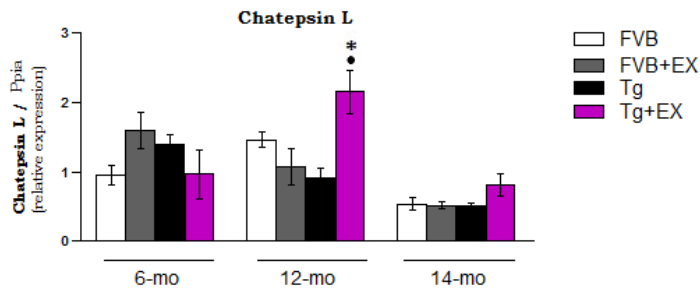
Gastrocnemius

B
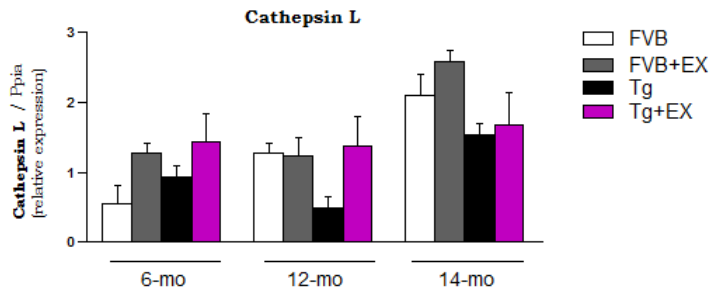
Soleus

Fig. 33: Gene expression analysis of CathepsinL normalized on Ppia gene. Relative mRNA expression in Gastrocnemius muscle **(A)** and relative mRNA expression in soleus muscle **(B)** at 6, 12 and 14 months of age, in FVB, FVB+EX, Tg and Tg+EX respectively. n=4 for each group in Gas; n=3 for each group in soleus. Data are shown as mean±s.e.m. Two-way ANOVA analysis-Bonferroni *post hoc* test; level of significance set to p≤0.05.

A: CathepsinL gene expression; ● Tg+EX sign different from Tg; * Tg+EX sign different from FVB+EX

Discussion

While some studies claimed that poor exercise capacity in patients with HF is caused by a reduction in ejection fraction and cardiac output most researchers have suggested that changes in the periphery are the main contributors to poor exercise capacity in these patients. These alterations include an increase in peripheral vascular resistance, changes in skeletal muscle metabolism, and reduction in skeletal muscle blood flow, mass, and strength. Therefore, the concept has emerged that the impairments at the skeletal muscle level, contribute significantly to the exercise intolerance (EI) in CHF patients (Hirai et al., 2015; Poole et al., 2012; Massie et al., 1996).

The transgenic cardiopathic model used in this thesis is characterized by a gradual progression of the disease and, for this reason, it offers the great advantage of studying muscle adaptations from the early to the late stages of the disease.

The major findings of this study concern (i) the characterization of the muscle alterations in skeletal muscle in mice with dilated cardiomyopathy (DCM) and (ii) the analysis of how these alterations are related to in vivo functional performance over time.

Functional performance: effect of cardiomyopathy and exercise

In this study, the *in vivo* functional evaluation was carried out by measuring the total distance and the total time of activity covered by mice after 2 months of voluntary wheel running.
Various researchers have shown that forced and voluntary exercise produce very different effects on tested animals. Animals forced to exercise develop physical and mental stress, so the physical activity in our experiments occurred under non-stressful conditions (Ke et al., 2011; Li et al., 2014).
In general we have observed a substantial increase in the level of spontaneous activity, both in wild type and cardiopathic mice (Fig. 17A and B) demonstrating a beneficial effect of VWRA on muscle function.
Cardiopathic exercised mice performed a total distance significantly lower than wild type exercised mice, only at 14 months of age (Fig. 16A). The observations of exercise program restricted to this result strongly suggest a functional alteration only in the late stage of dilated cardiomyopathy (14 months).
Interestingly, comparing the functional basal activity of wild type and cardiopathic mice, a deficit in *in vivo* functional activity was found at 12 and 14 months of age before the VWRA. In fact, cardiopathic mice showed a daily activity lower than the age matched control mice (Fig.17C) slightly above the level of significance. 2 months of VWRA reduced the functional gap between control and cardiopathic mice found at 12 months (from 46% before VWRA to 32% at the end of VWRA) indicating that exercise was able to reduce the difference in exercise tolerance between the two groups (Fig. 17D). In contrast, at 14 months of age, the functional gap between cardiopathic and wild type mice was found increased (from 44% before VWRA to 58% at the end of VWRA) (Fig.17D) despite the positive effect of exercise on cardiopathic mice at all stage of the disease (Fig.17B).
These results suggest that (i) muscle function begins to decrease in the crucial period of cardiomyopathy, i.e. the transition from the compensated to the uncompensated phase (12 months), (ii) exercise has a positive effect on *in vivo* muscle function at all stages of the disease, therefore the voluntary wheel running represents a valid training intervention (iii) despite the positive effect of exercise, exercise intolerance is increased in cardiopathic mice in the late phase of the disease.

Muscle phenotype (MyHC): effect of cardiomyopathy and exercise

As skeletal muscle contain different fiber types with different functional and metabolic characteristics, in order to verify if DCM affects skeletal muscle fibers composition and therefore muscle function, we analyzed MyHCs composition of gastrocnemius and soleus muscle of cardiopathic and control mice. The MyHC isoforms distribution was shifted toward fast MyHC2B in gastrocnemius of mice with cardiomyopathy, consistent with studies that reported a shift from slow to fast fibers both in human (Drexler et al., 1992; Sullivan et al., 1990; Caforio et al., 1989; Mancini et al 1989) and animal (De Sousa et al., 2000). Interestingly, in gastrocnemius muscle MyHC isoforms distribution changed when the animals did not yet exhibit the cardiac abnormalities (at 6 months) (Fig. 18A) and persisted during all stages of the disease (12 and 14 months) (Fig. 18C and E).

Differently from gastrocnemius, cardiomyopathy affected soleus MyHC isoforms distribution only in the early phase of the disease (Fig. 18B), after that muscle phenotype was preserved until the overt disease (Fig. 18D and F). These observations are in agreement with other studies demonstrating a major involvement of fast muscle in HF condition (Garnier et al., 2003).

Exercise-induced skeletal muscle adaptations to voluntary wheel running and involuntary treadmill training have been evaluated in several studies and appear dependent to type and amount of exercise. Chronic voluntary wheel running had no effect on muscle phenotype of control animals neither in the gastrocnemius nor in the soleus (Fig. 18). This is in agreement with evidences in which no effect on muscle phenotype were found following this training regime (Pellegrino et al., 2005). In other words, the positive effect on in *vivo* muscle function in control mice found in this study is not correlated with muscle phenotype suggesting that functional performance improvements of skeletal muscle occurred independently from fiber types transition. A similar *scenario* has been described in human undergoing moderate-intensity endurance training (Zoladz et al., 2013), in which the improvements in muscle performance was not accompanied by a change in muscle myosin heavy chain distribution and mitochondrial biogenesis. These considerations are useful for interpreting the time course of molecular adaptations in DCM and the effect of endurance training, together with the functional consequences on exercise tolerance. However, although exercise did not affect control healthy mice, our data strongly suggest that it was able to prevent the modulation of fiber types toward the more glycolytic metabolic pattern, both in gastrocnemius and soleus of cardiopathic mice, restoring a muscle phenotype similar to the control healthy mice (Fig. 18). This is a positive effect of exercise, in fact an alteration in fiber type from type I to type IIb imply slow vs fast and oxidative vs glycolytic properties twitching, therefore affecting aerobic exercise capacity adversely.

Metabolic and energetic adaptation: effect of cardiomyopathy and exercise

Numerous studies in patients (Mancini et al., 1989; Sullivan et al., 1990; Drexler et al., 1992; Massie et al., 1996; Sullivan et al., 1997) and animal models of heart failure (Arnolda et al., 1991; Sabbah et al., 1993; Bernocchi et al., 1996; Simonini et al., 1996b; Simonini et al., 1996a; Delp et al., 1997) have described reduction in oxidative enzyme activity. However, whether these abnormalities result in functional alterations of the contractile machinery, has never been directly assessed.

In order to better characterize this aspect, we performed an analysis of energy metabolism, before and during the development of the disease (at 6, 12 and 14 months of age). In general, we found that slow and fast muscles differently adapted to cardiomyopathy, with slow muscle more protected from metabolic alteration than fast muscle.

PCG-1α is the master control of mitochondrial biogenesis and oxidative metabolism, enhancing fatty acid β-oxidation, oxidative phosphorylation and ATP production (Liang & Ward, 2006).

Decrease of PCG-1α levels have been found in animal model of heart failure, both in cardiac (Knowlton, Chen and Malik 2014) and skeletal muscle (Garnier A. et al., 2003). Accordingly with this, we found lower level of PCG-1α in gastrocnemius muscle of cardiopathic mice respect to age matched control (Fig. 19A). Interestingly, the decrease in PGC-1α protein expression in gastrocnemius muscle occurred early into DCM, and precede the development of disease (Fig. 19A). Considering that PGC-1α is expressed preferentially in muscle enriched in type I fibers, reduction of PGC-1α observed in this study could be in part dependent on a shift in muscle phenotype (Fig. 18A, C and E). However, at 12 months of age, in the face of PGC-1α reduction, no differences in gastrocnemius phenotype between cardiopathic and control mice were observed. Therefore it is unlikely that adaptations of PGC-1α could be solely dependent on a shift in muscle phenotype. Therefore it seems that these adaptations in part reflect a primary metabolic impairment.

Differently from gastrocnemius, in soleus of cardiopathic mice, the PGC-1α protein levels were found similar to those observed in control mice at all stages of the disease (fig. 19B), despite the reduced PGC-1α mRNA expression found at 14 months of age (Fig. 20B). Taken together, these results suggest that fast muscles are most affected by the disease than the slow muscles.

Since the PGC-1α has a prominent role in the metabolic adaptations to the energetic status, its activity might be targeted by cellular mechanism capable to sense the perturbations in availability of energy of the cell. One of them is represented by 5′-AMP-activated protein kinase (AMPK), a cellular energy sensor. When intracellular levels of ATP decrease, a corresponding increase in AMP leads to activation of AMPK, a step that is essential for restoring intracellular energy balance via AMPK-dependent inhibition of energy-consuming biosynthetic processes and concomitant activation of pathways that increase ATP production (Dasgupta et al., 2012).

Mice lacking AMPK show drastic reduction in mitochondrial content and exercise capacity (Dasgupta eta la 2012, Jørgensen et al 2007, Steinberg et al 2010). Consistent with this, our data showed AMPK down-regulation in gastrocnemius muscle of cardiopathic mice, at all phases of DCM (6, 12 and 14-months) (Fig. 21A) suggesting basal AMPK signaling could be suppressed by cardiomyopathy with possible decrease in ability to tolerate metabolic stress such as muscle contraction.

Interestingly, recent findings have demonstrated a closer link between AMPK and PGC-1α, showing that AMPK can directly interact and phosphorylate PGC-1α (Jäger et al 2007). Direct phosphorylation of PGC-1α by AMPK seems to increase transcriptional activity of PGC-1α, even though the reasons why, where, and how that happens, are still elusive. Phosphorylation of PGC-1α by AMPK may, hence, be part of the link between the sensing of the energetic status and the induction of transcriptional programs that control energy expenditure. The lower PGC-1α expression we have shown in gastrocnemius of cardiopathic mice provide further evidence of the essential role that AMPK plays in maintaining mitochondrial function. Interestingly, despite the mitochondrial biogenesis and AMPK reduction in mice with cardiomyopathy, their *in vivo* basal performance was not significantly different from that of age-matched control mice (Fig. 17C) highlighting the large functional reserve of skeletal muscle to maintain resting/basal energy homeostasis.

As for PGC-1α, also for AMPK activation, soleus of cardiopathic mice did not show any alteration, with AMPK levels similar to those of control mice (Fig.21B). This result, together with PGC-1α adaptation, further suggests that the slow muscle is less affected by the disease.

It is widely established that AMPK is activated by muscle contraction and exercise in both human and rodents (Winder and Hardie, 1996; Durante et al., 2002) in an intensity-dependent manner. AMPK activation in skeletal muscle during exercise improves athletic performance (Jørgensen et al. 2005), and mice treated with AMPK activating compounds exhibit superendurance (Jäger et

al., 2007; Narkar et al., 2008). In gastrocnemius of wild type mice, exercise determined a reduction of AMPK activation (Fig.21A) and a decreasing trend of PGC-1α content (Fig. 19A). This apparent contradiction could be due to the fact that gene expression can vary significantly with time and muscle type after physical exercise. In our study muscles were collected 24h post-exercise. Similar results have been observed by Dasgupta (Dasgupta et al 2012) in which expression of PGC-1α and other mitochondrial genes have been found significantly reduced in gastrocnemius muscle already to 6h post-exercise. In soleus of wild type mice, exercise did not induce any variation in terms of PGC-1α and AMPK expression. A similar *scenario* has been found in a recent paper of Lira (Lira et al., 2013) in which no changes of PGC-1α, Cyc and Cox4 protein expression have been found with voluntary wheel running in soleus muscle. This is in agreement with the concept that because of its high postural and locomotive activities soleus muscle has already a highly oxidative phenotype that is minimally enhanced by the long-term increases in contractile activity during voluntary running. Consistent with this concept, here we found that cardiopathic mice were much more responsive to exercise than wild type mice. In fact, at least for soleus at 6 months of age and gastrocnemius at all stages of the disease (6, 12 and 14 months of age), muscle phenotype of cardiopathic mice was faster than that of wild type mice (Fig. 18), therefore, these muscles could be more susceptible to the effects of exercise.

Exercised cardiopathic mice showed higher levels of AMPK both in gastrocnemius and soleus, respect to the untrained cardiopathic mice, that resulted in PGC-1α increase only in gastrocnemius (Fig. 19A). Interestingly, after exercise we observed a fast to slow shift of MyHC isoforms in both muscles (Fig. 18), despite the lack of increase of PGC-1α in soleus (Fig. 19B). This result is not surprising, since there are several evidences indicating that endurance exercise-induced fiber-type transformation in skeletal muscle could occur independent of the function of the PGC1alpha. In fact, in this regard, Geng and coworkers (Geng et al., 2010), using PGC-1α knockout mice, showed that voluntary exercise-induced IIb-to-IIa transformation was not affected by the deletion of the PGC-1α gene in skeletal muscle. Consistent with this, overexpression of active upstream signaling molecules in skeletal muscle that upregulate PGC-1α expression can promote mitochondrial biogenesis without inducing shifts in fiber-type composition (Akimoto et al., 2005, Garcia-Roves et al., 2008).

Mitochondrial dynamic network: effect of cardiomyopathy and exercise

Since in cardiopathic fast muscle we found a deficit of key markers regulating oxidative metabolism, and considering that PGC-1α alpha down-regulation could be also linked to events of mitochondrial network related to changing shape phenomena, to better characterize this issue, we studied the mitochondrial dynamics through the analyses of pro-fusion (Mfn1, Mfn2) and pro-fission (DRP1) related proteins expression. Mitochondrial fission was found down regulated at all stages of the disease in gastrocnemius muscle (Fig. 22A) together with the decrease of pro-fusion Mfn1 at 12 months of age and no changes in pro-fusion Mfn2 (Fig. 23). Mitochondrial fusion and fission are crucial mechanisms for maintaining mitochondrial function and preserving energy production. A balance between these two systems is essential for a physiological maintenance of the cell. In particular, mitochondrial fusion is required to fuse new mitochondria, and mitochondrial fission allows for selective segregation of damaged mitochondria, which are afterward eliminated by DRP1-dependent mitochondrial autophagy (Ikeda et al., 2015). These results are in line with the reduced PGC-1α and AMPK levels found in these muscles and consistent with the hypothesis that mitochondrial dysfunction occurs, already when the mice were not yet affected by DCM (i.e. at 6 months of age).

Redox status: effect of cardiomyopathy and exercise

An important aspect, which is connected to the presence of mitochondrial alteration, is the excessive production of reactive oxygen species (ROS). Whenever the body is subjected to an insult which results in an increase of the intracellular concentration of ROS, it triggers a response by the endogenous antioxidant defense system, aimed to decrease ROS concentration. As explained above, the main proteins involved in the response of the antioxidant system are represented by the superoxide dismutase (SOD) and Catalase, whose expression increase in response to increased ROS. The SOD converts superoxide ion into hydrogen peroxide and catalase works downstream of SOD converting the hydrogen peroxide into water, avoiding in this way the oxidative damage operated by the accumulation of the hydroxyl radical consequent to the peroxide hydrogen accumulation. In this study the concomitant analysis of different parameters related to oxidative stress, combined together, provide strong indication that (i) redox imbalance affects gastrocnemius muscle and could be involved in the development of exercise intolerance and (ii) the soleus muscle was preserved from the oxidative damage.

At 6 months of age, i.e. when mice did not yet exhibit cardiac abnormalities, gastrocnemius was characterized by low, but no significant, levels of SOD1 (Fig. 27A) and catalase (Fig. 28A) with possible ROS accumulation and oxidative damage (Lawler et al., 2006). In the later stages of the disease, the persistent downregulation of catalase, at 12 months (Fig. 28A), and SOD1, at 14 months (Fig. 27A), resulted in protein oxidation (Fig. 29A). Instead, slow muscle was protected by oxidative damage (Fig. 29B), in agreemente with the normal expression of SOD and catalase at all stages of the disease (Fig. 27B and 28B).

Therefore, these results indicate an early and persistent impairment of the cellular responses against ROS that could be involved in the development of exercise intolerance. Several evidences indicate that a relationship between oxidative damage and functional performance exists (Kuwahara et al., 2010; Reid 2007). Kuwahara and coworkers demonstrated that the presence of oxidative damage worsens the functional performance in mice. In fact, the in vivo performance of mice lacking SOD2 and characterized by the presence of oxidative damage in skeletal muscle, has been found compromised. The subsequent administration of an antioxidant improved the in vivo performance. Therefore, it is reasonable to consider oxidative damage a potential mechanism responsible for the development of exercise intolerance in cardiopathic mice. Since this deficit in antioxidant systems occurred before the appearance of cardiac abnormalities and persist in the later phases of the disease (12 and 14 months of age) it can be considered one of the primary mechanisms of the exercise intolerance.

It is well established that, during contractile activity, the increase in metabolic rate in skeletal muscle results in an increased production of oxidants. Failure to remove these oxidants during exercise can result in significant oxidative damage of cellular biomolecules. Fortunately, regular endurance exercise results in adaptations in the skeletal muscle antioxidant capacity, which protects myocytes against the deleterious effects of oxidants and prevents extensive cellular damage. Consistent with this concept, we found that, in wild type mice, both fast and slow muscle was protected by oxidative damage during exercise (Fig. 29) despite the reduced SOD level at 14 months of age and the unchanged SOD and catalase levels at 6 and 12 months. Probably other antioxidant systems come into play in protecting the muscle from oxidative damage. In fact, the free radicals are neutralized by an elaborate antioxidant defense system consisting of enzymes such as catalase, superoxide dismutase, glutathione peroxidase, and numerous non-enzymatic antioxidants, including vitamin A, E and C, glutathione, ubiquinone, and flavonoids.

Endurance exercise, in cardiopathic mice, was able to reduce skeletal muscle damage found at 12 months of age but no at 14 months (Fig. 29A), despite the increase of SOD level in this last phase of the disease (Fig. 27A). As explained before, the antioxidant effect of exercise found in cardiopathic mice may depend on activation of other antioxidant systems, in fact, also in this case

no improvement of SOD and catalase expression were found at 12 months. Interestingly, the positive effect of exercise on oxidative damage was correlated with the improvements of in vivo function observed in trained cardiopathic mice at 12 months (Fig. 17D). Hence, exercise represent a useful therapeutic modality to reduce oxidative damage associated with the disease, especially in the crucial period of cardiomyopathy, i.e. the transition from the compensated to the uncompensated phase (12 months of age). These observation are in agreement with evidences that demonstrated a beneficial effect of aerobic exercise on anti-oxidant defences in the muscle of HF patients (Poole et al., 2012).

Effect of cardiomyopathy and exercise on tournover

Two main proteolytic pathway controlling protein degradation in skeletal muscle are the ubiquitine proteasome and autophagy system (Sandri, 2008).
The ubiquitine proteasome is responsible for degradation of soluble and myofibrillar muscle protein after the substrates are tagged by a polyubiquitin chain (Reid, 2005) and subsequently cleaved by proteasome 26S (Solomon and Goldberg, 1996). Autophagy involves the sequestration of proteins and/or organelles by double-membrane structures that form autophagosomes, which then fuse with lysosomes to degrade engulfed materials.
In addition to its role in simply maintaining proteostasis, proteolysis is an essential part of the production of new skeletal muscle fibers and adapting muscle fibers to cellular stress. Current research clearly indicates a critical role of protein degradation in the regulation of the myogenic differentiation program, ensuring timely protein expression for myoblast differentiation while also mediating myoblast fusion and myotube formation. The mature muscle fiber then relies on appropriate protein degradation to rid the cell of damaged proteins from the mechanical and oxidative stress that accompanies the force-bearing/force-generating function of skeletal muscle. Additionally, during nutrient deprivation the organism depends on skeletal muscle proteolysis to maintain whole-body energy homeostasis. Not surprisingly, defects within these proteolytic systems often result in the development of myopathic conditions (Jokl and Blanco, al 2016).
Defective activity of ubiquitine ligases and autophagy can lead to deleterious effect on skeletal muscle and cover a pathogenic role in several forms of muscle diseases (Grumati et al., 2011). Basal autophagy, is a continuous baseline process responsible for removal of dysfunctional cellular components and is required for normal cell function (Levine and Klionsky 2004; Lee et al., 2010).
Here, the ubiquitin proteasome markers (Atrogin1 and MuRF1) were found lower than the control basal level in 12 months old cardiopathic mice, both in gastrocnemius (Fig. 30A and 31A) and soleus muscle (Fig. 30B and 31B). A similar results were found for autophagic markers (Fig. 32 and 33) that resulted down-regulated under the basal level at 12 mo (trend to decrease in the CathepsinL level, both in fast and slow muscle) (Fig. 33A and B) and at 14 mo (significant decrease in the LC3 level in fast muscle) (Fig. 32A) in mice with cardiomyopathy. In other words, it seems that a deficit in the basal catabolic process is present in cardiopathic muscles starting from the crucial period of the transition from compensated hypertrophy to decompensated HF (i.e.12 months).
Since high level of AMPK causes Atrogin1 and MuRF1 induction via a FoxO3-dependent mechanism (Tong et al., 2009), it is reasonable to think that deficit in catabolic process found in mice with cardiomyopathy could be due to the low levels of AMPK that prevent catabolic induction. This mechanism would seem to prevail on the effect of the reduced PGC-1α content on catabolic pathways activation (Cannavino et al 2014).
Muscle maintenance relies on a baseline turnover of mechanically unfolded proteins to prevent cytotoxic accumulation of aggregates, as well as the turnover of damaged organelles, particularly mitochondria.

Exercise training-induced skeletal muscle adaptation likely requires both addition and clearance of cellular components. Several evidences indicate that exercise induces a general upregulation of ubiquitine proteasome basal level both in human (Stefanetti et al., 2015) and mice (Cunha et al., 2012). Furthermore, recent studies have shown that an intense, single bout of forced treadmill exercise in mice resulted in activation of autophagy and increased autophagy flux in skeletal muscle (Grumati et al., 2011; He et al 2012) as well as long time voluntary wheel-running exercise (Lira et al., 2013).

In this context, it is believed that Atrogin1 and MuRF1 may play a role in healthy skeletal muscle adaptation and remodelling post-exercise. It is also believed that endurance exercise-induced increase in ubiquitine proteasome may play a role in precluding type I fiber growth to optimize oxygen supply to the mitochondria (vanWessel et al., 2010).

Consistent with this, our findings indicate that in vivo skeletal muscle enhancements found in cardiopathic mice at 6 and 12 months of age, as evidenced by increased running capacity (Fig. 17D), occurred in spite of the upregulated ubiquitine proteasome (Fig. 30 and 31) and autophagy system (Fig. 33) suggesting that (i) a contribution of the catabolic systems to metabolic turnover of myofibrillar proteins and skeletal muscle adaptations to exercise occurs and (ii) overactivation of skeletal muscle proteolytic systems is not restricted to atrophying states.

In agreement with the positive effect of catabolic system activation on protein turnover, the late phase of the disease (14 months), where we found exercise intolerance (Fig. 16), is not accompanied by an increase of the catabolic systems which resulted even down-regulated or unchanged (Fig. 30, 31, 32 and 33).

Considering the high oxidation index found in gastrocnemius of cardiopathic exercised mice at the late stage of the disease (Fig. 29A), it is reasonable to think that catabolic systems and in particular the ubiquitine proteasome, for which a central role is recognized in removing oxidized proteins (Grune et al., 2003), become ineffective because themselves could be damaged by oxidation. Our results are therefore in line with those concerning different skeletal muscle disease models, in which an altered basal level of catabolic pathway is associated to an altered clearance of damaged protein and/or organelles, leading to an alteration in cellular homeostasys (Kroemer, Mariño and Levine, 2010; Kroemer 2010).

Surpraisingly, we did not found changes in catabolic processes in exercised wild type mice. A possible explanation for these results, could be due to transient expression of ubiquitine ligase (Cannavino et al., 2014), together with a possible different times of these events between wild type and Tg exercised mice.

Conclusions

In order to get a comprehensive picture of the complex adaptations of human skeletal muscle to dilated cardiomyopathy and exercise intolerance and further the understanding of the underlying mechanisms, we participated to Harmonia Project.

Results of this thesis provide information on the time course by which mice with cardiomyopathy develop muscular molecular alteration and exercise intolerance during the progression of the disease.

Because $Tg\alpha_q*44$ transgenic mice develop progressive cardiomyopathy they are a useful animal model for investigating the physiopathology of the disorder.

According to the "peripheral muscle hypothesis", results of this study have shown that (i) substantial modifications occur to muscles as a consequence of cardiomyopathy: shift in muscle phenotype, deficit in energetic and oxidative metabolic markers (AMPK and PGC1α), alteration in mitochondrial dynamic (DRP1 reduction), deficit in the basal catabolism (ubiquitine proteasome and autophagy reduction) and oxidative stress. Firstly, most of these alterations occurred only in gastrocnemius suggesting that fast muscles are more affected by cardiomyopathy than slow muscles. Secondly, the timing of adaptations was different with a) muscle phenotype, PGC1α, AMPK, and DRP1 changes preceding the onset of the disease b) oxidative stress occurring in the crucial period of cardiomyopathy, i.e. the transition from the compensated to the uncompensated phase (12 months) and persisting overtime c) atrogin1 and Murf1 deficit occurring in the late phase of the disease.

The recovery of altered parameters in the early and crucial phase of the disease (6 and 12 months) induced by exercise resulted in an in vivo functional improvement which prevented the occurrence of exercise intolerance. Instead, in the late phase of the disease (14 months) muscle response to exercise was compromised showing inability to counteract the oxidative stress and inefficacy to increase catabolic process which ensure an adequate proteins turnover during exercise.

Therefore, the decline of protein quality control system and the accumulation of oxidized proteins seem primarily involved in determining the exercise intolerance observed in cardiopathic mice.

Bibliography

Adamopoulos, S., Parissis, J. T. & Kremastinos, D. T. 2001. A glossary of circulating cytokines in chronic heart failure. Eur J Heart Fail, 3, 517-26.

Adamopoulos, S., Parissis, J., Karatzas, D., Kroupis, C., Georgiadis, M., Karavolias, G., Paraskevaidis, J., Koniavitou, K., Coats, A. J. & Kremastinos, D. T. 2002. Physical training modulates proinflammatory cytokines and the soluble Fas/soluble Fas ligand system in patients with chronic heart failure. J Am Coll Cardiol, 39, 653-63.

Adler, V., Yin, Z., Fuchs, S. Y., Benezra, M., Rosario, L., Tew, K. D., Pincus, M. R., Sardana, M., Henderson, C. J., Wolf, C. R., Davis, R. J. & Ronai, Z. 1999. Regulation of JNK signaling by GSTp. EMBO J, 18, 1321-34.

Aguiló, A., Tauler, P., Fuentespina, E., Tur, J. A., Córdova, A. & Pons, A. 2005. Antioxidant response to oxidative stress induced by exhaustive exercise. Physiol Behav, 84, 1-7.

Akhter, S. A., Luttrell, L. M., Rockman, H. A., Iaccarino, G., Lefkowitz, R. J. & Koch, W. J. 1998. Targeting the receptor-Gq interface to inhibit in vivo pressure overload myocardial hypertrophy. Science, 280, 574-7.

Akimoto, T., S. C. Pohnert, P. Li, M. Zhang, C. Gumbs, P. B. Rosenberg, R. S. Williams & Z. Yan (2005) Exercise stimulates Pgc-1alpha transcription in skeletal muscle through activation of the p38 MAPK pathway. J Biol Chem, 280, 19587-93.

Anand, I. S., Fisher, L. D., Chiang, Y. T., Latini, R., Masson, S., Maggioni, A. P., Glazer, R. D., Tognoni, G., Cohn, J. N. & Investigators, V.-H. 2003. Changes in brain natriuretic peptide and norepinephrine over time and mortality and morbidity in the Valsartan Heart Failure Trial (Val-HeFT). Circulation, 107, 1278-83.

Anderson, E. J. & Neufer, P. D. 2006. Type II skeletal myofibers possess unique properties that potentiate mitochondrial H(2)O(2) generation. Am J Physiol Cell Physiol, 290, C844-51.

Apple, F. S. & Tesch, P. A. 1989. CK and LD isozymes in human single muscle fibers in trained athletes. J Appl Physiol (1985), 66, 2717-20.

Arany, Z., Foo, S. Y., Ma, Y., Ruas, J. L., Bommi-Reddy, A., Girnun, G., Cooper, M., Laznik, D., Chinsomboon, J., Rangwala, S. M., Baek, K. H., Rosenzweig, A. & Spiegelman, B. M. 2008. HIF-independent regulation of VEGF and angiogenesis by the transcriptional coactivator PGC-1alpha. Nature, 451, 1008-12.

Arena, R., Myers, J., Abella, J., Peberdy, M. A., Bensimhon, D., Chase, P. & Guazzi, M. 2008a. Prognostic characteristics of cardiopulmonary exercise testing in caucasian and African American patients with heart failure. Congest Heart Fail, 14, 310-5.

Arena, R., Myers, J., Abella, J., Pinkstaff, S., Brubaker, P., Moore, B., Kitzman, D., Peberdy, M. A., Bensimhon, D., Chase, P. & Guazzi, M. 2008b. The partial pressure of resting end-tidal carbon dioxide predicts major cardiac events in patients with systolic heart failure. Am Heart J, 156, 982-8.

Argadine, H. M., Hellyer, N. J., Mantilla, C. B., Zhan, W. Z. & Sieck, G. C. 2009. The effect of denervation on protein synthesis and degradation in adult rat diaphragm muscle. J Appl Physiol (1985), 107, 438-44.

Arnér, E. S. & Holmgren, A. 2000. Physiological functions of thioredoxin and thioredoxin reductase. Eur J Biochem, 267, 6102-9.

Arnold, A. S., Egger, A. & Handschin, C. 2011. PGC-1α and myokines in the aging muscle - a mini-review. Gerontology, 57, 37-43.

Arnolda, L., Brosnan, J., Rajagopalan, B. & Radda, G. K. 1991. Skeletal muscle metabolism in heart failure in rats. Am J Physiol, 261, H434-42.

Arthur, J. R. 2000. The glutathione peroxidases. Cell Mol Life Sci, 57, 1825-35.

Azevedo, E. R., Newton, G. E., Floras, J. S. & Parker, J. D. 2000. Reducing cardiac filling pressure lowers norepinephrine spillover in patients with chronic heart failure. Circulation, 101, 2053-9.

Baehr, L. M., Furlow, J. D. & Bodine, S. C. 2011. Muscle sparing in muscle RING finger 1 null mice: response to synthetic glucocorticoids. J Physiol, 589, 4759-76.

Balagopal, P., Ljungqvist, O. & Nair, K. S. 1997. Skeletal muscle myosin heavy-chain synthesis rate in healthy humans. Am J Physiol, 272, E45-50.

Balasubramanian, V. P. & Varkey, B. 2006. Chronic obstructive pulmonary disease: effects beyond the lungs. Curr Opin Pulm Med, 12, 106-12.

Bär, A. & Pette, D. 1988. Three fast myosin heavy chains in adult rat skeletal muscle. FEBS Lett, 235, 153-5.

Batista, M. L., Santos, R. V., Lopes, R. D., Lopes, A. C., Costa Rosa, L. F. & Seelaender, M. C. 2008. Endurance training modulates lymphocyte function in rats with post-MI CHF. Med Sci Sports Exerc, 40, 549-56.

Batista, M. L., Santos, R. V., Oliveira, E. M., Seelaender, M. C. & Costa Rosa, L. F. 2007. Endurance training restores peritoneal macrophage function in post-MI congestive heart failure rats. J Appl Physiol (1985), 102, 2033-9.

Batista, R. J., Santos, J. L., Takeshita, N., Bocchino, L., Lima, P. N. & Cunha, M. A. 1996. Partial left ventriculectomy to improve left ventricular function in end-stage heart disease. J Card Surg, 11, 96-7; discussion 98.

Beckers, P. J., Denollet, J., Possemiers, N. M., Wuyts, F. L., Vrints, C. J. & Conraads, V. M. 2008. Combined endurance-resistance training vs. endurance training in patients with chronic heart failure: a prospective randomized study. Eur Heart J, 29, 1858-66.

Belardinelli, R., Georgiou, D., Scocco, V., Barstow, T. J. & Purcaro, A. 1995. Low intensity exercise training in patients with chronic heart failure. J Am Coll Cardiol, 26, 975-82.

Benard, G., Bellance, N., James, D., Parrone, P., Fernandez, H., Letellier, T. & Rossignol, R. 2007. Mitochondrial bioenergetics and structural network organization. J Cell Sci, 120, 838-48.

Benedict, C. R., Johnstone, D. E., Weiner, D. H., Bourassa, M. G., Bittner, V., Kay, R., Kirlin, P., Greenberg, B., Kohn, R. M. & Nicklas, J. M. 1994. Relation of neurohumoral activation to clinical variables and degree of ventricular dysfunction: a report from the Registry of Studies of Left Ventricular Dysfunction. SOLVD Investigators. J Am Coll Cardiol, 23, 1410-20.

Bensimhon, D. R., Leifer, E. S., Ellis, S. J., Fleg, J. L., Keteyian, S. J., Piña, I. L., Kitzman, D. W., McKelvie, R. S., Kraus, W. E., Forman, D. E., Kao, A. J., Whellan, D. J., O'Connor, C. M., Russell, S. D. & Investigators, H.-A. T. 2008. Reproducibility of peak oxygen uptake and other cardiopulmonary exercise testing parameters in patients with heart failure (from the Heart Failure and A Controlled Trial Investigating Outcomes of exercise traiNing). Am J Cardiol, 102, 712-7.

Bentzinger, C. F., Romanino, K., Cloëtta, D., Lin, S., Mascarenhas, J. B., Oliveri, F., Xia, J., Casanova, E., Costa, C. F., Brink, M., Zorzato, F., Hall, M. N. & Rüegg, M. A. 2008. Skeletal muscle-specific ablation of raptor, but not of rictor, causes metabolic changes and results in muscle dystrophy. Cell Metab, 8, 411-24.

Bergendi, L., Benes, L., Duracková, Z. & Ferencik, M. 1999. Chemistry, physiology and pathology of free radicals. Life Sci, 65, 1865-74.

Bernardi, P. & Bonaldo, P. 2008. Dysfunction of mitochondria and sarcoplasmic reticulum in the pathogenesis of collagen VI muscular dystrophies. Ann N Y Acad Sci, 1147, 303-11.

Berndt, C., Lillig, C. H. & Holmgren, A. 2007. Thiol-based mechanisms of the thioredoxin and glutaredoxin systems: implications for diseases in the cardiovascular system. Am J Physiol Heart Circ Physiol, 292, H1227-36.

Bernocchi, P., Ceconi, C., Pedersini, P., Pasini, E., Curello, S. & Ferrari, R. 1996. Skeletal muscle metabolism in experimental heart failure. J Mol Cell Cardiol, 28, 2263-73.

Bhandari, P., Song, M. & Dorn, G. W. 2015. Dissociation of mitochondrial from sarcoplasmic reticular stress in Drosophila cardiomyopathy induced by molecularly distinct mitochondrial fusion defects. J Mol Cell Cardiol, 80, 71-80.

Birben, E., Sahiner, U. M., Sackesen, C., Erzurum, S. & Kalayci, O. 2012. Oxidative stress and antioxidant defense. World Allergy Organ J, 5, 9-19.

Bjørnstad, H. H., Bruvik, J., Bjørnstad, A. B., Hjellestad, B. L., Damås, J. K. & Aukrust, P. 2008. Exercise training decreases plasma levels of soluble CD40 ligand and P-selectin in patients with chronic heart failure. Eur J Cardiovasc Prev Rehabil, 15, 43-8.

Björnstedt, M., Kumar, S., Björkhem, L., Spyrou, G. & Holmgren, A. 1997. Selenium and the thioredoxin and glutaredoxin systems. Biomed Environ Sci, 10, 271-9.

Björnstedt, M., Xue, J., Huang, W., Akesson, B. & Holmgren, A. 1994. The thioredoxin and glutaredoxin systems are efficient electron donors to human plasma glutathione peroxidase. J Biol Chem, 269, 29382-4.

Blaauw, B., Canato, M., Agatea, L., Toniolo, L., Mammucari, C., Masiero, E., Abraham, R., Sandri, M., Schiaffino, S. & Reggiani, C. 2009. Inducible activation of Akt increases skeletal muscle mass and force without satellite cell activation. FASEB J, 23, 3896-905.

Blaauw, B., Schiaffino, S. & Reggiani, C. 2013. Mechanisms modulating skeletal muscle phenotype. Compr Physiol, 3, 1645-87.

Blättler, S. M., Cunningham, J. T., Verdeguer, F., Chim, H., Haas, W., Liu, H., Romanino, K., Rüegg, M. A., Gygi, S. P., Shi, Y. & Puigserver, P. 2012. Yin Yang 1 deficiency in skeletal muscle protects against rapamycin-induced diabetic-like symptoms through activation of insulin/IGF signaling. Cell Metab, 15, 505-17.

Blum, A. & Miller, H. 2001. Pathophysiological role of cytokines in congestive heart failure. Annu Rev Med, 52, 15-27.

Bodine, S. C. 2006. mTOR signaling and the molecular adaptation to resistance exercise. Med Sci Sports Exerc, 38, 1950-7.

Bodine, S. C., Latres, E., Baumhueter, S., Lai, V. K., Nunez, L., Clarke, B. A., Poueymirou, W. T., Panaro, F. J., Na, E., Dharmarajan, K., Pan, Z. Q., Valenzuela, D. M., DeChiara, T. M., Stitt,

T. N., Yancopoulos, G. D. & Glass, D. J. 2001a. Identification of ubiquitin ligases required for skeletal muscle atrophy. Science, 294, 1704-8.

Bodine, S. C., Stitt, T. N., Gonzalez, M., Kline, W. O., Stover, G. L., Bauerlein, R., Zlotchenko, E., Scrimgeour, A., Lawrence, J. C., Glass, D. J. & Yancopoulos, G. D. 2001b. Akt/mTOR pathway is a crucial regulator of skeletal muscle hypertrophy and can prevent muscle atrophy in vivo. Nat Cell Biol, 3, 1014-9.

Bonaldo, P. & Sandri, M. 2013. Cellular and molecular mechanisms of muscle atrophy. Dis Model Mech, 6, 25-39.

Bothe, G. W., Haspel, J. A., Smith, C. L., Wiener, H. H. & Burden, S. J. 2000. Selective expression of Cre recombinase in skeletal muscle fibers. Genesis, 26, 165-6.

Bottinelli, R. & Reggiani, C. 2000. Human skeletal muscle fibres: molecular and functional diversity. Prog Biophys Mol Biol, 73, 195-262.

Bottinelli, R., Schiaffino, S. & Reggiani, C. 1991. Force-velocity relations and myosin heavy chain isoform compositions of skinned fibres from rat skeletal muscle. J Physiol, 437, 655-72.

Bozkurt, B., Kribbs, S. B., Clubb, F. J., Michael, L. H., Didenko, V. V., Hornsby, P. J., Seta, Y., Oral, H., Spinale, F. G. & Mann, D. L. 1998. Pathophysiologically relevant concentrations of tumor necrosis factor-alpha promote progressive left ventricular dysfunction and remodeling in rats. Circulation, 97, 1382-91.

Braith, R. W., Welsch, M. A., Feigenbaum, M. S., Kluess, H. A. & Pepine, C. J. 1999. Neuroendocrine activation in heart failure is modified by endurance exercise training. J Am Coll Cardiol, 34, 1170-5.

Brault, J. J., Jespersen, J. G. & Goldberg, A. L. 2010. Peroxisome proliferator-activated receptor gamma coactivator 1alpha or 1beta overexpression inhibits muscle protein degradation, induction of ubiquitin ligases, and disuse atrophy. J Biol Chem, 285, 19460-71.

Brigelius-Flohé, R. (2009) Commentary: oxidative stress reconsidered. Genes Nutr, 4, 161-3.

Brigelius-Flohé, R. 1999. Tissue-specific functions of individual glutathione peroxidases. Free Radic Biol Med, 27, 951-65.

Brigelius-Flohé, R. 2006. Glutathione peroxidases and redox-regulated transcription factors. Biol Chem, 387, 1329-35.

Brunotte, F., Thompson, C. H., Adamopoulos, S., Coats, A., Unitt, J., Lindsay, D., Kaklamanis, L., Radda, G. K. & Rajagopalan, B. 1995. Rat skeletal muscle metabolism in experimental heart failure: effects of physical training. Acta Physiol Scand, 154, 439-47.

Bunker, V. W. 1992. Free radicals, antioxidants and ageing. Med Lab Sci, 49, 299-312.

Burke, R. E., Levine, D. N., Tsairis, P. & Zajac, F. E. 1973. Physiological types and histochemical profiles in motor units of the cat gastrocnemius. J Physiol, 234, 723-48.

Cadenas, E. & Sies, H. 1998. The lag phase. Free Radic Res, 28, 601-9.

Caforio, A. L., B. Rossi, R. Risaliti, G. Siciliano, A. Marchetti, C. Angelini, F. Crea, M. Mariani & A. Muratorio (1989) Type 1 fiber abnormalities in skeletal muscle of patients with hypertrophic and dilated cardiomyopathy: evidence of subclinical myogenic myopathy. J Am Coll Cardiol, 14, 1464-73.

Calnan, D. R. & Brunet, A. 2008. The FoxO code. Oncogene, 27, 2276-88.

Calvani, R., Joseph, A. M., Adhihetty, P. J., Miccheli, A., Bossola, M., Leeuwenburgh, C., Bernabei, R. & Marzetti, E. 2013. Mitochondrial pathways in sarcopenia of aging and disuse muscle atrophy. Biol Chem, 394, 393-414.

Cannavino, J., L. Brocca, M. Sandri, R. Bottinelli & M. A. Pellegrino (2014) PGC1-α over-expression prevents metabolic alterations and soleus muscle atrophy in hindlimb unloaded mice. J Physiol, 592, 4575-89.

Chang, N. C., Nguyen, M., Bourdon, J., Risse, P. A., Martin, J., Danialou, G., Rizzuto, R., Petrof, B. J. & Shore, G. C. 2012. Bcl-2-associated autophagy regulator Naf-1 required for maintenance of skeletal muscle. Hum Mol Genet, 21, 2277-87.

Chase, P., Arena, R., Myers, J., Abella, J., Peberdy, M. A., Guazzi, M., Kenjale, A. & Bensimhon, D. 2008. Prognostic usefulness of dyspnea versus fatigue as reason for exercise test termination in patients with heart failure. Am J Cardiol, 102, 879-82.

Chemello, F., Bean, C., Cancellara, P., Laveder, P., Reggiani, C. & Lanfranchi, G. 2011. Microgenomic analysis in skeletal muscle: expression signatures of individual fast and slow myofibers. PLoS One, 6, e16807.

Chen, Y. & Dorn, G. W. 2013. PINK1-phosphorylated mitofusin 2 is a Parkin receptor for culling damaged mitochondria. Science, 340, 471-5.

Cho, S. G., Lee, Y. H., Park, H. S., Ryoo, K., Kang, K. W., Park, J., Eom, S. J., Kim, M. J., Chang, T. S., Choi, S. Y., Shim, J., Kim, Y., Dong, M. S., Lee, M. J., Kim, S. G., Ichijo, H., et al. 2001. Glutathione S-transferase mu modulates the stress-activated signals by suppressing apoptosis signal-regulating kinase 1. J Biol Chem, 276, 12749-55.

Chou, J. L., Su, H. Y., Chen, L. Y., Liao, Y. P., Hartman-Frey, C., Lai, Y. H., Yang, H. W., Deatherage, D. E., Kuo, C. T., Huang, Y. W., Yan, P. S., Hsiao, S. H., Tai, C. K., Lin, H. J., Davuluri, R. V., Chao, T. K., et al. 2010. Promoter hypermethylation of FBXO32, a novel TGF-beta/SMAD4 target gene and tumor suppressor, is associated with poor prognosis in human ovarian cancer. Lab Invest, 90, 414-25.

Cipolat, S., Martins de Brito, O., Dal Zilio, B. & Scorrano, L. 2004. OPA1 requires mitofusin 1 to promote mitochondrial fusion. Proc Natl Acad Sci U S A, 101, 15927-32.

Clarke, B. A., Drujan, D., Willis, M. S., Murphy, L. O., Corpina, R. A., Burova, E., Rakhilin, S. V., Stitt, T. N., Patterson, C., Latres, E. & Glass, D. J. 2007. The E3 Ligase MuRF1 degrades myosin heavy chain protein in dexamethasone-treated skeletal muscle. Cell Metab, 6, 376-85.

CLOSE, R. 1964. DYNAMIC PROPERTIES OF FAST AND SLOW SKELETAL MUSCLES OF THE RAT DURING DEVELOPMENT. J Physiol, 173, 74-95.

Coats, A. J., Adamopoulos, S., Radaelli, A., McCance, A., Meyer, T. E., Bernardi, L., Solda, P. L., Davey, P., Ormerod, O. & Forfar, C. 1992. Controlled trial of physical training in chronic heart failure. Exercise performance, hemodynamics, ventilation, and autonomic function. Circulation, 85, 2119-31.

Coats, A. J., Clark, A. L., Piepoli, M., Volterrani, M. & Poole-Wilson, P. A. 1994. Symptoms and quality of life in heart failure: the muscle hypothesis. Br Heart J, 72, S36-9.

Cohen, S., Zhai, B., Gygi, S. P. & Goldberg, A. L. 2012. Ubiquitylation by Trim32 causes coupled loss of desmin, Z-bands, and thin filaments in muscle atrophy. J Cell Biol, 198, 575-89.

Conery, A. R., Cao, Y., Thompson, E. A., Townsend, C. M., Ko, T. C. & Luo, K. 2004. Akt interacts directly with Smad3 to regulate the sensitivity to TGF-beta induced apoptosis. Nat Cell Biol, 6, 366-72.

Cong, H., Sun, L., Liu, C. & Tien, P. 2011. Inhibition of atrogin-1/MAFbx expression by adenovirus-delivered small hairpin RNAs attenuates muscle atrophy in fasting mice. Hum Gene Ther, 22, 313-24.

Cornwell, E. W., Mirbod, A., Wu, C. L., Kandarian, S. C. & Jackman, R. W. 2014. C26 cancer-induced muscle wasting is IKKβ-dependent and NF-kappaB-independent. PLoS One, 9, e87776.

Crimi, E., Ignarro, L. J., Cacciatore, F. & Napoli, C. 2009. Mechanisms by which exercise training benefits patients with heart failure. Nat Rev Cardiol, 6, 292-300.

Criswell, D., Powers, S., Dodd, S., Lawler, J., Edwards, W., Renshler, K. & Grinton, S. 1993. High intensity training-induced changes in skeletal muscle antioxidant enzyme activity. Med Sci Sports Exerc, 25, 1135-40.

Csibi, A., Cornille, K., Leibovitch, M. P., Poupon, A., Tintignac, L. A., Sanchez, A. M. & Leibovitch, S. A. 2010. The translation regulatory subunit eIF3f controls the kinase-dependent mTOR signaling required for muscle differentiation and hypertrophy in mouse. PLoS One, 5, e8994.

Culotta, V. C., Yang, M. & O'Halloran, T. V. 2006. Activation of superoxide dismutases: putting the metal to the pedal. Biochim Biophys Acta, 1763, 747-58.

Cunha, T. F., J. B. Moreira, N. A. Paixão, J. C. Campos, A. W. Monteiro, A. V. Bacurau, C. R. Bueno, J. C. Ferreira & P. C. Brum (2012) Aerobic exercise training upregulates skeletal muscle calpain and ubiquitin-proteasome systems in healthy mice. J Appl Physiol (1985), 112, 1839-46.

Cunningham, J. T., Rodgers, J. T., Arlow, D. H., Vazquez, F., Mootha, V. K. & Puigserver, P. 2007. mTOR controls mitochondrial oxidative function through a YY1-PGC-1alpha transcriptional complex. Nature, 450, 736-40.

Curello, S., Ceconi, C., Bigoli, C., Ferrari, R., Albertini, A. & Guarnieri, C. 1985. Changes in the cardiac glutathione status after ischemia and reperfusion. Experientia, 41, 42-3.

Damy, T., Ratajczak, P., Shah, A. M., Camors, E., Marty, I., Hasenfuss, G., Marotte, F., Samuel, J. L. & Heymes, C. 2004. Increased neuronal nitric oxide synthase-derived NO production in the failing human heart. Lancet, 363, 1365-7.

D'Angelo, D. D., Sakata, Y., Lorenz, J. N., Boivin, G. P., Walsh, R. A., Liggett, S. B. & Dorn, G. W. 1997. Transgenic Galphaq overexpression induces cardiac contractile failure in mice. Proc Natl Acad Sci U S A, 94, 8121-6.

Dasgupta, B., J. S. Ju, Y. Sasaki, X. Liu, S. R. Jung, K. Higashida, D. Lindquist & J. Milbrandt (2012) The AMPK β2 subunit is required for energy homeostasis during metabolic stress. Mol Cell Biol, 32, 2837-48.

Davies, K. J. 1987. Protein damage and degradation by oxygen radicals. I. general aspects. J Biol Chem, 262, 9895-901.

de Brito, O. M. & Scorrano, L. 2009. Mitofusin-2 regulates mitochondrial and endoplasmic reticulum morphology and tethering: the role of Ras. Mitochondrion, 9, 222-6.

de Mello Franco, F. G., Santos, A. C., Rondon, M. U., Trombetta, I. C., Strunz, C., Braga, A. M., Middlekauff, H., Negrão, C. E. & Pereira Barretto, A. C. 2006. Effects of home-based exercise training on neurovascular control in patients with heart failure. Eur J Heart Fail, 8, 851-5.

De Sousa, E., Lechêne, P., Fortin, D., N'Guessan, B., Belmadani, S., Bigard, X., Veksler, V. & Ventura-Clapier, R. 2002. Cardiac and skeletal muscle energy metabolism in heart failure: beneficial effects of voluntary activity. Cardiovasc Res, 56, 260-8.

De Sousa, E., V. Veksler, X. Bigard, P. Mateo & R. Ventura-Clapier (2000) Heart failure affects mitochondrial but not myofibrillar intrinsic properties of skeletal muscle. Circulation, 102, 1847-53.

de Waard, M. C., van der Velden, J., Bito, V., Ozdemir, S., Biesmans, L., Boontje, N. M., Dekkers, D. H., Schoonderwoerd, K., Schuurbiers, H. C., de Crom, R., Stienen, G. J., Sipido, K. R., Lamers, J. M. & Duncker, D. J. 2007. Early exercise training normalizes myofilament function and attenuates left ventricular pump dysfunction in mice with a large myocardial infarction. Circ Res, 100, 1079-88.

Dec, G. W. & Fuster, V. 1994. Idiopathic dilated cardiomyopathy. N Engl J Med, 331, 1564-75.

Delp, M. D., Duan, C., Mattson, J. P. & Musch, T. I. 1997. Changes in skeletal muscle biochemistry and histology relative to fiber type in rats with heart failure. J Appl Physiol (1985), 83, 1291-9.

Demontis, F. & Perrimon, N. 2010. FOXO/4E-BP signaling in Drosophila muscles regulates organism-wide proteostasis during aging. Cell, 143, 813-25.

Deter, R. L. & De Duve, C. 1967. Influence of glucagon, an inducer of cellular autophagy, on some physical properties of rat liver lysosomes. J Cell Biol, 33, 437-49.

Deval, C., Mordier, S., Obled, C., Bechet, D., Combaret, L., Attaix, D. & Ferrara, M. 2001. Identification of cathepsin L as a differentially expressed message associated with skeletal muscle wasting. Biochem J, 360, 143-50.

Di Valentino, M., Maeder, M. T., Jaggi, S., Schumann, J., Sommerfeld, K., Piazzalonga, S. & Hoffmann, A. 2010. Prognostic value of cycle exercise testing prior to and after outpatient cardiac rehabilitation. Int J Cardiol, 140, 34-41.

Díaz-Troya, S., Pérez-Pérez, M. E., Florencio, F. J. & Crespo, J. L. 2008. The role of TOR in autophagy regulation from yeast to plants and mammals. Autophagy, 4, 851-65.

Dickinson, D. A. & Forman, H. J. 2002. Glutathione in defense and signaling: lessons from a small thiol. Ann N Y Acad Sci, 973, 488-504.

Donato, L. J. & Noy, N. 2005. Suppression of mammary carcinoma growth by retinoic acid: proapoptotic genes are targets for retinoic acid receptor and cellular retinoic acid-binding protein II signaling. Cancer Res, 65, 8193-9.

Dorion, S., Lambert, H. & Landry, J. 2002. Activation of the p38 signaling pathway by heat shock involves the dissociation of glutathione S-transferase Mu from Ask1. J Biol Chem, 277, 30792-7.

Dowal, L., Provitera, P. & Scarlata, S. 2006. Stable association between G alpha(q) and phospholipase C beta 1 in living cells. J Biol Chem, 281, 23999-4014.

Drelicharz, Ł., Woźniak, M., Skórka, T., Tyrankiewicz, U., Heinze-Paluchowska, S., Jabłońska, M., Gebska, A. & Chłopicki, S. 2009. Application of magnetic resonance imaging in vivo for the assessment of the progression of systolic and diastolic dysfunction in a mouse model of dilated cardiomyopathy. Kardiol Pol, 67, 386-95.

Drevet, J. R. 2006. The antioxidant glutathione peroxidase family and spermatozoa: a complex story. Mol Cell Endocrinol, 250, 70-9.

Drexler, H., Riede, U., Münzel, T., König, H., Funke, E. & Just, H. 1992. Alterations of skeletal muscle in chronic heart failure. Circulation, 85, 1751-9.

Dröge, W. (2002) Free radicals in the physiological control of cell function. Physiol Rev, 82, 47-95.

Drummond, M. J., Dreyer, H. C., Pennings, B., Fry, C. S., Dhanani, S., Dillon, E. L., Sheffield-Moore, M., Volpi, E. & Rasmussen, B. B. 2008. Skeletal muscle protein anabolic response to resistance exercise and essential amino acids is delayed with aging. J Appl Physiol (1985), 104, 1452-61.

Durante, P. E., K. J. Mustard, S. H. Park, W. W. Winder & D. G. Hardie (2002) Effects of endurance training on activity and expression of AMP-activated protein kinase isoforms in rat muscles. Am J Physiol Endocrinol Metab, 283, E178-86.

Edes, I. F., Tóth, A., Csányi, G., Lomnicka, M., Chłopicki, S., Edes, I. & Papp, Z. 2008. Late-stage alterations in myofibrillar contractile function in a transgenic mouse model of dilated cardiomyopathy (Tgalphaq*44). J Mol Cell Cardiol, 45, 363-72.

El-Agamey, A., Lowe, G. M., McGarvey, D. J., Mortensen, A., Phillip, D. M., Truscott, T. G. & Young, A. J. 2004. Carotenoid radical chemistry and antioxidant/pro-oxidant properties. Arch Biochem Biophys, 430, 37-48.

Elahi, M., Mahmood, M., Shahbaz, A., Malick, N., Sajid, J., Asopa, S. & Matata, B. M. 2010. Current concepts underlying benefits of exercise training in congestive heart failure patients. Curr Cardiol Rev, 6, 104-11.

Feige, J. N. & Auwerx, J. 2007. Transcriptional coregulators in the control of energy homeostasis. Trends Cell Biol, 17, 292-301.

Ferdinandy, P., Danial, H., Ambrus, I., Rothery, R. A. & Schulz, R. 2000. Peroxynitrite is a major contributor to cytokine-induced myocardial contractile failure. Circ Res, 87, 241-7.

Fielitz, J., Kim, M. S., Shelton, J. M., Latif, S., Spencer, J. A., Glass, D. J., Richardson, J. A., Bassel-Duby, R. & Olson, E. N. 2007. Myosin accumulation and striated muscle myopathy result from the loss of muscle RING finger 1 and 3. J Clin Invest, 117, 2486-95.

Fimia, G. M., Stoykova, A., Romagnoli, A., Giunta, L., Di Bartolomeo, S., Nardacci, R., Corazzari, M., Fuoco, C., Ucar, A., Schwartz, P., Gruss, P., Piacentini, M., Chowdhury, K. & Cecconi, F. 2007. Ambra1 regulates autophagy and development of the nervous system. Nature, 447, 1121-5.

Flohé, L. 1988. Glutathione peroxidase. Basic Life Sci, 49, 663-8.

Flohé, L., Budde, H. & Hofmann, B. 2003. Peroxiredoxins in antioxidant defense and redox regulation. Biofactors, 19, 3-10.

Frolov, A., Chahwan, S., Ochs, M., Arnoletti, J. P., Pan, Z. Z., Favorova, O., Fletcher, J., von Mehren, M., Eisenberg, B. & Godwin, A. K. 2003. Response markers and the molecular mechanisms of action of Gleevec in gastrointestinal stromal tumors. Mol Cancer Ther, 2, 699-709.

Furuno, K., Goodman, M. N. & Goldberg, A. L. 1990. Role of different proteolytic systems in the degradation of muscle proteins during denervation atrophy. J Biol Chem, 265, 8550-7.

Garcia-Roves, P. M., M. E. Osler, M. H. Holmström & J. R. Zierath (2008) Gain-of-function R225Q mutation in AMP-activated protein kinase gamma3 subunit increases mitochondrial biogenesis in glycolytic skeletal muscle. J Biol Chem, 283, 35724-34.

Garnier, A., D. Fortin, C. Deloménie, I. Momken, V. Veksler & R. Ventura-Clapier (2003) Depressed mitochondrial transcription factors and oxidative capacity in rat failing cardiac and skeletal muscles. J Physiol, 551, 491-501.

Garnier, A., Fortin, D., Zoll, J., N'Guessan, B., Mettauer, B., Lampert, E., Veksler, V. & Ventura-Clapier, R. 2005. Coordinated changes in mitochondrial function and biogenesis in healthy and diseased human skeletal muscle. FASEB J, 19, 43-52.

Geng, T., Li, P., Okutsu, M., Yin, X., Kwek, J., Zhang, M. & Yan, Z. 2010. PGC-1alpha plays a functional role in exercise-induced mitochondrial biogenesis and angiogenesis but not fiber-type transformation in mouse skeletal muscle. Am J Physiol Cell Physiol, 298, C572-9.

Geng, T., Li, P., Yin, X. & Yan, Z. 2011. PGC-1α promotes nitric oxide antioxidant defenses and inhibits FOXO signaling against cardiac cachexia in mice. Am J Pathol, 178, 1738-48.

Ghezzi, P. 2005. Regulation of protein function by glutathionylation. Free Radic Res, 39, 573-80.

Gil-del Valle, L., de la C Milian, L., Toledo, A., Vilaró, N., Tápanes, R. & Otero, M. A. 2005. Altered redox status in patients with diabetes mellitus type I. Pharmacol Res, 51, 375-80.

Goldberg, A. L. 1969. Protein turnover in skeletal muscle. I. Protein catabolism during work-induced hypertrophy and growth induced with growth hormone. J Biol Chem, 244, 3217-22.

Gomes, A. V., Waddell, D. S., Siu, R., Stein, M., Dewey, S., Furlow, J. D. & Bodine, S. C. 2012. Upregulation of proteasome activity in muscle RING finger 1-null mice following denervation. FASEB J, 26, 2986-99.

Goodman, C. A., Frey, J. W., Mabrey, D. M., Jacobs, B. L., Lincoln, H. C., You, J. S. & Hornberger, T. A. 2011. The role of skeletal muscle mTOR in the regulation of mechanical load-induced growth. J Physiol, 589, 5485-501.

Gordon, A., Tyni-Lenné, R., Jansson, E., Kaijser, L., Theodorsson-Norheim, E. & Sylvén, C. 1997. Improved ventilation and decreased sympathetic stress in chronic heart failure patients following local endurance training with leg muscles. J Card Fail, 3, 3-12.

Green, H. J., Helyar, R., Ball-Burnett, M., Kowalchuk, N., Symon, S. & Farrance, B. 1992. Metabolic adaptations to training precede changes in muscle mitochondrial capacity. J Appl Physiol (1985), 72, 484-91.

Green, H. J., Reichmann, H. & Pette, D. 1982. A comparison of two ATPase based schemes for histochemical muscle fibre typing in various mammals. Histochemistry, 76, 21-31.

Greenhaff, P. L., Söderlund, K., Ren, J. M. & Hultman, E. 1993. Energy metabolism in single human muscle fibres during intermittent contraction with occluded circulation. J Physiol, 460, 443-53.

Greer, E. L., Dowlatshahi, D., Banko, M. R., Villen, J., Hoang, K., Blanchard, D., Gygi, S. P. & Brunet, A. 2007a. An AMPK-FOXO pathway mediates longevity induced by a novel method of dietary restriction in C. elegans. Curr Biol, 17, 1646-56.

Greer, E. L., Oskoui, P. R., Banko, M. R., Maniar, J. M., Gygi, M. P., Gygi, S. P. & Brunet, A. 2007b. The energy sensor AMP-activated protein kinase directly regulates the mammalian FOXO3 transcription factor. J Biol Chem, 282, 30107-19.

Gromer, S., Urig, S. & Becker, K. 2004. The thioredoxin system--from science to clinic. Med Res Rev, 24, 40-89.

Grumati, P., Coletto, L., Sabatelli, P., Cescon, M., Angelin, A., Bertaggia, E., Blaauw, B., Urciuolo, A., Tiepolo, T., Merlini, L., Maraldi, N. M., Bernardi, P., Sandri, M. & Bonaldo, P. 2010. Autophagy is defective in collagen VI muscular dystrophies, and its reactivation rescues myofiber degeneration. Nat Med, 16, 1313-20.

Grune, T., Merker, K., Sandig, G. & Davies, K. J. 2003. Selective degradation of oxidatively modified protein substrates by the proteasome. Biochem Biophys Res Commun, 305, 709-18.

Gustafsson, T., Bodin, K., Sylvén, C., Gordon, A., Tyni-Lenné, R. & Jansson, E. 2001. Increased expression of VEGF following exercise training in patients with heart failure. Eur J Clin Invest, 31, 362-6.

Gutteridge, J. M. & Mitchell, J. 1999. Redox imbalance in the critically ill. Br Med Bull, 55, 49-75.

Halliwell, B. 2007. Biochemistry of oxidative stress. Biochem Soc Trans, 35, 1147-50.

Hambrecht, R., Fiehn, E., Yu, J., Niebauer, J., Weigl, C., Hilbrich, L., Adams, V., Riede, U. & Schuler, G. 1997. Effects of endurance training on mitochondrial ultrastructure and fiber type distribution in skeletal muscle of patients with stable chronic heart failure. J Am Coll Cardiol, 29, 1067-73.

Hambrecht, R., Gielen, S., Linke, A., Fiehn, E., Yu, J., Walther, C., Schoene, N. & Schuler, G. 2000. Effects of exercise training on left ventricular function and peripheral resistance in patients with chronic heart failure: A randomized trial. JAMA, 283, 3095-101.

Hambrecht, R., Niebauer, J., Fiehn, E., Kälberer, B., Offner, B., Hauer, K., Riede, U., Schlierf, G., Kübler, W. & Schuler, G. 1995. Physical training in patients with stable chronic heart failure: effects on cardiorespiratory fitness and ultrastructural abnormalities of leg muscles. J Am Coll Cardiol, 25, 1239-49.

Handschin, C. 2009. Peroxisome proliferator-activated receptor-gamma coactivator-1alpha in muscle links metabolism to inflammation. Clin Exp Pharmacol Physiol, 36, 1139-43.

Handschin, C., Chin, S., Li, P., Liu, F., Maratos-Flier, E., Lebrasseur, N. K., Yan, Z. & Spiegelman, B. M. 2007. Skeletal muscle fiber-type switching, exercise intolerance, and myopathy in PGC-1alpha muscle-specific knock-out animals. J Biol Chem, 282, 30014-21.

Hanna, R. A., Quinsay, M. N., Orogo, A. M., Giang, K., Rikka, S. & Gustafsson, Å. 2012. Microtubule-associated protein 1 light chain 3 (LC3) interacts with Bnip3 protein to selectively remove endoplasmic reticulum and mitochondria via autophagy. J Biol Chem, 287, 19094-104.

HANSON, J. & HUXLEY, H. E. 1953. Structural basis of the cross-striations in muscle. Nature, 172, 530-2.

Hara, T., Nakamura, K., Matsui, M., Yamamoto, A., Nakahara, Y., Suzuki-Migishima, R., Yokoyama, M., Mishima, K., Saito, I., Okano, H. & Mizushima, N. 2006. Suppression of basal autophagy in neural cells causes neurodegenerative disease in mice. Nature, 441, 885-9.

Haykowsky, M. J., Liang, Y., Pechter, D., Jones, L. W., McAlister, F. A. & Clark, A. M. 2007. A meta-analysis of the effect of exercise training on left ventricular remodeling in heart failure patients: the benefit depends on the type of training performed. J Am Coll Cardiol, 49, 2329-36.

Hirai, D. M., T. I. Musch & D. C. Poole (2015) Exercise training in chronic heart failure: improving skeletal muscle O2 transport and utilization. Am J Physiol Heart Circ Physiol, 309, H1419-39.

Holmgren, A. 1985. Thioredoxin. Annu Rev Biochem, 54, 237-71.

Holmgren, A., Johansson, C., Berndt, C., Lönn, M. E., Hudemann, C. & Lillig, C. H. 2005. Thiol redox control via thioredoxin and glutaredoxin systems. Biochem Soc Trans, 33, 1375-7.

Hoppeler, H., Howald, H., Conley, K., Lindstedt, S. L., Claassen, H., Vock, P. & Weibel, E. R. 1985. Endurance training in humans: aerobic capacity and structure of skeletal muscle. J Appl Physiol (1985), 59, 320-7.

Huang, H. & Tindall, D. J. 2007. Dynamic FoxO transcription factors. J Cell Sci, 120, 2479-87.

Hunt, S. A., Baker, D. W., Chin, M. H., Cinquegrani, M. P., Feldman, A. M., Francis, G. S., Ganiats, T. G., Goldstein, S., Gregoratos, G., Jessup, M. L., Noble, R. J., Packer, M., Silver, M. A., Stevenson, L. W., Gibbons, R. J., Antman, E. M., et al. 2001. ACC/AHA guidelines for the evaluation and management of chronic heart failure in the adult: executive summary. A report of the American College of Cardiology/American Heart Association Task Force on Practice Guidelines (Committee to revise the 1995 Guidelines for the Evaluation and Management of Heart Failure). J Am Coll Cardiol, 38, 2101-13.

Huss, J. M., Kopp, R. P. & Kelly, D. P. 2002. Peroxisome proliferator-activated receptor coactivator-1alpha (PGC-1alpha) coactivates the cardiac-enriched nuclear receptors estrogen-related receptor-alpha and -gamma. Identification of novel leucine-rich interaction motif within PGC-1alpha. J Biol Chem, 277, 40265-74.

Hwee, D. T., Baehr, L. M., Philp, A., Baar, K. & Bodine, S. C. 2014. Maintenance of muscle mass and load-induced growth in Muscle RING Finger 1 null mice with age. Aging Cell, 13, 92-101.

Ikeda, Y., A. Shirakabe, C. Brady, D. Zablocki, M. Ohishi & J. Sadoshima (2015) Molecular mechanisms mediating mitochondrial dynamics and mitophagy and their functional roles in the cardiovascular system. J Mol Cell Cardiol, 78, 116-22.

Ishihara, N., Eura, Y. & Mihara, K. 2004. Mitofusin 1 and 2 play distinct roles in mitochondrial fusion reactions via GTPase activity. J Cell Sci, 117, 6535-46.

Izumiya, Y., Hopkins, T., Morris, C., Sato, K., Zeng, L., Viereck, J., Hamilton, J. A., Ouchi, N., LeBrasseur, N. K. & Walsh, K. 2008. Fast/Glycolytic muscle fiber growth reduces fat mass and improves metabolic parameters in obese mice. Cell Metab, 7, 159-72.

Jackman, M. R. & Willis, W. T. 1996. Characteristics of mitochondria isolated from type I and type IIb skeletal muscle. Am J Physiol, 270, C673-8.

Jackson, M. J., Papa, S., Bolaños, J., Bruckdorfer, R., Carlsen, H., Elliott, R. M., Flier, J., Griffiths, H. R., Heales, S., Holst, B., Lorusso, M., Lund, E., Øivind Moskaug, J., Moser, U., Di Paola, M., Polidori, M. C., et al. 2002. Antioxidants, reactive oxygen and nitrogen species, gene induction and mitochondrial function. Mol Aspects Med, 23, 209-85.

Jäger, S., C. Handschin, J. St-Pierre & B. M. Spiegelman (2007) AMP-activated protein kinase (AMPK) action in skeletal muscle via direct phosphorylation of PGC-1alpha. Proc Natl Acad Sci U S A, 104, 12017-22.

James, D. I., Parone, P. A., Mattenberger, Y. & Martinou, J. C. 2003. hFis1, a novel component of the mammalian mitochondrial fission machinery. J Biol Chem, 278, 36373-9.

Janssen-Heininger, Y. M., Mossman, B. T., Heintz, N. H., Forman, H. J., Kalyanaraman, B., Finkel, T., Stamler, J. S., Rhee, S. G. & van der Vliet, A. 2008. Redox-based regulation of signal transduction: principles, pitfalls, and promises. Free Radic Biol Med, 45, 1-17.

Ji, L. L., Gomez-Cabrera, M. C., Steinhafel, N. & Vina, J. 2004. Acute exercise activates nuclear factor (NF)-kappaB signaling pathway in rat skeletal muscle. FASEB J, 18, 1499-506.

Johansen, T. & Lamark, T. 2011. Selective autophagy mediated by autophagic adapter proteins. Autophagy, 7, 279-96.

Jokl, E. J. & G. Blanco (2016) Disrupted autophagy undermines skeletal muscle adaptation and integrity. Mamm Genome.

Jørgensen, S. B., J. F. Wojtaszewski, B. Viollet, F. Andreelli, J. B. Birk, Y. Hellsten, P. Schjerling, S. Vaulont, P. D. Neufer, E. A. Richter & H. Pilegaard (2005) Effects of alpha-AMPK knockout on exercise-induced gene activation in mouse skeletal muscle. FASEB J, 19, 1146-8.

Jørgensen, S. B., J. T. Treebak, B. Viollet, P. Schjerling, S. Vaulont, J. F. Wojtaszewski & E. A. Richter (2007) Role of AMPKalpha2 in basal, training-, and AICAR-induced GLUT4, hexokinase II, and mitochondrial protein expression in mouse muscle. Am J Physiol Endocrinol Metab, 292, E331-9.

Kamei, Y., Miura, S., Suzuki, M., Kai, Y., Mizukami, J., Taniguchi, T., Mochida, K., Hata, T., Matsuda, J., Aburatani, H., Nishino, I. & Ezaki, O. 2004. Skeletal muscle FOXO1 (FKHR) transgenic mice have less skeletal muscle mass, down-regulated Type I (slow twitch/red muscle) fiber genes, and impaired glycemic control. J Biol Chem, 279, 41114-23.

Kang, S. W., Rhee, S. G., Chang, T. S., Jeong, W. & Choi, M. H. 2005. 2-Cys peroxiredoxin function in intracellular signal transduction: therapeutic implications. Trends Mol Med, 11, 571-8.

Karren, M. A., Coonrod, E. M., Anderson, T. K. & Shaw, J. M. 2005. The role of Fis1p-Mdv1p interactions in mitochondrial fission complex assembly. J Cell Biol, 171, 291-301.

Katz, S. D., Khan, T., Zeballos, G. A., Mathew, L., Potharlanka, P., Knecht, M. & Whelan, J. 1999. Decreased activity of the L-arginine-nitric oxide metabolic pathway in patients with congestive heart failure. Circulation, 99, 2113-7.

Ke, Z., S. P. Yip, L. Li, X. X. Zheng, W. K. Tam & K. Y. Tong (2011) The effects of voluntary, involuntary, and forced exercises on motor recovery in a stroke rat model. Conf Proc IEEE Eng Med Biol Soc, 2011, 8223-6.

Kedar, V., McDonough, H., Arya, R., Li, H. H., Rockman, H. A. & Patterson, C. 2004. Muscle-specific RING finger 1 is a bona fide ubiquitin ligase that degrades cardiac troponin I. Proc Natl Acad Sci U S A, 101, 18135-40.

Kemi, O. J., Høydal, M. A., Haram, P. M., Garnier, A., Fortin, D., Ventura-Clapier, R. & Ellingsen, O. 2007. Exercise training restores aerobic capacity and energy transfer systems in heart failure treated with losartan. Cardiovasc Res, 76, 91-9.

Kenchaiah, S., Sesso, H. D. & Gaziano, J. M. 2009. Body mass index and vigorous physical activity and the risk of heart failure among men. Circulation, 119, 44-52.

Keteyian, S. J., Duscha, B. D., Brawner, C. A., Green, H. J., Marks, C. R., Schachat, F. H., Annex, B. H. & Kraus, W. E. 2003. Differential effects of exercise training in men and women with chronic heart failure. Am Heart J, 145, 912-8.

Kim, J. Y., Koves, T. R., Yu, G. S., Gulick, T., Cortright, R. N., Dohm, G. L. & Muoio, D. M. 2002. Evidence of a malonyl-CoA-insensitive carnitine palmitoyltransferase I activity in red skeletal muscle. Am J Physiol Endocrinol Metab, 282, E1014-22.

Kim, K., Rhee, S. G. & Stadtman, E. R. 1985. Nonenzymatic cleavage of proteins by reactive oxygen species generated by dithiothreitol and iron. J Biol Chem, 260, 15394-7.

Kirkin, V., Lamark, T., Sou, Y. S., Bjørkøy, G., Nunn, J. L., Bruun, J. A., Shvets, E., McEwan, D. G., Clausen, T. H., Wild, P., Bilusic, I., Theurillat, J. P., Øvervatn, A., Ishii, T., Elazar, Z., Komatsu, M., et al. 2009a. A role for NBR1 in autophagosomal degradation of ubiquitinated substrates. Mol Cell, 33, 505-16.

Kirkin, V., McEwan, D. G., Novak, I. & Dikic, I. 2009b. A role for ubiquitin in selective autophagy. Mol Cell, 34, 259-69.

Kirkman, H. N., Rolfo, M., Ferraris, A. M. & Gaetani, G. F. 1999. Mechanisms of protection of catalase by NADPH. Kinetics and stoichiometry. J Biol Chem, 274, 13908-14.

Klionsky, D. J. 2007. Autophagy: from phenomenology to molecular understanding in less than a decade. Nat Rev Mol Cell Biol, 8, 931-7.

Klionsky, D. J.Abeliovich, H.Agostinis, P.Agrawal, D. K.Aliev, G.Askew, D. S.Baba, M.Baehrecke, E. H.Bahr, B. A.Ballabio, A.Bamber, B. A.Bassham, D. C.Bergamini, E.Bi, X.Biard-Piechaczyk, M.Blum, J. S., et al. 2008. Guidelines for the use and interpretation of assays for monitoring autophagy in higher eukaryotes. Autophagy, 4, 151-75.

Knowlton, A. A., Chen, L. & Malik, Z. A. 2014. Heart failure and mitochondrial dysfunction: the role of mitochondrial fission/fusion abnormalities and new therapeutic strategies. J Cardiovasc Pharmacol, 63, 196-206.

Koike, M., Shibata, M., Waguri, S., Yoshimura, K., Tanida, I., Kominami, E., Gotow, T., Peters, C., von Figura, K., Mizushima, N., Saftig, P. & Uchiyama, Y. 2005. Participation of autophagy

in storage of lysosomes in neurons from mouse models of neuronal ceroid-lipofuscinoses (Batten disease). Am J Pathol, 167, 1713-28.

Komatsu, M., Waguri, S., Koike, M., Sou, Y. S., Ueno, T., Hara, T., Mizushima, N., Iwata, J., Ezaki, J., Murata, S., Hamazaki, J., Nishito, Y., Iemura, S., Natsume, T., Yanagawa, T., Uwayama, J., et al. 2007. Homeostatic levels of p62 control cytoplasmic inclusion body formation in autophagy-deficient mice. Cell, 131, 1149-63.

Komatsu, M., Waguri, S., Ueno, T., Iwata, J., Murata, S., Tanida, I., Ezaki, J., Mizushima, N., Ohsumi, Y., Uchiyama, Y., Kominami, E., Tanaka, K. & Chiba, T. 2005. Impairment of starvation-induced and constitutive autophagy in Atg7-deficient mice. J Cell Biol, 169, 425-34.

Kon, M. & Cuervo, A. M. 2010. Chaperone-mediated autophagy in health and disease. FEBS Lett, 584, 1399-404.

Koshiba, T., Detmer, S. A., Kaiser, J. T., Chen, H., McCaffery, J. M. & Chan, D. C. 2004. Structural basis of mitochondrial tethering by mitofusin complexes. Science, 305, 858-62.

Kovacic, P. & Jacintho, J. D. 2001. Mechanisms of carcinogenesis: focus on oxidative stress and electron transfer. Curr Med Chem, 8, 773-96.

Kroemer, G. (2010) Pathophysiological implications of mithochondrial cell death control. Bull Mem Acad R Med Belg, 165, 205-10.

Kroemer, G., G. Mariño & B. Levine (2010) Autophagy and the integrated stress response. Mol Cell, 40, 280-93.

Kudryashova, E., Kramerova, I. & Spencer, M. J. 2012. Satellite cell senescence underlies myopathy in a mouse model of limb-girdle muscular dystrophy 2H. J Clin Invest, 122, 1764-76.

Kuma, A., Hatano, M., Matsui, M., Yamamoto, A., Nakaya, H., Yoshimori, T., Ohsumi, Y., Tokuhisa, T. & Mizushima, N. 2004. The role of autophagy during the early neonatal starvation period. Nature, 432, 1032-6.

Kumar, A., Bhatnagar, S. & Paul, P. K. 2012. TWEAK and TRAF6 regulate skeletal muscle atrophy. Curr Opin Clin Nutr Metab Care, 15, 233-9.

Kundu, M. & Thompson, C. B. 2005. Macroautophagy versus mitochondrial autophagy: a question of fate? Cell Death Differ, 12 Suppl 2, 1484-9.

Kundu, M., Lindsten, T., Yang, C. Y., Wu, J., Zhao, F., Zhang, J., Selak, M. A., Ney, P. A. & Thompson, C. B. 2008. Ulk1 plays a critical role in the autophagic clearance of mitochondria and ribosomes during reticulocyte maturation. Blood, 112, 1493-502.

Kuwahara, H., T. Horie, S. Ishikawa, C. Tsuda, S. Kawakami, Y. Noda, T. Kaneko, S. Tahara, T. Tachibana, M. Okabe, J. Melki, R. Takano, T. Toda, D. Morikawa, H. Nojiri, H. Kurosawa, T. Shirasawa & T. Shimizu (2010) Oxidative stress in skeletal muscle causes severe disturbance of exercise activity without muscle atrophy. Free Radic Biol Med, 48, 1252-62.

Ladner, J. E., Parsons, J. F., Rife, C. L., Gilliland, G. L. & Armstrong, R. N. 2004. Parallel evolutionary pathways for glutathione transferases: structure and mechanism of the mitochondrial class kappa enzyme rGSTK1-1. Biochemistry, 43, 352-61.

Laemmli, U. K. 1970. Cleavage of structural proteins during the assembly of the head of bacteriophage T4. Nature, 227, 680-5.

Lai, K. M., Gonzalez, M., Poueymirou, W. T., Kline, W. O., Na, E., Zlotchenko, E., Stitt, T. N., Economides, A. N., Yancopoulos, G. D. & Glass, D. J. 2004. Conditional activation of akt in adult skeletal muscle induces rapid hypertrophy. Mol Cell Biol, 24, 9295-304.

Lapierre, L. R., Kumsta, C., Sandri, M., Ballabio, A. & Hansen, M. 2015. Transcriptional and epigenetic regulation of autophagy in aging. Autophagy, 11, 867-80.

Laplante, M. & Sabatini, D. M. 2012. mTOR signaling in growth control and disease. Cell, 149, 274-93.

Larsen, A. I., Lindal, S., Aukrust, P., Toft, I., Aarsland, T. & Dickstein, K. 2002. Effect of exercise training on skeletal muscle fibre characteristics in men with chronic heart failure. Correlation between skeletal uscle alterations, cytokines and exercise capacity. Int J Cardiol, 83, 25-32.

Larsen, R. G., Maynard, L. & Kent, J. A. 2014. High-intensity interval training alters ATP pathway flux during maximal muscle contractions in humans. Acta Physiol (Oxf), 211, 147-60.

Larsson, L. & Moss, R. L. 1993. Maximum velocity of shortening in relation to myosin isoform composition in single fibres from human skeletal muscles. J Physiol, 472, 595-614.

Latres, E., Amini, A. R., Amini, A. A., Griffiths, J., Martin, F. J., Wei, Y., Lin, H. C., Yancopoulos, G. D. & Glass, D. J. 2005. Insulin-like growth factor-1 (IGF-1) inversely regulates atrophy-induced genes via the phosphatidylinositol 3-kinase/Akt/mammalian target of rapamycin (PI3K/Akt/mTOR) pathway. J Biol Chem, 280, 2737-44.

Laughlin, M. H., Simpson, T., Sexton, W. L., Brown, O. R., Smith, J. K. & Korthuis, R. J. 1990. Skeletal muscle oxidative capacity, antioxidant enzymes, and exercise training. J Appl Physiol (1985), 68, 2337-43.

Lawler, J. M. & Demaree, S. R. 2001. Relationship between NADP-specific isocitrate dehydrogenase and glutathione peroxidase in aging rat skeletal muscle. Mech Ageing Dev, 122, 291-304.

Lawler, J. M., Kwak, H. B., Song, W. & Parker, J. L. 2006. Exercise training reverses downregulation of HSP70 and antioxidant enzymes in porcine skeletal muscle after chronic coronary artery occlusion. Am J Physiol Regul Integr Comp Physiol, 291, R1756-63.

Lawler, J. M., Powers, S. K. & Criswell, D. S. 1993. Inducibility of NADP-specific isocitrate dehydrogenase with endurance training in skeletal muscle. Acta Physiol Scand, 149, 177-81.

Le Bacquer, O., Petroulakis, E., Paglialunga, S., Poulin, F., Richard, D., Cianflone, K. & Sonenberg, N. 2007. Elevated sensitivity to diet-induced obesity and insulin resistance in mice lacking 4E-BP1 and 4E-BP2. J Clin Invest, 117, 387-96.

Leblanc, P. J., Harris, R. A. & Peters, S. J. 2007. Skeletal muscle fiber type comparison of pyruvate dehydrogenase phosphatase activity and isoform expression in fed and food-deprived rats. Am J Physiol Endocrinol Metab, 292, E571-6.

Leboucher, G. P., Tsai, Y. C., Yang, M., Shaw, K. C., Zhou, M., Veenstra, T. D., Glickman, M. H. & Weissman, A. M. 2012. Stress-induced phosphorylation and proteasomal degradation of mitofusin 2 facilitates mitochondrial fragmentation and apoptosis. Mol Cell, 47, 547-57.

Lecker, S. H., Jagoe, R. T., Gilbert, A., Gomes, M., Baracos, V., Bailey, J., Price, S. R., Mitch, W. E. & Goldberg, A. L. 2004. Multiple types of skeletal muscle atrophy involve a common program of changes in gene expression. FASEB J, 18, 39-51.

Lee, J. H., Bodmer, R., Bier, E. & Karin, M. 2010. Sestrins at the crossroad between stress and aging. Aging (Albany NY), 2, 369-74.

Lee, J. Y., H. Koga, Y. Kawaguchi, W. Tang, E. Wong, Y. S. Gao, U. B. Pandey, S. Kaushik, E. Tresse, J. Lu, J. P. Taylor, A. M. Cuervo & T. P. Yao (2010) HDAC6 controls autophagosome maturation essential for ubiquitin-selective quality-control autophagy. EMBO J, 29, 969-80.

Lee, S. J. 2004. Regulation of muscle mass by myostatin. Annu Rev Cell Dev Biol, 20, 61-86.

Leeuwenburgh, C., Fiebig, R., Chandwaney, R. & Ji, L. L. 1994. Aging and exercise training in skeletal muscle: responses of glutathione and antioxidant enzyme systems. Am J Physiol, 267, R439-45.

Lehman, J. J., Barger, P. M., Kovacs, A., Saffitz, J. E., Medeiros, D. M. & Kelly, D. P. 2000. Peroxisome proliferator-activated receptor gamma coactivator-1 promotes cardiac mitochondrial biogenesis. J Clin Invest, 106, 847-56.

Lei, K. F., Liu, B. Y., Wang, Y. F., Chen, X. H., Yu, B. Q., Guo, Y. & Zhu, Z. G. 2011. SerpinB5 interacts with KHDRBS3 and FBXO32 in gastric cancer cells. Oncol Rep, 26, 1115-20.

Leick, L., Lyngby, S. S., Wojtaszewski, J. F., Wojtasewski, J. F. & Pilegaard, H. 2010. PGC-1alpha is required for training-induced prevention of age-associated decline in mitochondrial enzymes in mouse skeletal muscle. Exp Gerontol, 45, 336-42.

Leick, L., Wojtaszewski, J. F., Johansen, S. T., Kiilerich, K., Comes, G., Hellsten, Y., Hidalgo, J. & Pilegaard, H. 2008. PGC-1alpha is not mandatory for exercise- and training-induced adaptive gene responses in mouse skeletal muscle. Am J Physiol Endocrinol Metab, 294, E463-74.

Lerman, A., Kubo, S. H., Tschumperlin, L. K. & Burnett, J. C. 1992. Plasma endothelin concentrations in humans with end-stage heart failure and after heart transplantation. J Am Coll Cardiol, 20, 849-53.

Levin, H. R., Oz, M. C., Chen, J. M., Packer, M., Rose, E. A. & Burkhoff, D. 1995. Reversal of chronic ventricular dilation in patients with end-stage cardiomyopathy by prolonged mechanical unloading. Circulation, 91, 2717-20.

Levine, B. & D. J. Klionsky (2004) Development by self-digestion: molecular mechanisms and biological functions of autophagy. Dev Cell, 6, 463-77.

Li, H. H., Kedar, V., Zhang, C., McDonough, H., Arya, R., Wang, D. Z. & Patterson, C. 2004. Atrogin-1/muscle atrophy F-box inhibits calcineurin-dependent cardiac hypertrophy by participating in an SCF ubiquitin ligase complex. J Clin Invest, 114, 1058-71.

Li, J. B. & Goldberg, A. L. 1976. Effects of food deprivation on protein synthesis and degradation in rat skeletal muscles. Am J Physiol, 231, 441-8.

Li, J. Y., T. B. Kuo, J. C. Yen, S. C. Tsai & C. C. Yang (2014) Voluntary and involuntary running in the rat show different patterns of theta rhythm, physical activity, and heart rate. J Neurophysiol, 111, 2061-70.

Liang, C., Feng, P., Ku, B., Dotan, I., Canaani, D., Oh, B. H. & Jung, J. U. 2006. Autophagic and tumour suppressor activity of a novel Beclin1-binding protein UVRAG. Nat Cell Biol, 8, 688-99.

Liang, H. & W. F. Ward (2006) PGC-1alpha: a key regulator of energy metabolism. Adv Physiol Educ, 30, 145-51.

Lin, J., Wu, H., Tarr, P. T., Zhang, C. Y., Wu, Z., Boss, O., Michael, L. F., Puigserver, P., Isotani, E., Olson, E. N., Lowell, B. B., Bassel-Duby, R. & Spiegelman, B. M. 2002. Transcriptional co-activator PGC-1 alpha drives the formation of slow-twitch muscle fibres. Nature, 418, 797-801.

Lin, M. T. & Beal, M. F. 2006. Mitochondrial dysfunction and oxidative stress in neurodegenerative diseases. Nature, 443, 787-95.

Lindquist, S. & Craig, E. A. 1988. The heat-shock proteins. Annu Rev Genet, 22, 631-77.

Linke, A., Recchia, F., Zhang, X. & Hintze, T. H. 2003. Acute and chronic endothelial dysfunction: implications for the development of heart failure. Heart Fail Rev, 8, 87-97.

Liochev, S. I. & Fridovich, I. 2002. Nitroxyl (NO-): a substrate for superoxide dismutase. Arch Biochem Biophys, 402, 166-71.

Lira, V. A., M. Okutsu, M. Zhang, N. P. Greene, R. C. Laker, D. S. Breen, K. L. Hoehn & Z. Yan (2013) Autophagy is required for exercise training-induced skeletal muscle adaptation and improvement of physical performance. FASEB J, 27, 4184-93.

Liu, C. M., Yang, Z., Liu, C. W., Wang, R., Tien, P., Dale, R. & Sun, L. Q. 2007. Effect of RNA oligonucleotide targeting Foxo-1 on muscle growth in normal and cancer cachexia mice. Cancer Gene Ther, 14, 945-52.

Lo Verso, F., Carnio, S., Vainshtein, A. & Sandri, M. 2014. Autophagy is not required to sustain exercise and PRKAA1/AMPK activity but is important to prevent mitochondrial damage during physical activity. Autophagy, 10, 1883-94.

Lokireddy, S., Wijesoma, I. W., Sze, S. K., McFarlane, C., Kambadur, R. & Sharma, M. 2012a. Identification of atrogin-1-targeted proteins during the myostatin-induced skeletal muscle wasting. Am J Physiol Cell Physiol, 303, C512-29.

Lokireddy, S., Wijesoma, I. W., Teng, S., Bonala, S., Gluckman, P. D., McFarlane, C., Sharma, M. & Kambadur, R. 2012. The ubiquitin ligase Mul1 induces mitophagy in skeletal muscle in response to muscle-wasting stimuli. Cell Metab, 16, 613-24.

Lokireddy, S., Wijesoma, I. W., Teng, S., Bonala, S., Gluckman, P. D., McFarlane, C., Sharma, M. & Kambadur, R. 2012. The ubiquitin ligase Mul1 induces mitophagy in skeletal muscle in response to muscle-wasting stimuli. Cell Metab, 16, 613-24.

LOWRY, O. H., ROSEBROUGH, N. J., FARR, A. L. & RANDALL, R. J. 1951. Protein measurement with the Folin phenol reagent. J Biol Chem, 193, 265-75.

Lu, L., Mei, D. F., Gu, A. G., Wang, S., Lentzner, B., Gutstein, D. E., Zwas, D., Homma, S., Yi, G. H. & Wang, J. 2002. Exercise training normalizes altered calcium-handling proteins during development of heart failure. J Appl Physiol (1985), 92, 1524-30.

Maiuri, M. C., Zalckvar, E., Kimchi, A. & Kroemer, G. 2007. Self-eating and self-killing: crosstalk between autophagy and apoptosis. Nat Rev Mol Cell Biol, 8, 741-52.

Mancini, D. M., Coyle, E., Coggan, A., Beltz, J., Ferraro, N., Montain, S. & Wilson, J. R. 1989. Contribution of intrinsic skeletal muscle changes to 31P NMR skeletal muscle metabolic abnormalities in patients with chronic heart failure. Circulation, 80, 1338-46.

Manevich, Y., Feinstein, S. I. & Fisher, A. B. 2004. Activation of the antioxidant enzyme 1-CYS peroxiredoxin requires glutathionylation mediated by heterodimerization with pi GST. Proc Natl Acad Sci U S A, 101, 3780-5.

Marzetti, E., Lees, H. A., Wohlgemuth, S. E. & Leeuwenburgh, C. 2009. Sarcopenia of aging: underlying cellular mechanisms and protection by calorie restriction. Biofactors, 35, 28-35.

Mascarello, F., Maccatrozzo, L., Patruno, M., Toniolo, L. & Reggiani, C. 2004. 2B myosin heavy chain isoform expression in bovine skeletal muscle. Vet Res Commun, 28 Suppl 1, 201-4.

Masella, R., Di Benedetto, R., Varì, R., Filesi, C. & Giovannini, C. 2005. Novel mechanisms of natural antioxidant compounds in biological systems: involvement of glutathione and glutathione-related enzymes. J Nutr Biochem, 16, 577-86.

Masiero, E. & Sandri, M. 2010. Autophagy inhibition induces atrophy and myopathy in adult skeletal muscles. Autophagy, 6, 307-9.

Masiero, E., Agatea, L., Mammucari, C., Blaauw, B., Loro, E., Komatsu, M., Metzger, D., Reggiani, C., Schiaffino, S. & Sandri, M. 2009. Autophagy is required to maintain muscle mass. Cell Metab, 10, 507-15.

Massie, B. M., Simonini, A., Sahgal, P., Wells, L. & Dudley, G. A. 1996. Relation of systemic and local muscle exercise capacity to skeletal muscle characteristics in men with congestive heart failure. J Am Coll Cardiol, 27, 140-5.

Matés, J. M., Segura, J. A., Alonso, F. J. & Márquez, J. 2008. Intracellular redox status and oxidative stress: implications for cell proliferation, apoptosis, and carcinogenesis. Arch Toxicol, 82, 273-99.

Matsunaga, K., Saitoh, T., Tabata, K., Omori, H., Satoh, T., Kurotori, N., Maejima, I., Shirahama-Noda, K., Ichimura, T., Isobe, T., Akira, S., Noda, T. & Yoshimori, T. 2009. Two Beclin 1-binding proteins, Atg14L and Rubicon, reciprocally regulate autophagy at different stages. Nat Cell Biol, 11, 385-96.

Mavalli, M. D., DiGirolamo, D. J., Fan, Y., Riddle, R. C., Campbell, K. S., van Groen, T., Frank, S. J., Sperling, M. A., Esser, K. A., Bamman, M. M. & Clemens, T. L. 2010. Distinct growth hormone receptor signaling modes regulate skeletal muscle development and insulin sensitivity in mice. J Clin Invest, 120, 4007-20.

McCord, J. M. & Fridovich, I. 1969. Superoxide dismutase. An enzymic function for erythrocuprein (hemocuprein). J Biol Chem, 244, 6049-55.

McTiernan, C. F., Lemster, B. H., Frye, C., Brooks, S., Combes, A. & Feldman, A. M. 1997. Interleukin-1 beta inhibits phospholamban gene expression in cultured cardiomyocytes. Circ Res, 81, 493-503.

Medeiros, A., Rolim, N. P., Oliveira, R. S., Rosa, K. T., Mattos, K. C., Casarini, D. E., Irigoyen, M. C., Krieger, E. M., Krieger, J. E., Negrão, C. E. & Brum, P. C. 2008. Exercise training delays cardiac dysfunction and prevents calcium handling abnormalities in sympathetic hyperactivity-induced heart failure mice. J Appl Physiol (1985), 104, 103-9.

Mei, Z., Zhang, D., Hu, B., Wang, J., Shen, X. & Xiao, W. 2015. FBXO32 Targets c-Myc for Proteasomal Degradation and Inhibits c-Myc Activity. J Biol Chem, 290, 16202-14.

Mende, U., Kagen, A., Cohen, A., Aramburu, J., Schoen, F. J. & Neer, E. J. 1998. Transient cardiac expression of constitutively active Galphaq leads to hypertrophy and dilated cardiomyopathy by calcineurin-dependent and independent pathways. Proc Natl Acad Sci U S A, 95, 13893-8.

Mende, U., Kagen, A., Meister, M. & Neer, E. J. 1999. Signal transduction in atria and ventricles of mice with transient cardiac expression of activated G protein alpha(q). Circ Res, 85, 1085-91.

Mende, U., Semsarian, C., Martins, D. C., Kagen, A., Duffy, C., Schoen, F. J. & Neer, E. J. 2001. Dilated cardiomyopathy in two transgenic mouse lines expressing activated G protein alpha(q): lack of correlation between phospholipase C activation and the phenotype. J Mol Cell Cardiol, 33, 1477-91.

Mezzetti, A., Lapenna, D., Romano, F., Costantini, F., Pierdomenico, S. D., De Cesare, D., Cuccurullo, F., Riario-Sforza, G., Zuliani, G. & Fellin, R. 1996. Systemic oxidative stress and its relationship with age and illness. Associazione Medica "Sabin". J Am Geriatr Soc, 44, 823-7.

Michael, L. F., Wu, Z., Cheatham, R. B., Puigserver, P., Adelmant, G., Lehman, J. J., Kelly, D. P. & Spiegelman, B. M. 2001. Restoration of insulin-sensitive glucose transporter (GLUT4) gene expression in muscle cells by the transcriptional coactivator PGC-1. Proc Natl Acad Sci U S A, 98, 3820-5.

Milan, G., Romanello, V., Pescatore, F., Armani, A., Paik, J. H., Frasson, L., Seydel, A., Zhao, J., Abraham, R., Goldberg, A. L., Blaauw, B., DePinho, R. A. & Sandri, M. 2015. Regulation of autophagy and the ubiquitin-proteasome system by the FoxO transcriptional network during muscle atrophy. Nat Commun, 6, 6670.

Milano, C. A., Dolber, P. C., Rockman, H. A., Bond, R. A., Venable, M. E., Allen, L. F. & Lefkowitz, R. J. 1994. Myocardial expression of a constitutively active alpha 1B-adrenergic receptor in transgenic mice induces cardiac hypertrophy. Proc Natl Acad Sci U S A, 91, 10109-13.

Miller, D. M., Buettner, G. R. & Aust, S. D. 1990. Transition metals as catalysts of "autoxidation" reactions. Free Radic Biol Med, 8, 95-108.

Milligan, G. & Kostenis, E. 2006. Heterotrimeric G-proteins: a short history. Br J Pharmacol, 147 Suppl 1, S46-55.

Mishra, S. K. & Misra, V. 2003. Muscle sarcopenia: an overview. Acta Myol, 22, 43-7.

Mitch, W. E. & Goldberg, A. L. 1996. Mechanisms of muscle wasting. The role of the ubiquitin-proteasome pathway. N Engl J Med, 335, 1897-905.

Mizushima, N. 2007. Autophagy: process and function. Genes Dev, 21, 2861-73.

Mizushima, N., Levine, B., Cuervo, A. M. & Klionsky, D. J. 2008. Autophagy fights disease through cellular self-digestion. Nature, 451, 1069-75.

Mizushima, N., Yamamoto, A., Matsui, M., Yoshimori, T. & Ohsumi, Y. 2004. In vivo analysis of autophagy in response to nutrient starvation using transgenic mice expressing a fluorescent autophagosome marker. Mol Biol Cell, 15, 1101-11.

Mootha, V. K., Handschin, C., Arlow, D., Xie, X., St Pierre, J., Sihag, S., Yang, W., Altshuler, D., Puigserver, P., Patterson, N., Willy, P. J., Schulman, I. G., Heyman, R. A., Lander, E. S. & Spiegelman, B. M. 2004. Erralpha and Gabpa/b specify PGC-1alpha-dependent oxidative phosphorylation gene expression that is altered in diabetic muscle. Proc Natl Acad Sci U S A, 101, 6570-5.

Mootha, V. K., Lindgren, C. M., Eriksson, K. F., Subramanian, A., Sihag, S., Lehar, J., Puigserver, P., Carlsson, E., Ridderstråle, M., Laurila, E., Houstis, N., Daly, M. J., Patterson, N.,

Mesirov, J. P., Golub, T. R., Tamayo, P., et al. 2003. PGC-1alpha-responsive genes involved in oxidative phosphorylation are coordinately downregulated in human diabetes. Nat Genet, 34, 267-73.

Mounier, R., Lantier, L., Leclerc, J., Sotiropoulos, A., Foretz, M. & Viollet, B. 2011. Antagonistic control of muscle cell size by AMPK and mTORC1. Cell Cycle, 10, 2640-6.

Muñoz, J. P., Ivanova, S., Sánchez-Wandelmer, J., Martínez-Cristóbal, P., Noguera, E., Sancho, A., Díaz-Ramos, A., Hernández-Alvarez, M. I., Sebastián, D., Mauvezin, C., Palacín, M. & Zorzano, A. 2013. Mfn2 modulates the UPR and mitochondrial function via repression of PERK. EMBO J, 32, 2348-61.

Murgia, M., Serrano, A. L., Calabria, E., Pallafacchina, G., Lomo, T. & Schiaffino, S. 2000. Ras is involved in nerve-activity-dependent regulation of muscle genes. Nat Cell Biol, 2, 142-7.

Musarò, A., McCullagh, K., Paul, A., Houghton, L., Dobrowolny, G., Molinaro, M., Barton, E. R., Sweeney, H. L. & Rosenthal, N. 2001. Localized Igf-1 transgene expression sustains hypertrophy and regeneration in senescent skeletal muscle. Nat Genet, 27, 195-200.

Musarò, A., S. Fulle & G. Fanò (2010) Oxidative stress and muscle homeostasis. Curr Opin Clin Nutr Metab Care, 13, 236-42.

Myers, J., Arena, R., Dewey, F., Bensimhon, D., Abella, J., Hsu, L., Chase, P., Guazzi, M. & Peberdy, M. A. 2008. A cardiopulmonary exercise testing score for predicting outcomes in patients with heart failure. Am Heart J, 156, 1177-83.

Nakashima, K. & Yakabe, Y. 2007. AMPK activation stimulates myofibrillar protein degradation and expression of atrophy-related ubiquitin ligases by increasing FOXO transcription factors in C2C12 myotubes. Biosci Biotechnol Biochem, 71, 1650-6.

Napoli, C., Williams-Ignarro, S., de Nigris, F., Lerman, L. O., D'Armiento, F. P., Crimi, E., Byrns, R. E., Casamassimi, A., Lanza, A., Gombos, F., Sica, V. & Ignarro, L. J. 2006. Physical training and metabolic supplementation reduce spontaneous atherosclerotic plaque rupture and prolong survival in hypercholesterolemic mice. Proc Natl Acad Sci U S A, 103, 10479-84.

Napoli, C., Williams-Ignarro, S., De Nigris, F., Lerman, L. O., Rossi, L., Guarino, C., Mansueto, G., Di Tuoro, F., Pignalosa, O., De Rosa, G., Sica, V. & Ignarro, L. J. 2004. Long-term combined beneficial effects of physical training and metabolic treatment on atherosclerosis in hypercholesterolemic mice. Proc Natl Acad Sci U S A, 101, 8797-802.

Narendra, D. P. & Youle, R. J. 2011. Targeting mitochondrial dysfunction: role for PINK1 and Parkin in mitochondrial quality control. Antioxid Redox Signal, 14, 1929-38.

Narkar, V. A., M. Downes, R. T. Yu, E. Embler, Y. X. Wang, E. Banayo, M. M. Mihaylova, M. C. Nelson, Y. Zou, H. Juguilon, H. Kang, R. J. Shaw & R. M. Evans (2008) AMPK and PPARdelta agonists are exercise mimetics. Cell, 134, 405-15.

Nazio, F., Strappazzon, F., Antonioli, M., Bielli, P., Cianfanelli, V., Bordi, M., Gretzmeier, C., Dengjel, J., Piacentini, M., Fimia, G. M. & Cecconi, F. 2013. mTOR inhibits autophagy by controlling ULK1 ubiquitylation, self-association and function through AMBRA1 and TRAF6. Nat Cell Biol, 15, 406-16.

Ngoh, G. A., Papanicolaou, K. N. & Walsh, K. 2012. Loss of mitofusin 2 promotes endoplasmic reticulum stress. J Biol Chem, 287, 20321-32.

Niizuma, H., Nakamura, Y., Ozaki, T., Nakanishi, H., Ohira, M., Isogai, E., Kageyama, H., Imaizumi, M. & Nakagawara, A. 2006. Bcl-2 is a key regulator for the retinoic acid-induced apoptotic cell death in neuroblastoma. Oncogene, 25, 5046-55.

Niles, R. M. 2004. Signaling pathways in retinoid chemoprevention and treatment of cancer. Mutat Res, 555, 81-96.

Nilsson, B. B., Westheim, A. & Risberg, M. A. 2008. Long-term effects of a group-based high-intensity aerobic interval-training program in patients with chronic heart failure. Am J Cardiol, 102, 1220-4.

Nishida, Y., Arakawa, S., Fujitani, K., Yamaguchi, H., Mizuta, T., Kanaseki, T., Komatsu, M., Otsu, K., Tsujimoto, Y. & Shimizu, S. 2009. Discovery of Atg5/Atg7-independent alternative macroautophagy. Nature, 461, 654-8.

Novak, I., Kirkin, V., McEwan, D. G., Zhang, J., Wild, P., Rozenknop, A., Rogov, V., Löhr, F., Popovic, D., Occhipinti, A., Reichert, A. S., Terzic, J., Dötsch, V., Ney, P. A. & Dikic, I. 2010. Nix is a selective autophagy receptor for mitochondrial clearance. EMBO Rep, 11, 45-51.

Nunes, R. B., Tonetto, M., Machado, N., Chazan, M., Heck, T. G., Veiga, A. B. & Dall'Ago, P. 2008. Physical exercise improves plasmatic levels of IL-10, left ventricular end-diastolic pressure, and muscle lipid peroxidation in chronic heart failure rats. J Appl Physiol (1985), 104, 1641-7.

Ogata, T. & Yamasaki, Y. 1997. Ultra-high-resolution scanning electron microscopy of mitochondria and sarcoplasmic reticulum arrangement in human red, white, and intermediate muscle fibers. Anat Rec, 248, 214-23.

Oka, Y., Saraiva, L. R., Kwan, Y. Y. & Korsching, S. I. 2009. The fifth class of Galpha proteins. Proc Natl Acad Sci U S A, 106, 1484-9.

O'Neill, H. M., Holloway, G. P. & Steinberg, G. R. 2013. AMPK regulation of fatty acid metabolism and mitochondrial biogenesis: implications for obesity. Mol Cell Endocrinol, 366, 135-51.

Otera, H. & Mihara, K. 2011. Molecular mechanisms and physiologic functions of mitochondrial dynamics. J Biochem, 149, 241-51.

Palazzetti, S., Richard, M. J., Favier, A. & Margaritis, I. 2003. Overloaded training increases exercise-induced oxidative stress and damage. Can J Appl Physiol, 28, 588-604.

Pallafacchina, G., Calabria, E., Serrano, A. L., Kalhovde, J. M. & Schiaffino, S. 2002. A protein kinase B-dependent and rapamycin-sensitive pathway controls skeletal muscle growth but not fiber type specification. Proc Natl Acad Sci U S A, 99, 9213-8.

Pankiv, S., Clausen, T. H., Lamark, T., Brech, A., Bruun, J. A., Outzen, H., Øvervatn, A., Bjørkøy, G. & Johansen, T. 2007. p62/SQSTM1 binds directly to Atg8/LC3 to facilitate degradation of ubiquitinated protein aggregates by autophagy. J Biol Chem, 282, 24131-45.

Passino, C., Severino, S., Poletti, R., Piepoli, M. F., Mammini, C., Clerico, A., Gabutti, A., Nassi, G. & Emdin, M. 2006. Aerobic training decreases B-type natriuretic peptide expression and adrenergic activation in patients with heart failure. J Am Coll Cardiol, 47, 1835-9.

Patti, M. E., Butte, A. J., Crunkhorn, S., Cusi, K., Berria, R., Kashyap, S., Miyazaki, Y., Kohane, I., Costello, M., Saccone, R., Landaker, E. J., Goldfine, A. B., Mun, E., DeFronzo, R., Finlayson, J., Kahn, C. R., et al. 2003. Coordinated reduction of genes of oxidative metabolism in humans

with insulin resistance and diabetes: Potential role of PGC1 and NRF1. Proc Natl Acad Sci U S A, 100, 8466-71.

Pattingre, S., Tassa, A., Qu, X., Garuti, R., Liang, X. H., Mizushima, N., Packer, M., Schneider, M. D. & Levine, B. 2005. Bcl-2 antiapoptotic proteins inhibit Beclin 1-dependent autophagy. Cell, 122, 927-39.

Paul, P. K., Bhatnagar, S., Mishra, V., Srivastava, S., Darnay, B. G., Choi, Y. & Kumar, A. 2012. The E3 ubiquitin ligase TRAF6 intercedes in starvation-induced skeletal muscle atrophy through multiple mechanisms. Mol Cell Biol, 32, 1248-59.

Paul, P. K., Gupta, S. K., Bhatnagar, S., Panguluri, S. K., Darnay, B. G., Choi, Y. & Kumar, A. 2010. Targeted ablation of TRAF6 inhibits skeletal muscle wasting in mice. J Cell Biol, 191, 1395-411.

Pearson, T., Kabayo, T., Ng, R., Chamberlain, J., McArdle, A. & Jackson, M. J. 2014. Skeletal muscle contractions induce acute changes in cytosolic superoxide, but slower responses in mitochondrial superoxide and cellular hydrogen peroxide. PLoS One, 9, e96378.

Pedersen, B. K. & Saltin, B. 2006. Evidence for prescribing exercise as therapy in chronic disease. Scand J Med Sci Sports, 16 Suppl 1, 3-63.

Pellegrino, M. A., Canepari, M., Rossi, R., D'Antona, G., Reggiani, C. & Bottinelli, R. 2003. Orthologous myosin isoforms and scaling of shortening velocity with body size in mouse, rat, rabbit and human muscles. J Physiol, 546, 677-89.

Pellegrino, M. A., L. Brocca, F. S. Dioguardi, R. Bottinelli & G. D'Antona (2005) Effects of voluntary wheel running and amino acid supplementation on skeletal muscle of mice. Eur J Appl Physiol, 93, 655-64.

Pereira, B., Costa Rosa, L. F., Safi, D. A., Medeiros, M. H., Curi, R. & Bechara, E. J. 1994. Superoxide dismutase, catalase, and glutathione peroxidase activities in muscle and lymphoid organs of sedentary and exercise-trained rats. Physiol Behav, 56, 1095-9.

Peters, S. J., Harris, R. A., Heigenhauser, G. J. & Spriet, L. L. 2001. Muscle fiber type comparison of PDH kinase activity and isoform expression in fed and fasted rats. Am J Physiol Regul Integr Comp Physiol, 280, R661-8.

Pette, D. & Staron, R. S. 1990. Cellular and molecular diversities of mammalian skeletal muscle fibers. Rev Physiol Biochem Pharmacol, 116, 1-76.

Piepoli, M. F., Conraads, V., Corrà, U., Dickstein, K., Francis, D. P., Jaarsma, T., McMurray, J., Pieske, B., Piotrowicz, E., Schmid, J. P., Anker, S. D., Solal, A. C., Filippatos, G. S., Hoes, A. W., Gielen, S., Giannuzzi, P., et al. 2011. Exercise training in heart failure: from theory to practice. A consensus document of the Heart Failure Association and the European Association for Cardiovascular Prevention and Rehabilitation. Eur J Heart Fail, 13, 347-57.

Piepoli, M. F., Davos, C., Francis, D. P., Coats, A. J. & Collaborative, E. 2004. Exercise training meta-analysis of trials in patients with chronic heart failure (ExTraMATCH). BMJ, 328, 189.

Plomgaard, P., Penkowa, M., Leick, L., Pedersen, B. K., Saltin, B. & Pilegaard, H. 2006. The mRNA expression profile of metabolic genes relative to MHC isoform pattern in human skeletal muscles. J Appl Physiol (1985), 101, 817-25.

Polge, C., Heng, A. E., Jarzaguet, M., Ventadour, S., Claustre, A., Combaret, L., Béchet, D., Matondo, M., Uttenweiler-Joseph, S., Monsarrat, B., Attaix, D. & Taillandier, D. 2011. Muscle actin is polyubiquitinylated in vitro and in vivo and targeted for breakdown by the E3 ligase MuRF1. FASEB J, 25, 3790-802.

Poole, D. C., Hirai, D. M., Copp, S. W. & Musch, T. I. 2012. Muscle oxygen transport and utilization in heart failure: implications for exercise (in)tolerance. Am J Physiol Heart Circ Physiol, 302, H1050-63.

Poole, L. B. 2015. The basics of thiols and cysteines in redox biology and chemistry. Free Radic Biol Med, 80, 148-57.

Powers, S. K. & Jackson, M. J. 2008. Exercise-induced oxidative stress: cellular mechanisms and impact on muscle force production. Physiol Rev, 88, 1243-76.

Powers, S. K., Criswell, D., Lawler, J., Ji, L. L., Martin, D., Herb, R. A. & Dudley, G. 1994. Influence of exercise and fiber type on antioxidant enzyme activity in rat skeletal muscle. Am J Physiol, 266, R375-80.

Powers, S. K., Duarte, J., Kavazis, A. N. & Talbert, E. E. 2010. Reactive oxygen species are signalling molecules for skeletal muscle adaptation. Exp Physiol, 95, 1-9.

Powers, S. K., Kavazis, A. N. & DeRuisseau, K. C. 2005. Mechanisms of disuse muscle atrophy: role of oxidative stress. Am J Physiol Regul Integr Comp Physiol, 288, R337-44.

Puigserver, P., Rhee, J., Donovan, J., Walkey, C. J., Yoon, J. C., Oriente, F., Kitamura, Y., Altomonte, J., Dong, H., Accili, D. & Spiegelman, B. M. 2003. Insulin-regulated hepatic gluconeogenesis through FOXO1-PGC-1alpha interaction. Nature, 423, 550-5.

Puigserver, P., Wu, Z., Park, C. W., Graves, R., Wright, M. & Spiegelman, B. M. 1998. A cold-inducible coactivator of nuclear receptors linked to adaptive thermogenesis. Cell, 92, 829-39.

Quy, P. N., Kuma, A., Pierre, P. & Mizushima, N. 2013. Proteasome-dependent activation of mammalian target of rapamycin complex 1 (mTORC1) is essential for autophagy suppression and muscle remodeling following denervation. J Biol Chem, 288, 1125-34.

Raben, N., Hill, V., Shea, L., Takikita, S., Baum, R., Mizushima, N., Ralston, E. & Plotz, P. 2008. Suppression of autophagy in skeletal muscle uncovers the accumulation of ubiquitinated proteins and their potential role in muscle damage in Pompe disease. Hum Mol Genet, 17, 3897-908.

Raffaello, A., Milan, G., Masiero, E., Carnio, S., Lee, D., Lanfranchi, G., Goldberg, A. L. & Sandri, M. 2010. JunB transcription factor maintains skeletal muscle mass and promotes hypertrophy. J Cell Biol, 191, 101-13.

Rajawat, Y. S., Hilioti, Z. & Bossis, I. 2009. Aging: central role for autophagy and the lysosomal degradative system. Ageing Res Rev, 8, 199-213.

Ramsey, M. W., Goodfellow, J., Jones, C. J., Luddington, L. A., Lewis, M. J. & Henderson, A. H. 1995. Endothelial control of arterial distensibility is impaired in chronic heart failure. Circulation, 92, 3212-9.

Reed, S. A., Sandesara, P. B., Senf, S. M. & Judge, A. R. 2012. Inhibition of FoxO transcriptional activity prevents muscle fiber atrophy during cachexia and induces hypertrophy. FASEB J, 26, 987-1000.

Reid, M. B. (2005) Response of the ubiquitin-proteasome pathway to changes in muscle activity. Am J Physiol Regul Integr Comp Physiol, 288, R1423-31.

Remme, W. J., Swedberg, K. & Task Force for the Diagnosis and Treatment of Chronic Heart Failure, E. r. S. o. C. 2001. Guidelines for the diagnosis and treatment of chronic heart failure. Eur Heart J, 22, 1527-60.

Remy, I., Montmarquette, A. & Michnick, S. W. 2004. PKB/Akt modulates TGF-beta signalling through a direct interaction with Smad3. Nat Cell Biol, 6, 358-65.

Rhee, S. G. 2001. Regulation of phosphoinositide-specific phospholipase C. Annu Rev Biochem, 70, 281-312.

Rhee, S. G., Chae, H. Z. & Kim, K. 2005a. Peroxiredoxins: a historical overview and speculative preview of novel mechanisms and emerging concepts in cell signaling. Free Radic Biol Med, 38, 1543-52.

Rhee, S. G., Kang, S. W., Jeong, W., Chang, T. S., Yang, K. S. & Woo, H. A. 2005b. Intracellular messenger function of hydrogen peroxide and its regulation by peroxiredoxins. Curr Opin Cell Biol, 17, 183-9.

Rhee, S. G., Yang, K. S., Kang, S. W., Woo, H. A. & Chang, T. S. 2005c. Controlled elimination of intracellular H_2O_2: regulation of peroxiredoxin, catalase, and glutathione peroxidase via post-translational modification. Antioxid Redox Signal, 7, 619-26.

Rice-Evans, C. A., Sampson, J., Bramley, P. M. & Holloway, D. E. 1997. Why do we expect carotenoids to be antioxidants in vivo? Free Radic Res, 26, 381-98.

Richardson, P., McKenna, W., Bristow, M., Maisch, B., Mautner, B., O'Connell, J., Olsen, E., Thiene, G., Goodwin, J., Gyarfas, I., Martin, I. & Nordet, P. 1996. Report of the 1995 World Health Organization/International Society and Federation of Cardiology Task Force on the Definition and Classification of cardiomyopathies. Circulation, 93, 841-2.

Ridnour, L. A., Sim, J. E., Choi, J., Dickinson, D. A., Forman, H. J., Ahmad, I. M., Coleman, M. C., Hunt, C. R., Goswami, P. C. & Spitz, D. R. 2005. Nitric oxide-induced resistance to hydrogen peroxide stress is a glutamate cysteine ligase activity-dependent process. Free Radic Biol Med, 38, 1361-71.

Risson, V., Mazelin, L., Roceri, M., Sanchez, H., Moncollin, V., Corneloup, C., Richard-Bulteau, H., Vignaud, A., Baas, D., Defour, A., Freyssenet, D., Tanti, J. F., Le-Marchand-Brustel, Y., Ferrier, B., Conjard-Duplany, A., Romanino, K., et al. 2009. Muscle inactivation of mTOR causes metabolic and dystrophin defects leading to severe myopathy. J Cell Biol, 187, 859-74.

Ristow, M., Zarse, K., Oberbach, A., Klöting, N., Birringer, M., Kiehntopf, M., Stumvoll, M., Kahn, C. R. & Blüher, M. 2009. Antioxidants prevent health-promoting effects of physical exercise in humans. Proc Natl Acad Sci U S A, 106, 8665-70.

Robinson, A., Huttley, G. A., Booth, H. S. & Board, P. G. 2004. Modelling and bioinformatics studies of the human Kappa-class glutathione transferase predict a novel third glutathione transferase family with similarity to prokaryotic 2-hydroxychromene-2-carboxylate isomerases. Biochem J, 379, 541-52.

Rogov, V., Dötsch, V., Johansen, T. & Kirkin, V. 2014. Interactions between autophagy receptors and ubiquitin-like proteins form the molecular basis for selective autophagy. Mol Cell, 53, 167-78.

Rolim, N. P., Medeiros, A., Rosa, K. T., Mattos, K. C., Irigoyen, M. C., Krieger, E. M., Krieger, J. E., Negrão, C. E. & Brum, P. C. 2007. Exercise training improves the net balance of cardiac Ca2+ handling protein expression in heart failure. Physiol Genomics, 29, 246-52.

Romanello, V. & Sandri, M. 2010. Mitochondrial biogenesis and fragmentation as regulators of muscle protein degradation. Curr Hypertens Rep, 12, 433-9.

Romanello, V. & Sandri, M. 2015. Mitochondrial Quality Control and Muscle Mass Maintenance. Front Physiol, 6, 422.

Romanello, V., Guadagnin, E., Gomes, L., Roder, I., Sandri, C., Petersen, Y., Milan, G., Masiero, E., Del Piccolo, P., Foretz, M., Scorrano, L., Rudolf, R. & Sandri, M. 2010. Mitochondrial fission and remodelling contributes to muscle atrophy. EMBO J, 29, 1774-85.

Rush, J. W., Denniss, S. G. & Graham, D. A. 2005. Vascular nitric oxide and oxidative stress: determinants of endothelial adaptations to cardiovascular disease and to physical activity. Can J Appl Physiol, 30, 442-74.

Sabatini, D. M. 2006. mTOR and cancer: insights into a complex relationship. Nat Rev Cancer, 6, 729-34.

Sabbah, H. N., Hansen-Smith, F., Sharov, V. G., Kono, T., Lesch, M., Gengo, P. J., Steffen, R. P., Levine, T. B. & Goldstein, S. 1993. Decreased proportion of type I myofibers in skeletal muscle of dogs with chronic heart failure. Circulation, 87, 1729-37.

Sahlin, K., Söderlund, K., Tonkonogi, M. & Hirakoba, K. 1997. Phosphocreatine content in single fibers of human muscle after sustained submaximal exercise. Am J Physiol, 273, C172-8.

Sakellariou, G. K., A. Vasilaki, J. Palomero, A. Kayani, L. Zibrik, A. McArdle & M. J. Jackson (2013) Studies of mitochondrial and nonmitochondrial sources implicate nicotinamide adenine dinucleotide phosphate oxidase(s) in the increased skeletal muscle superoxide generation that occurs during contractile activity. Antioxid Redox Signal, 18, 603-21.

Sakellariou, G. K., Jackson, M. J. & Vasilaki, A. 2014. Redefining the major contributors to superoxide production in contracting skeletal muscle. The role of NAD(P)H oxidases. Free Radic Res, 48, 12-29.

Sakellariou, G. K., Vasilaki, A., Palomero, J., Kayani, A., Zibrik, L., McArdle, A. & Jackson, M. J. 2013. Studies of mitochondrial and nonmitochondrial sources implicate nicotinamide adenine dinucleotide phosphate oxidase(s) in the increased skeletal muscle superoxide generation that occurs during contractile activity. Antioxid Redox Signal, 18, 603-21.

Sánchez-Fernández, G., Cabezudo, S., García-Hoz, C., Benincá, C., Aragay, A. M., Mayor, F. & Ribas, C. 2014. Gαq signalling: the new and the old. Cell Signal, 26, 833-48.

Sandri, M. 2008. Signaling in muscle atrophy and hypertrophy. Physiology (Bethesda), 23, 160-70.

Sandri, M. 2015. Protein breakdown in cancer cachexia. Semin Cell Dev Biol.

Sandri, M. 2016. Protein breakdown in cancer cachexia. Semin Cell Dev Biol, 54, 11-9.

Sandri, M., Barberi, L., Bijlsma, A. Y., Blaauw, B., Dyar, K. A., Milan, G., Mammucari, C., Meskers, C. G., Pallafacchina, G., Paoli, A., Pion, D., Roceri, M., Romanello, V., Serrano, A. L., Toniolo, L., Larsson, L., et al. 2013. Signalling pathways regulating muscle mass in ageing skeletal muscle: the role of the IGF1-Akt-mTOR-FoxO pathway. Biogerontology, 14, 303-23.

Sandri, M., Lin, J., Handschin, C., Yang, W., Arany, Z. P., Lecker, S. H., Goldberg, A. L. & Spiegelman, B. M. 2006. PGC-1alpha protects skeletal muscle from atrophy by suppressing FoxO3 action and atrophy-specific gene transcription. Proc Natl Acad Sci U S A, 103, 16260-5.

Sandri, M., Sandri, C., Gilbert, A., Skurk, C., Calabria, E., Picard, A., Walsh, K., Schiaffino, S., Lecker, S. H. & Goldberg, A. L. 2004. Foxo transcription factors induce the atrophy-related ubiquitin ligase atrogin-1 and cause skeletal muscle atrophy. Cell, 117, 399-412.

Sant'Ana Pereira, J. A., Sargeant, A. J., Rademaker, A. C., de Haan, A. & van Mechelen, W. 1996. Myosin heavy chain isoform expression and high energy phosphate content in human muscle fibres at rest and post-exercise. J Physiol, 496 (Pt 2), 583-8.

Sarto, P., Balducci, E., Balconi, G., Fiordaliso, F., Merlo, L., Tuzzato, G., Pappagallo, G. L., Frigato, N., Zanocco, A., Forestieri, C., Azzarello, G., Mazzucco, A., Valenti, M. T., Alborino, F., Noventa, D., Vinante, O., et al. 2007. Effects of exercise training on endothelial progenitor cells in patients with chronic heart failure. J Card Fail, 13, 701-8.

Sartori, R., Milan, G., Patron, M., Mammucari, C., Blaauw, B., Abraham, R. & Sandri, M. 2009. Smad2 and 3 transcription factors control muscle mass in adulthood. Am J Physiol Cell Physiol, 296, C1248-57.

Sartori, R., Schirwis, E., Blaauw, B., Bortolanza, S., Zhao, J., Enzo, E., Stantzou, A., Mouisel, E., Toniolo, L., Ferry, A., Stricker, S., Goldberg, A. L., Dupont, S., Piccolo, S., Amthor, H. & Sandri, M. 2013. BMP signaling controls muscle mass. Nat Genet, 45, 1309-18.

Sastre, J., Asensi, M., Gascó, E., Pallardó, F. V., Ferrero, J. A., Furukawa, T. & Viña, J. 1992. Exhaustive physical exercise causes oxidation of glutathione status in blood: prevention by antioxidant administration. Am J Physiol, 263, R992-5.

Schiaffino, S. & Hanzlíková, V. 1972. Studies on the effect of denervation in developing muscle. II. The lysosomal system. J Ultrastruct Res, 39, 1-14.

Schiaffino, S. & Mammucari, C. 2011. Regulation of skeletal muscle growth by the IGF1-Akt/PKB pathway: insights from genetic models. Skelet Muscle, 1, 4.

Schiaffino, S. & Reggiani, C. 1996. Molecular diversity of myofibrillar proteins: gene regulation and functional significance. Physiol Rev, 76, 371-423.

Schiaffino, S., Dyar, K. A., Ciciliot, S., Blaauw, B. & Sandri, M. 2013. Mechanisms regulating skeletal muscle growth and atrophy. FEBS J, 280, 4294-314.

Schiaffino, S., Gorza, L., Sartore, S., Saggin, L., Ausoni, S., Vianello, M., Gundersen, K. & Lømo, T. 1989. Three myosin heavy chain isoforms in type 2 skeletal muscle fibres. J Muscle Res Cell Motil, 10, 197-205.

Schlesinger, M. J. 1990. Heat shock proteins. J Biol Chem, 265, 12111-4.

Schrader, M. 2006. Shared components of mitochondrial and peroxisomal division. Biochim Biophys Acta, 1763, 531-41.

Schreiber, S. N., Knutti, D., Brogli, K., Uhlmann, T. & Kralli, A. 2003. The transcriptional coactivator PGC-1 regulates the expression and activity of the orphan nuclear receptor estrogen-related receptor alpha (ERRalpha). J Biol Chem, 278, 9013-8.

Sebastián, D., Hernández-Alvarez, M. I., Segalés, J., Sorianello, E., Muñoz, J. P., Sala, D., Waget, A., Liesa, M., Paz, J. C., Gopalacharyulu, P., Orešič, M., Pich, S., Burcelin, R., Palacín, M. &

Zorzano, A. 2012. Mitofusin 2 (Mfn2) links mitochondrial and endoplasmic reticulum function with insulin signaling and is essential for normal glucose homeostasis. Proc Natl Acad Sci U S A, 109, 5523-8.

Sellers, J. R., Goodson, H. V. & Wang, F. 1996. A myosin family reunion. J Muscle Res Cell Motil, 17, 7-22.

Shang, F., Gong, X. & Taylor, A. 1997. Activity of ubiquitin-dependent pathway in response to oxidative stress. Ubiquitin-activating enzyme is transiently up-regulated. J Biol Chem, 272, 23086-93.

Shemesh, J., Grossman, E., Peleg, E., Steinmetz, A., Rosenthal, T. & Motro, M. 1995. Norepinephrine and atrial natriuretic peptide responses to exercise testing in rehabilitated and nonrehabilitated men with ischemic cardiomyopathy after healing of anterior wall acute myocardial infarction. Am J Cardiol, 75, 1072-4.

Sies, H. 1999. Glutathione and its role in cellular functions. Free Radic Biol Med, 27, 916-21.

Simon, M. I., Strathmann, M. P. & Gautam, N. 1991. Diversity of G proteins in signal transduction. Science, 252, 802-8.

Simonini, A., Long, C. S., Dudley, G. A., Yue, P., McElhinny, J. & Massie, B. M. 1996a. Heart failure in rats causes changes in skeletal muscle morphology and gene expression that are not explained by reduced activity. Circ Res, 79, 128-36.

Simonini, A., Massie, B. M., Long, C. S., Qi, M. & Samarel, A. M. 1996b. Alterations in skeletal muscle gene expression in the rat with chronic congestive heart failure. J Mol Cell Cardiol, 28, 1683-91.

Simonsen, A. & Tooze, S. A. 2009. Coordination of membrane events during autophagy by multiple class III PI3-kinase complexes. J Cell Biol, 186, 773-82.

Sinoway, L. I. & Li, J. 2005. A perspective on the muscle reflex: implications for congestive heart failure. J Appl Physiol (1985), 99, 5-22.

Smirnova, E., Griparic, L., Shurland, D. L. & van der Bliek, A. M. 2001. Dynamin-related protein Drp1 is required for mitochondrial division in mammalian cells. Mol Biol Cell, 12, 2245-56.

Smith, M. A. & M. B. Reid (2006) Redox modulation of contractile function in respiratory and limb skeletal muscle. Respir Physiol Neurobiol, 151, 229-41.

Smuder, A. J., Kavazis, A. N., Hudson, M. B., Nelson, W. B. & Powers, S. K. 2010. Oxidation enhances myofibrillar protein degradation via calpain and caspase-3. Free Radic Biol Med, 49, 1152-60.

Solomon, V. & A. L. Goldberg (1996) Importance of the ATP-ubiquitin-proteasome pathway in the degradation of soluble and myofibrillar proteins in rabbit muscle extracts. J Biol Chem, 271, 26690-7.

Song, M. & Dorn, G. W. 2015. Mitoconfusion: noncanonical functioning of dynamism factors in static mitochondria of the heart. Cell Metab, 21, 195-205.

Southgate, R. J., Neill, B., Prelovsek, O., El-Osta, A., Kamei, Y., Miura, S., Ezaki, O., McLoughlin, T. J., Zhang, W., Unterman, T. G. & Febbraio, M. A. 2007. FOXO1 regulates the expression of 4E-BP1 and inhibits mTOR signaling in mammalian skeletal muscle. J Biol Chem, 282, 21176-86.

Stefanetti, R. J., S. Lamon, M. Wallace, M. H. Vendelbo, A. P. Russell & K. Vissing (2015) Regulation of ubiquitin proteasome pathway molecular markers in response to endurance and resistance exercise and training. Pflugers Arch, 467, 1523-37.

Steinberg, G. R., H. M. O'Neill, N. L. Dzamko, S. Galic, T. Naim, R. Koopman, S. B. Jørgensen, J. Honeyman, K. Hewitt, Z. P. Chen, J. D. Schertzer, J. W. Scott, F. Koentgen, G. S. Lynch, M. J. Watt, B. J. van Denderen, D. J. Campbell & B. E. Kemp (2010) Whole body deletion of AMP-activated protein kinase {beta}2 reduces muscle AMPK activity and exercise capacity. J Biol Chem, 285, 37198-209.

Stitt, T. N., Drujan, D., Clarke, B. A., Panaro, F., Timofeyva, Y., Kline, W. O., Gonzalez, M., Yancopoulos, G. D. & Glass, D. J. 2004. The IGF-1/PI3K/Akt pathway prevents expression of muscle atrophy-induced ubiquitin ligases by inhibiting FOXO transcription factors. Mol Cell, 14, 395-403.

Stølen, T. O., Høydal, M. A., Kemi, O. J., Catalucci, D., Ceci, M., Aasum, E., Larsen, T., Rolim, N., Condorelli, G., Smith, G. L. & Wisløff, U. 2009. Interval training normalizes cardiomyocyte function, diastolic Ca2+ control, and SR Ca2+ release synchronicity in a mouse model of diabetic cardiomyopathy. Circ Res, 105, 527-36.

St-Pierre, J., Lin, J., Krauss, S., Tarr, P. T., Yang, R., Newgard, C. B. & Spiegelman, B. M. 2003. Bioenergetic analysis of peroxisome proliferator-activated receptor gamma coactivators 1alpha and 1beta (PGC-1alpha and PGC-1beta) in muscle cells. J Biol Chem, 278, 26597-603.

Sullivan, M. J., Duscha, B. D., Klitgaard, H., Kraus, W. E., Cobb, F. R. & Saltin, B. 1997. Altered expression of myosin heavy chain in human skeletal muscle in chronic heart failure. Med Sci Sports Exerc, 29, 860-6.

Sullivan, M. J., Green, H. J. & Cobb, F. R. 1990. Skeletal muscle biochemistry and histology in ambulatory patients with long-term heart failure. Circulation, 81, 518-27.

Sun, Q. A., Wang, B., Miyagi, M., Hess, D. T. & Stamler, J. S. 2013. Oxygen-coupled redox regulation of the skeletal muscle ryanodine receptor/Ca2+ release channel (RyR1): sites and nature of oxidative modification. J Biol Chem, 288, 22961-71.

Sun, Y. S., Ye, Z. Y., Qian, Z. Y., Xu, X. D. & Hu, J. F. 2012. Expression of TRAF6 and ubiquitin mRNA in skeletal muscle of gastric cancer patients. J Exp Clin Cancer Res, 31, 81.

Suzuki, N., Motohashi, N., Uezumi, A., Fukada, S., Yoshimura, T., Itoyama, Y., Aoki, M., Miyagoe-Suzuki, Y. & Takeda, S. 2007. NO production results in suspension-induced muscle atrophy through dislocation of neuronal NOS. J Clin Invest, 117, 2468-76.

Takikita, S., Schreiner, C., Baum, R., Xie, T., Ralston, E., Plotz, P. H. & Raben, N. 2010. Fiber type conversion by PGC-1α activates lysosomal and autophagosomal biogenesis in both unaffected and Pompe skeletal muscle. PLoS One, 5, e15239.

Talmadge, R. J., Grossman, E. J. & Roy, R. R. 1996. Myosin heavy chain composition of adult feline (Felis catus) limb and diaphragm muscles. J Exp Zool, 275, 413-20.

Taylor, W. E., Bhasin, S., Artaza, J., Byhower, F., Azam, M., Willard, D. H., Kull, F. C. & Gonzalez-Cadavid, N. 2001. Myostatin inhibits cell proliferation and protein synthesis in C2C12 muscle cells. Am J Physiol Endocrinol Metab, 280, E221-8.

Teerlink, J. R. 2005. Endothelins: pathophysiology and treatment implications in chronic heart failure. Curr Heart Fail Rep, 2, 191-7.

Thomas, G. D., Zhang, W. & Victor, R. G. 2001. Impaired modulation of sympathetic vasoconstriction in contracting skeletal muscle of rats with chronic myocardial infarctions: role of oxidative stress. Circ Res, 88, 816-23.

Thorstensson, A., Grimby, G. & Karlsson, J. 1976. Force-velocity relations and fiber composition in human knee extensor muscles. J Appl Physiol, 40, 12-6.

Tintignac, L. A., Lagirand, J., Batonnet, S., Sirri, V., Leibovitch, M. P. & Leibovitch, S. A. 2005. Degradation of MyoD mediated by the SCF (MAFbx) ubiquitin ligase. J Biol Chem, 280, 2847-56.

Tong, J. F., X. Yan, M. J. Zhu & M. Du (2009) AMP-activated protein kinase enhances the expression of muscle-specific ubiquitin ligases despite its activation of IGF-1/Akt signaling in C2C12 myotubes. J Cell Biochem, 108, 458-68.

Tong, X., Hou, X., Jourd'heuil, D., Weisbrod, R. M. & Cohen, R. A. 2010. Upregulation of Nox4 by TGF{beta}1 oxidizes SERCA and inhibits NO in arterial smooth muscle of the prediabetic Zucker rat. Circ Res, 107, 975-83.

Torre-Amione, G., Kapadia, S., Benedict, C., Oral, H., Young, J. B. & Mann, D. L. 1996. Proinflammatory cytokine levels in patients with depressed left ventricular ejection fraction: a report from the Studies of Left Ventricular Dysfunction (SOLVD). J Am Coll Cardiol, 27, 1201-6.

Towbin, H., Staehelin, T. & Gordon, J. 1979. Electrophoretic transfer of proteins from polyacrylamide gels to nitrocellulose sheets: procedure and some applications. Proc Natl Acad Sci U S A, 76, 4350-4.

Trendelenburg, A. U., Meyer, A., Rohner, D., Boyle, J., Hatakeyama, S. & Glass, D. J. 2009. Myostatin reduces Akt/TORC1/p70S6K signaling, inhibiting myoblast differentiation and myotube size. Am J Physiol Cell Physiol, 296, C1258-70.

Tsutamoto, T., Hisanaga, T., Wada, A., Maeda, K., Ohnishi, M., Fukai, D., Mabuchi, N., Sawaki, M. & Kinoshita, M. 1998. Interleukin-6 spillover in the peripheral circulation increases with the severity of heart failure, and the high plasma level of interleukin-6 is an important prognostic predictor in patients with congestive heart failure. J Am Coll Cardiol, 31, 391-8.

Twig, G., Elorza, A., Molina, A. J., Mohamed, H., Wikstrom, J. D., Walzer, G., Stiles, L., Haigh, S. E., Katz, S., Las, G., Alroy, J., Wu, M., Py, B. F., Yuan, J., Deeney, J. T., Corkey, B. E., et al. 2008. Fission and selective fusion govern mitochondrial segregation and elimination by autophagy. EMBO J, 27, 433-46.

Valko, M., Leibfritz, D., Moncol, J., Cronin, M. T., Mazur, M. & Telser, J. 2007. Free radicals and antioxidants in normal physiological functions and human disease. Int J Biochem Cell Biol, 39, 44-84.

Valko, M., Morris, H. & Cronin, M. T. 2005. Metals, toxicity and oxidative stress. Curr Med Chem, 12, 1161-208.

Valko, M., Morris, H., Mazúr, M., Rapta, P. & Bilton, R. F. 2001. Oxygen free radical generating mechanisms in the colon: do the semiquinones of vitamin K play a role in the aetiology of colon cancer? Biochim Biophys Acta, 1527, 161-6.

Valko, M., Rhodes, C. J., Moncol, J., Izakovic, M. & Mazur, M. 2006. Free radicals, metals and antioxidants in oxidative stress-induced cancer. Chem Biol Interact, 160, 1-40.

van Tol, B. A., Huijsmans, R. J., Kroon, D. W., Schothorst, M. & Kwakkel, G. 2006. Effects of exercise training on cardiac performance, exercise capacity and quality of life in patients with heart failure: a meta-analysis. Eur J Heart Fail, 8, 841-50.

van Wessel, T., A. de Haan, W. J. van der Laarse & R. T. Jaspers (2010) The muscle fiber type-fiber size paradox: hypertrophy or oxidative metabolism? Eur J Appl Physiol, 110, 665-94.

Vega, R. B., Huss, J. M. & Kelly, D. P. 2000. The coactivator PGC-1 cooperates with peroxisome proliferator-activated receptor alpha in transcriptional control of nuclear genes encoding mitochondrial fatty acid oxidation enzymes. Mol Cell Biol, 20, 1868-76.

Ventura-Clapier, R., Mettauer, B. & Bigard, X. 2007. Beneficial effects of endurance training on cardiac and skeletal muscle energy metabolism in heart failure. Cardiovasc Res, 73, 10-8.

Vescovo, G., Zennaro, R., Sandri, M., Carraro, U., Leprotti, C., Ceconi, C., Ambrosio, G. B. & Dalla Libera, L. 1998. Apoptosis of skeletal muscle myofibers and interstitial cells in experimental heart failure. J Mol Cell Cardiol, 30, 2449-59.

Vøllestad, N. K., Tabata, I. & Medbø, J. I. 1992. Glycogen breakdown in different human muscle fibre types during exhaustive exercise of short duration. Acta Physiol Scand, 144, 135-41.

Wakasaki, H., Koya, D., Schoen, F. J., Jirousek, M. R., Ways, D. K., Hoit, B. D., Walsh, R. A. & King, G. L. 1997. Targeted overexpression of protein kinase C beta2 isoform in myocardium causes cardiomyopathy. Proc Natl Acad Sci U S A, 94, 9320-5.

Wang, Y. X., Lee, C. H., Tiep, S., Yu, R. T., Ham, J., Kang, H. & Evans, R. M. 2003. Peroxisome-proliferator-activated receptor delta activates fat metabolism to prevent obesity. Cell, 113, 159-70.

Ward, C. W., Prosser, B. L. & Lederer, W. J. 2014. Mechanical stretch-induced activation of ROS/RNS signaling in striated muscle. Antioxid Redox Signal, 20, 929-36.

Watanabe, T., Takeda, T., Omiya, S., Hikoso, S., Yamaguchi, O., Nakano, Y., Higuchi, Y., Nakai, A., Abe, Y., Aki-Jin, Y., Taniike, M., Mizote, I., Matsumura, Y., Shimizu, T., Nishida, K., Imai, K., et al. 2008. Reduction in hemoglobin-oxygen affinity results in the improvement of exercise capacity in mice with chronic heart failure. J Am Coll Cardiol, 52, 779-86.

Wei, Y., Pattingre, S., Sinha, S., Bassik, M. & Levine, B. 2008. JNK1-mediated phosphorylation of Bcl-2 regulates starvation-induced autophagy. Mol Cell, 30, 678-88.

Wenz, T., Rossi, S. G., Rotundo, R. L., Spiegelman, B. M. & Moraes, C. T. 2009. Increased muscle PGC-1alpha expression protects from sarcopenia and metabolic disease during aging. Proc Natl Acad Sci U S A, 106, 20405-10.

Wenz, T., Rossi, S. G., Rotundo, R. L., Spiegelman, B. M. & Moraes, C. T. 2009. Increased muscle PGC-1alpha expression protects from sarcopenia and metabolic disease during aging. Proc Natl Acad Sci U S A, 106, 20405-10.

White, E., Shannon, J. S. & Patterson, R. E. 1997. Relationship between vitamin and calcium supplement use and colon cancer. Cancer Epidemiol Biomarkers Prev, 6, 769-74.

Winder, W. W. & D. G. Hardie (1996) Inactivation of acetyl-CoA carboxylase and activation of AMP-activated protein kinase in muscle during exercise. Am J Physiol, 270, E299-304.

Wisløff, U., Loennechen, J. P., Currie, S., Smith, G. L. & Ellingsen, Ø. 2002. Aerobic exercise reduces cardiomyocyte hypertrophy and increases contractility, Ca2+ sensitivity and SERCA-2 in rat after myocardial infarction. Cardiovasc Res, 54, 162-74.

Wisløff, U., Støylen, A., Loennechen, J. P., Bruvold, M., Rognmo, Ø., Haram, P. M., Tjønna, A. E., Helgerud, J., Slørdahl, S. A., Lee, S. J., Videm, V., Bye, A., Smith, G. L., Najjar, S. M., Ellingsen, Ø. & Skjaerpe, T. 2007. Superior cardiovascular effect of aerobic interval training versus moderate continuous training in heart failure patients: a randomized study. Circulation, 115, 3086-94.

Wu, Z., Lee, S. T., Qiao, Y., Li, Z., Lee, P. L., Lee, Y. J., Jiang, X., Tan, J., Aau, M., Lim, C. Z. & Yu, Q. 2011. Polycomb protein EZH2 regulates cancer cell fate decision in response to DNA damage. Cell Death Differ, 18, 1771-9.

Wu, Z., Puigserver, P., Andersson, U., Zhang, C., Adelmant, G., Mootha, V., Troy, A., Cinti, S., Lowell, B., Scarpulla, R. C. & Spiegelman, B. M. 1999. Mechanisms controlling mitochondrial biogenesis and respiration through the thermogenic coactivator PGC-1. Cell, 98, 115-24.

Xie, Z. & Klionsky, D. J. 2007. Autophagosome formation: core machinery and adaptations. Nat Cell Biol, 9, 1102-9.

Yamashita, K. & Yoshioka, T. 1992. Activities of creatine kinase isoenzymes in single skeletal muscle fibres of trained and untrained rats. Pflugers Arch, 421, 270-3.

Yoshioka, J., Schreiter, E. R. & Lee, R. T. 2006. Role of thioredoxin in cell growth through interactions with signaling molecules. Antioxid Redox Signal, 8, 2143-51.

Youle, R. J. & Narendra, D. P. 2011. Mechanisms of mitophagy. Nat Rev Mol Cell Biol, 12, 9-14.

Zaglia, T., Milan, G., Ruhs, A., Franzoso, M., Bertaggia, E., Pianca, N., Carpi, A., Carullo, P., Pesce, P., Sacerdoti, D., Sarais, C., Catalucci, D., Krüger, M., Mongillo, M. & Sandri, M. 2014. Atrogin-1 deficiency promotes cardiomyopathy and premature death via impaired autophagy. J Clin Invest, 124, 2410-24.

Zhang, J., Randall, M. S., Loyd, M. R., Dorsey, F. C., Kundu, M., Cleveland, J. L. & Ney, P. A. 2009. Mitochondrial clearance is regulated by Atg7-dependent and -independent mechanisms during reticulocyte maturation. Blood, 114, 157-64.

Zoladz, J. A., Grassi, B., Majerczak, J., Szkutnik, Z., Korostyński, M., Karasiński, J., Kilarski, W. & Korzeniewski, B. 2013. Training-induced acceleration of O(2) uptake on-kinetics precedes muscle mitochondrial biogenesis in humans. Exp Physiol, 98, 883-98.

Acknowledgment

I have a great pleasure to thank Professor Roberto Bottinelli for giving me the opportunity to work in this scientific team under his leadership and the possibility to meet new realities and new motivations for my young ideas. Tank Prof.

Throughout my PhD I have had many opportunities of scientific interaction wich often resulted in ideas and suggestions. Particularly, I enjoyed the exciting and interesting discussions with all collaborators of this study, Prof. Bruno Grassi, Prof.Jerzy Zoladz, Dr. Joanna Majerczak and the younger colleagues Alessia and Desy.

But I am grateful to a special person, my supervisor Professor Maria Antonietta Pellegrino for her enthusiasm in sharing her vast scientific knowledge, for teaching me so patiently, ever listening my opinions, in a path for me constructive and productive. She is a teacher but also a friend and, maybe she does not know, she had represented my rock in this laboratory and in my life by now by four years. Your smile, that is perhaps the thing that unites us, it was important for me during this time. Thanks Maria.

I would also like to thank Cinzia that became one of my greatest friends. She helped me and encouraged me in my sad moments. From simple colleague, was born a unique friendship. I say thanks you but also I love you.

I can not forget the first people who made to love my job, Elena and my dear Professor Francesco Maria Megli, in the laboratory in Bari. I will always carry with me the memory of those happy days.

The achievement of this finish line I also have to my mom. Mom you are my perfect half, the only person from whom I expect only love and never a letdown. You are the person who gives me the strength every day, believing in my dreams without never to change, but always carrying on my ideas and never stooping to compromises with those who, for some reason, would like me different. Thanks Mom and I love you!

Finally, I can not find the right words for one person who I like to thank the most, you my love! Fra we started togheter this experience, we started from nothing, we had nothing, and now look where we are! We do not have much but we have collected so many job satisfaction and not only, believing in ourselves and helping each other. Because what you have made me realize that no matter what others think but what we are and what we want to become. Well, I thanks you and I love you!

In the end I dedicate my PhD thesys to Monyarella and Sara, like four years ago. Thanks also to my grandparents.

Thanks You all!